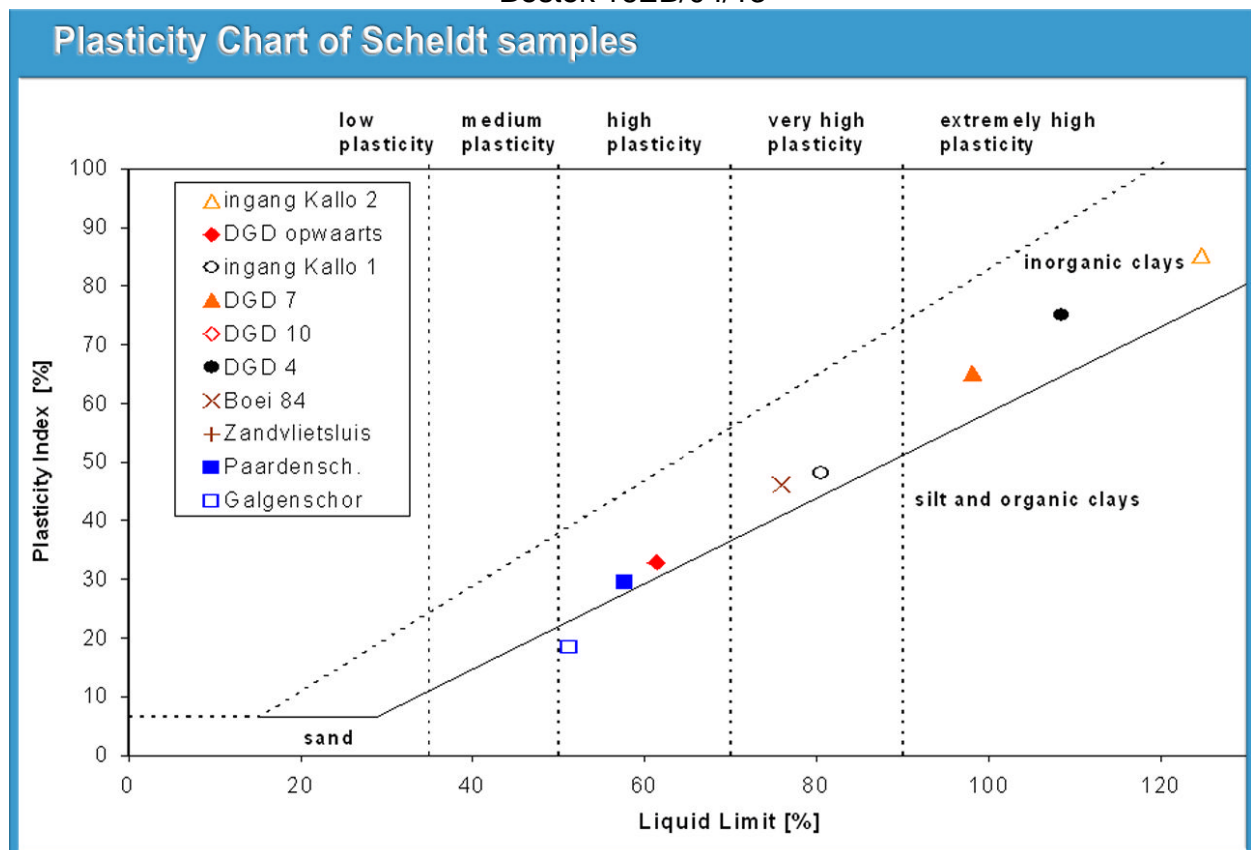


Uitbreiding studie denstiteitsstromingen in de Beneden Zeeschelde in het kader van LTV Meetcampagne naar hooggeconcentreerde slib suspensies

Bestek 16EB/04/13



Deelrapport 10 : Aanvullende slibparameters zomer 2006 Report 10 : Cohesive sediment properties summer 2006

31/10/2007

I/RA/11291/06.103/MSA



i.s.m



wl | delft hydraulics

en



Documentcontroleblad

Document Identificatie

Titel:	Deelrapport 10 : Aanvullende slibparameters zomer 2006 Report 10: Cohesive sediment properties summer 2006
Project:	Uitbreiding studie denstiteitsstromingen in de Beneden Zeeschelde in het kader van LTV Meetcampagne naar hooggeconcentreerde slibsuspensies Field measurements : high-concentration benthic suspensions (HCBS2)
Opdrachtgever	Waterbouwkundig Laboratorium
Documentref:	I/RA/11291/06.103/MSA
Documentnaam	K:\PROJECTS\11\11291 - HCBS Meetcampagne 2\10-Rap\10_RA06103_Slibeigenschappen\ra06103_Slibparameters_HCBS2_v20.doc

Revisies

Versie	Datum	Auteur	Omschrijving
0.8	15/06/07	T. van Kessel	pre-concept
0.9	21/06/07	T. van Kessel	1 ^e concept na review W.G.M. van Kesteren
1.0	9/8/07	TVK; JME	Toevoeging kaart en overzicht staalnames HCBS1 en 2
2.0	31/10/2007	TVK, JME	Final version

Verdeellijst

Naam	# ex.	Bedrijf/overheid	Functie m.b.t. het project
Joris Vanlede	7	Waterbouwkundig Laboratorium	Client
Frederik Roose	3	Maritieme Toegang	Client

Goedkeuring

Versie	Datum	Auteur	Projectleider	Diensthooft
2.0	31/10/07	JME	MSA	MSA
1.0	9/8/07	JME	MSA	MSA

TABLE OF CONTENTS

1. INTRODUCTION	4
1.1. THE ASSIGNMENT	4
1.2. PURPOSE OF THE STUDY	4
1.3. OVERVIEW OF THE STUDY	5
1.3.1. HCBS2 reports.....	5
1.3.2. HCBS1 reports.....	7
1.4. STRUCTURE OF THIS REPORT	7
2. LABORATORY TEST PROGRAM.....	8
2.1. INTRODUCTION COHESIVE SEDIMENT PROPERTIES	8
2.2. OVERVIEW OF SAMPLES	8
3. LABORATORY TEST RESULTS.....	15
3.1. GRAIN SIZE DISTRIBUTION, ORGANIC AND CARBONATE CONTENT	15
3.2. WATER CONTENT, UNDRAINED SHEAR STRENGTH AND ATTERBERG LIMITS	18
3.3. ZETA POTENTIAL	23
3.4. CST TESTS	24
3.5. CONSOLIDATION TESTS	26
4. CONCLUSIONS AND APPLICATION METHOD.....	29
4.1. CONCLUSIONS	29
4.2. APPLICATION OF RESULTS TO NUMERICAL MODELLING.....	29
5. REFERENCES.....	31

ANNEXES

ANNEX A. GRAIN SIZE DISTRIBUTIONS	A-1
ANNEX B. CONSOLIDATION TEST RESULTS.....	B-1

LIST OF TABLES

TABLE 1-1: OVERVIEW OF HCBS 2 REPORTS	5
TABLE 1-2: OVERVIEW OF HCBS 1 REPORTS	7
TABLE 2-1: SAMPLE ANALYSIS OF HCBS1.....	12
TABLE 2-2: SAMPLE ANALYSIS OF HCBS2.....	13
TABLE 2-3: OVERVIEW OF SAMPLES TAKEN AND SAMPLE LOCATIONS.	14
TABLE 3-1: RENUMBERING OF SAMPLES BY GEODELFT.....	15
TABLE 3-2: CARBONATE CONTENT, ORGANIC CONTENT (BASED ON LOI), AND GRAIN SIZE CHARACTERISTICS. ^A EXCLUDING THE CLAY FRACTION; ^B ACCORDING TO YOUD (1973).....	16
TABLE 3-3: WATER CONTENT, UNDRAINED SHEAR STRENGTH AND ATTERBERG LIMITS	18
TABLE 3-4: ZETA-POTENTIAL OF MUD SAMPLES IN FRESHWATER (CONDUCTIVITY 0.5 M ^S /CM) AND SALTWATER (CONDUCTIVITY 7.9 M ^S /CM AT 25 °C).....	23
TABLE 3-5: CAPILLARY SUCTION TIME AND INITIAL WATER CONTENT OF SAMPLES	25
TABLE 3-6: RESULTS FROM CONSOLIDATION TESTS	28
TABLE 4-1: EROSION PARAMETERS DETERMINED FROM SEDIMENT ANALYSIS.....	30

LIST OF FIGURES

FIGURE 2.1: MAPS OF HCBS1 (BLUE O) AND HCBS2 (RED +) SAMPLE LOCATIONS.....	11
FIGURE 3.1: BED COMPOSITION IN DEURGANCKDOK. IN BLACK: SAMPLE NO. IN PINK: PERCENTAGE SAND.	16
FIGURE 3.2: SAND-SILT-CLAY TRIANGLE OF SOIL SAMPLES.....	17
FIGURE 3.3: SILT CONTENT AS A FUNCTION OF CLAY CONTENT Ξ	17
FIGURE 3.4: PLASTICITY INDEX (PI) AS A FUNCTION OF LIQUID LIMIT (LL) (PLASTICITY CHART)	19
FIGURE 3.5: PLASTICITY INDEX (PI) AS A FUNCTION OF CLAY CONTENT Ξ (ACTIVITY PLOT).....	19
FIGURE 3.6: PERCENTAGE ORGANIC MATTER (OM) AS A FUNCTION OF CLAY CONTENT Ξ	20
FIGURE 3.7: CARBONATE CONTENT AS A FUNCTION OF CLAY CONTENT Ξ	21
FIGURE 3.8: UNDRAINED SHEAR STRENGTH C_u AS A FUNCTION OF LIQUIDITY INDEX (LI).....	21
FIGURE 3.9: UNDRAINED SHEAR STRENGTH C_u AS A FUNCTION OF CLAY WATER CONTENT w/N_{cl}	22
FIGURE 3.10: SEDIMENT PHASE DIAGRAM FOR THE LOWER SEA SCHELDT	22
FIGURE 3.11: ZETA-POTENTIAL OF SAMPLES AS A FUNCTION OF THEIR ACTIVITY	24
FIGURE 3.12: RESULTS FROM CST-TESTS	25
FIGURE 3.13: OVERVIEW OF CST-APPARATUS. $D_F = 1.10 \times 10^{-3}$ M, $D_c = 0.018$ M; $D_1 = 0.032$ M; $D_2 = 0.045$ M.....	26
FIGURE 3.14: EXAMPLE OF IMAGE CAPTURED WITH CANON DIGITAL SLR (3888 \times 2592) TO DETERMINE INTERFACE SETTLEMENT. COLUMN HEIGHT = 1 M; RULER LENGTH = 0.20 M; DISTANCE BETWEEN TWO RULER TICKS = 0.01 M.	28

LIST OF FIGURES IN ANNEXES

FIGURE 2.1: MAPS OF HCBS1 (BLUE O) AND HCBS2 (RED +) SAMPLE LOCATIONS.....	11
FIGURE 3.1: BED COMPOSITION IN DEURGANCKDOK. IN BLACK: SAMPLE NO. IN PINK: PERCENTAGE SAND.	16
FIGURE 3.2: SAND-SILT-CLAY TRIANGLE OF SOIL SAMPLES.....	17
FIGURE 3.3: SILT CONTENT AS A FUNCTION OF CLAY CONTENT Ξ	17
FIGURE 3.4: PLASTICITY INDEX (PI) AS A FUNCTION OF LIQUID LIMIT (LL) (PLASTICITY CHART)	19
FIGURE 3.5: PLASTICITY INDEX (PI) AS A FUNCTION OF CLAY CONTENT Ξ (ACTIVITY PLOT).....	19
FIGURE 3.6: PERCENTAGE ORGANIC MATTER (OM) AS A FUNCTION OF CLAY CONTENT Ξ	20
FIGURE 3.7: CARBONATE CONTENT AS A FUNCTION OF CLAY CONTENT Ξ	21
FIGURE 3.8: UNDRAINED SHEAR STRENGTH C_u AS A FUNCTION OF LIQUIDITY INDEX (LI).....	21
FIGURE 3.9: UNDRAINED SHEAR STRENGTH C_u AS A FUNCTION OF CLAY WATER CONTENT w/N_{cl}	22
FIGURE 3.10: SEDIMENT PHASE DIAGRAM FOR THE LOWER SEA SCHELDT	22
FIGURE 3.11: ZETA-POTENTIAL OF SAMPLES AS A FUNCTION OF THEIR ACTIVITY	24
FIGURE 3.12: RESULTS FROM CST-TESTS	25
FIGURE 3.13: OVERVIEW OF CST-APPARATUS. $D_F = 1.10 \times 10^{-3}$ M, $D_c = 0.018$ M; $D_1 = 0.032$ M; $D_2 = 0.045$ M.....	26
FIGURE 3.14: EXAMPLE OF IMAGE CAPTURED WITH CANON DIGITAL SLR (3888 \times 2592) TO DETERMINE INTERFACE SETTLEMENT. COLUMN HEIGHT = 1 M; RULER LENGTH = 0.20 M; DISTANCE BETWEEN TWO RULER TICKS = 0.01 M.	28

1. INTRODUCTION

1.1. The assignment

This report is part of the set of reports describing the results of the extension of the study about density currents in the Lower Sea Scheldt (Beneden Zeeschelde) as part of the Long Term Vision for the Scheldt estuary – Field measurements high-concentration benthic suspensions (HCBS 2)¹. It is complementary to the study ‘Monitoring and analysis of silt accretion in Deurganckdok.

The terms of reference for this study were prepared by the ‘Departement Mobiliteit en Openbare Werken van de Vlaamse Overheid, Waterbouwkundig Laboratorium’ (16EB/04/13). The repetition of this study was awarded to International Marine and Dredging Consultants NV in association with WL|Delft Hydraulics, dr. R. Kirby and Gems International on 09/12/2005.

‘Waterbouwkundig Laboratorium – Cel Hydrometrie Schelde’ provided data on discharge, tide, salinity and turbidity along the river Scheldt and provided survey vessels for the long term and through tide measurements.

The settling velocity measurements with INSSEV were subcontracted to the Coastal Processes Research Group (SEOES, University of Plymouth), with team leader Dr Andrew Manning.

1.2. Purpose of the study

The Lower Sea Scheldt is the stretch of the Scheldt estuary between the Belgium-Dutch border and Rupelmonde, where the entrance channels to the Antwerp sea locks are located. The navigation channel has a sandy bed, whereas the shallower areas (intertidal areas, mud flats, salt marshes) consist of sandy clay or even pure mud sometimes. This part of the Scheldt is characterized by large horizontal salinity gradients and the presence of a turbidity maximum with depth-averaged concentrations ranging from 50 to 500 mg/l at grain sizes of 60 - 100 μm . The salinity gradients generate significant density currents between the river and the entrance channels to the locks, causing large siltation rates. It is to be expected that in the near future also the Deurganckdok will suffer from such large siltation rates, which may double the amount of dredging material to be dumped in the Lower Sea Scheldt.

Another observation during the last years is that the composition of the sediment dredged at the Sill of Zandvliet became more muddy, resulting in a strong increase in dumping volumes at the allocated dumping sites since 2002.

To deal with these problems, and to facilitate the management of the Lower Sea Scheldt, more knowledge on the fine sediment dynamics is required. This can be obtained from in-situ measurements and the development of an advanced numerical sediment transport model.

In the past, already many surveys have been carried out to increase the understanding of the dynamics of fine sediment in the Lower Sea Scheldt. Also, salinity and turbidity is measured continuously at Prosperpolder and Oosterweel. However, none of these measurements have been carried out in the lower 1 m of the water column.

It is expected that temporary layers of soft mud may be formed in this lower part of the water column, which may move independently of the tidal water movement, in particular during slack

¹ Uitbreiding studie densiteitsstromingen in de Beneden Zeeschelde in het kader van LTV Meetcampagne naar hooggeconcentreerde slibsuspensies

water. These layers may be remixed during accelerating tide, an indication for which is the observation of mud clouds at the water surface during maximum ebb and flood velocities. If such layers exist, they may contribute significantly to the siltation rate in the Deurganckdok. This would imply that measures (for instance passive constructions) to minimize siltation in the Deurganckdok can only be successful if the dynamics of these soft mud layers are also affected. Therefore it is important to establish the role of these soft mud layers on the sediment dynamics in the Lower Sea Scheldt, both from a qualitative and quantitative point of view.

The goal of the first HCBS study (2005) was threefold:

1. The primary goal of the study (and the survey) is to detect the occurrence of near-bed high-concentration mud suspensions (referred to as **high-concentration benthic suspensions - HCBS**), their dynamic behaviour and the conditions and locations of their occurrence,
2. The second goal is to establish fluxes of fine sediment in the river with the purpose to calibrate a numerical 3D cohesive sediment transport model of the Lower Sea Scheldt,
3. The third goal is to establish the sediment properties required for the cohesive sediment transport model.

The second HCBS survey aims to complete the same HCBS and flux measurements after the opening of Deurganckdok in July 2005. The measurements are repeated under the same (seasonal and tidal) conditions as the original HCBS survey. These are referred to as the winter campaign. Seasonal influences are examined in September 2006 when the survey was repeated in summer conditions, being the summer campaign.

The settling velocity measurements are only conducted in summer conditions (August 2006).

1.3. Overview of the study

1.3.1. HCBS2 reports

The repetition of the study consists of two separate surveys. The first survey is a repetition of the first HCBS measurement campaign (winter campaign) and was conducted in March 2006. The second survey will be held in September 2006.

In situ calibrations were conducted on several dates to calibrate all turbidity and conductivity sensors.

This report, report 10, is part of the set of reports for the summer campaign, describing the study. An overview of these reports is given in Table 1-1.

Parallel with this study, measurement campaigns were conducted as a part of study to 'Monitoring and analysis of silt accretion in Deurganckdok. These measurements (see IMDC, 2006l to 2006o & IMDC, 2007m to 2007w) and in combination with measurements of this report could help to understand the tidal dynamics within Deurganckdok and on the river Scheldt.

Table 1-1: Overview of HCBS 2 Reports

Report	Description
Ambient Conditions Lower Sea Scheldt	
5.3	Overview of ambient conditions in the river Scheldt – January-June 2006 (I/RA/11291/06.088/MSA)
5.4	Overview of ambient conditions in the river Scheldt – July-December 2006 (I/RA/11291/06.089/MSA)

Report	Description
Ambient Conditions Lower Sea Scheldt	
5.5*	Overview of ambient conditions in the river Scheldt : RCM-9 buoy 84 & 97 (1/1/2007 – 31/3/2007) (I/RA/11291/06.090/MSA)
5.6	Analysis of ambient conditions during 2006 (I/RA/11291/06.091/MSA)
Calibration	
6.1	Winter Calibration (I/RA/11291/06.092/MSA)
6.2	Summer Calibration and Final Report (I/RA/11291/06.093/MSA)
Through tide Measurements Winter 2006	
7.1	21/3 Scheldewacht – Deurganckdok – Salinity Distribution (I/RA/11291/06.094/MSA)
7.2	22/3 Parel 2 – Deurganckdok (I/RA/11291/06.095/MSA)
7.3	22/3 Laure Marie – Liefkenshoek (I/RA/11291/06.096/MSA)
7.4	23/3 Parel 2 – Schelle (I/RA/11291/06.097/MSA)
7.5	23/3 Laure Marie – Deurganckdok (I/RA/11291/06.098/MSA)
7.6	23/3 Veremans Waarde (I/RA/11291/06.099/MSA)
HCBS Near bed continuous monitoring (Frames)	
8.1	Near bed continuous monitoring winter 2006 (I/RA/11291/06.100/MSA)
INSSEV	
9	Settling Velocity - INSSEV summer 2006 (I/RA/11291/06.102/MSA)
Cohesive Sediment	
10	Cohesive sediment properties summer 2006 (I/RA/11291/06.103/MSA)
Through tide Measurements Summer 2006	
11.1	Through Tide Measurement Sediview and Siltprofiler 27/9 Stream - Liefkenshoek (I/RA/11291/06.104/MSA)
11.2	Through Tide Measurement Sediview 27/9 Veremans - Raai K (I/RA/11291/06.105/MSA)
11.3	Through Tide Measurement Sediview and Siltprofiler 28/9 Stream - Raai K (I/RA/11291/06.106/MSA)
11.4	Through Tide Measurement Sediview 28/9 Veremans – Waarde (I/RA/11291/06.107/MSA)
11.5	Through Tide Measurements Sediview 28/9 Parel 2 - Schelle (I/RA/11291/06.108/MSA)
11.6	Through Tide measurement Longitudinal Salinity Distribution 26/9 Scheldewacht – Deurganckdok (I/RA/11291/06.161/MSA)
Analysis	
12	Report concerning the presence of HCBS layers in the Scheldt river (I/RA/11291/06.109/MSA)

* Report 5.5 will be handled in report 3.1. Boundary conditions: Three monthly report 1/1/2007 – 31/03/2007 (I/RA/11283/06.127/MSA) including HCBS 2 report 5.5 (Deurganckdok)..

1.3.2. HCBS1 reports

Reports of the first HCBS campaign are summarized in Table 1-2.

Table 1-2: Overview of HCBS 1 Reports

Report	Description
Test Survey	
1	Test survey 2-3 February 2005 (I/RA/11265/05.008/MSA)
Through tide and DON frame Measurements Winter 2005	
2.1	February survey – Deurganckdok 17 February 2005 (I/RA/11265/05.009/MSA)
2.2	February survey – Zandvliet 17 February 2005 (I/RA/11265/05.010/MSA)
2.3	February survey – Liefkenshoek 17 February 2005 (I/RA/11265/05.011/MSA)
2.4	February survey – Schelle 17 February 2005 (I/RA/11265/05.012/MSA)
2.5	February survey – Deurganckdok 16 February 2005 (I/RA/11265/05.013/MSA)
2.6	February survey – Kallosluis 18 February 2005 (I/RA/11265/05.014/MSA)
2.7	February survey – Near bed continuous monitoring (I/RA/11265/05.015/MSA)
INSSEV	
3	February survey – Settling velocity - INSSEV (I/RA/11265/05.016/MSA)
Cohesive Sediment	
4	February survey – Cohesive sediment properties (I/RA/11265/05.017/MSA)
Ambient Conditions Lower Sea Scheldt	
5.1	Overview of ambient conditions in the river Scheldt – January-June 2005 (I/RA/11265/05.018/MSA)
5.2	Overview of ambient conditions in the river Scheldt – July-December 2005 (I/RA/11265/05.019/MSA)
Analyse	
6.1**	Analysis of ambient conditions in the river Scheldt: RCM-9 buoy 84 & 97- (21/09/05-1/10/06) (I/RA/11265.162/MSA)

** Report 6.1 will be handled in report 5.6 (HCBS 2): Analysis of ambient conditions 21/09/05 - 31/3/2007 (I/RA/11291/06.091/MSA).

1.4. Structure of this report

The structure of this report is as follow. In Chapter 2 the laboratory test program is discussed. In Chapter 3 the results are presented. In Chapter 4 the results are discussed and conclusions are drawn.

2. LABORATORY TEST PROGRAM

2.1. Introduction cohesive sediment properties

The cohesive sediment properties are analysed to determine the consolidation and erosion properties of the sediment. These are required as input to the 3D mud transport model to be developed in a related study (Winterwerp et al, 2006).

The consolidation properties are determined using a settling column technique described by Merckelbach (2000) and Merckelbach and Kranenburg (2004).

The erodibility and critical shear stress for erosion is derived from a number of laboratory tests as explained in §4.2:

- Particle size distribution
- Organic and calcium content
- Atterberg limits
- Capillary Suction Time (CST) and water content
- Zeta-potential
- Bulk density
- Undrained shear strength

2.2. Overview of samples

On October 13th 2006, samples were taken in the Beneden Zeeschelde from the Dutch-Belgian border up to Antwerpen from the vessel Scheldewacht II (see Table 2-3).

Sampling was done with a Van Veen grab sampler (2 litre). Additionally 200 litre of water was collected from the river Scheldt for the consolidation tests.

The intertidal areas surface samples (2 l) were taken on October 20th 2006 using cylindrical PVC tubes of 50 mm diameter and 200 mm length (see Table 2-3).

On October 24, 2006, samples were delivered by IMDC to WL | Delft Hydraulics (see Table 2-1). From this set, the following 20 samples were selected and delivered to GeoDelft on May 4, 2007:

Zandvlietsluis no. 2, Galgenschoor no. GS2, Paardenschoor no. PS2, Boei 84 no. 9, ingang Kallo 2 no. 31, ingang Kallo 1 no. 33, DGD4 no. 12, DGD10 no. 18, DGD7 no. 21, sill (DGD opwaarts) no. 24, Berendrechtshuis no. 5, Zandvliet 2 no. 7, Groot Buitenschor no. GB10, Plaat van Boomke no. 35, Kallo afwaarts 2 no. 27, Oosterweel no. 36, DGD afwaarts 2 no. 10, DGD2 no. 22, DGD3 no. 23, DGD9 no. 20.

The samples GS2, PS2 and GB10 originate from the intertidal areas, nearby the locations where in situ erosion tests were executed in 1997 (IMDC-IN, 1998).

The 20 samples were analysed by GeoDelft on the following parameters (N.B. of the last 10 samples, no Atterberg limits and organic and lime content were determined for financial reasons):

- Grain size distribution (sieve for fraction > 32 µm and sedigraph for fraction < 32 µm)
- Bulk density and water content
- Organic and lime content
- Atterberg limits

The laboratory tests were carried out according to the following standards:

- Organic content ('humus'): RAW2000, test 158 (<http://www.crow.nl/raw>);
- Calcium content ('kalk'): RAW2000, test 159 (<http://www.crow.nl/raw>);
- Grain size distribution: sieve and sedigraph according to recommended practice NEN ISO/DTS17892-4 ('Geotechnisch onderzoek en beproeving - Beproeving van grond in het laboratorium - Deel 4: Bepaling van de korrelgrootte verdeling') (<http://normen.nen.nl/>);
- Atterberg limits: DIN 18122-1; ASTM D4318 and BS 1377 Parts 2-4 and 2-5.

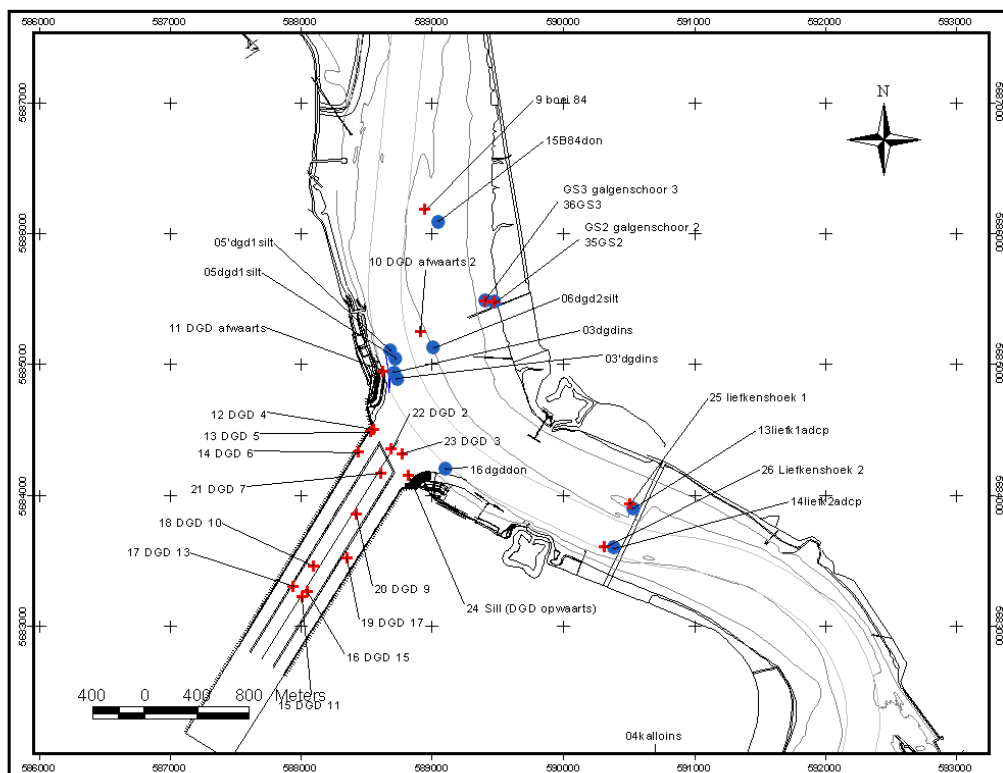
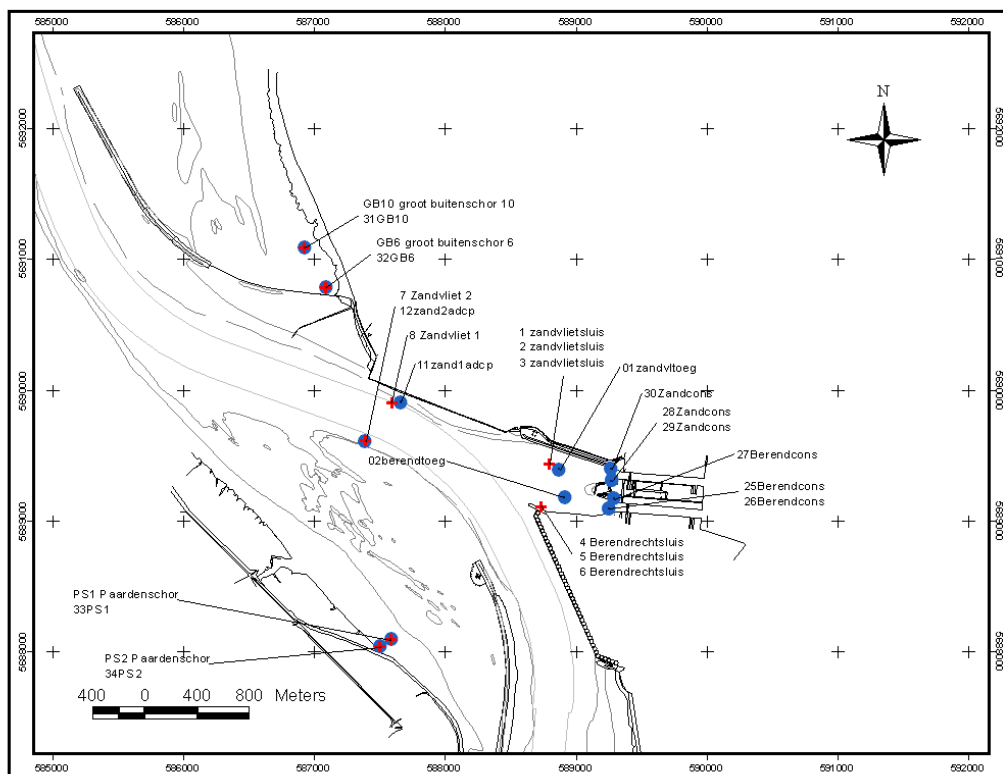
On June 1, 2007, the test results were delivered by GeoDelft to WL | Delft Hydraulics.

WL | Delft Hydraulics analysed the following 10 samples on shear strength, zeta-potential, CST-time and consolidation properties. Figure 2.1 shows a map of the sample locations.

Zandvlietsluis no. 2, Galgenschoor no. GS2, Paardenschoor no. PS2, Boei 84 no. 9, ingang Kallo 2 no. 31, ingang Kallo 1 no. 33, DGD4 no. 12, DGD10 no. 18, DGD7 no. 21, sill (DGD opwaarts) no. 24.

Regarding the CST-test, the procedure described by Huisman and Van Kesteren (1998) was applied. These tests are described in more detail in Section 3.4.

For the zeta-potential (see Section 3.3) no official standard exists. The zeta-potential of the mud particles was measured on a Malvern Zetasizer 3000 (www.malvern.co.uk) following the protocol from the user manual. Prior to use, the instrument was allowed to warm up for a sufficient time and the proper functioning of the system was checked with a -50 ± 5 mV transfer standard supplied by Malvern. A useful introduction to the measurement of zeta-potential in slurries is given by Hunter (2001).



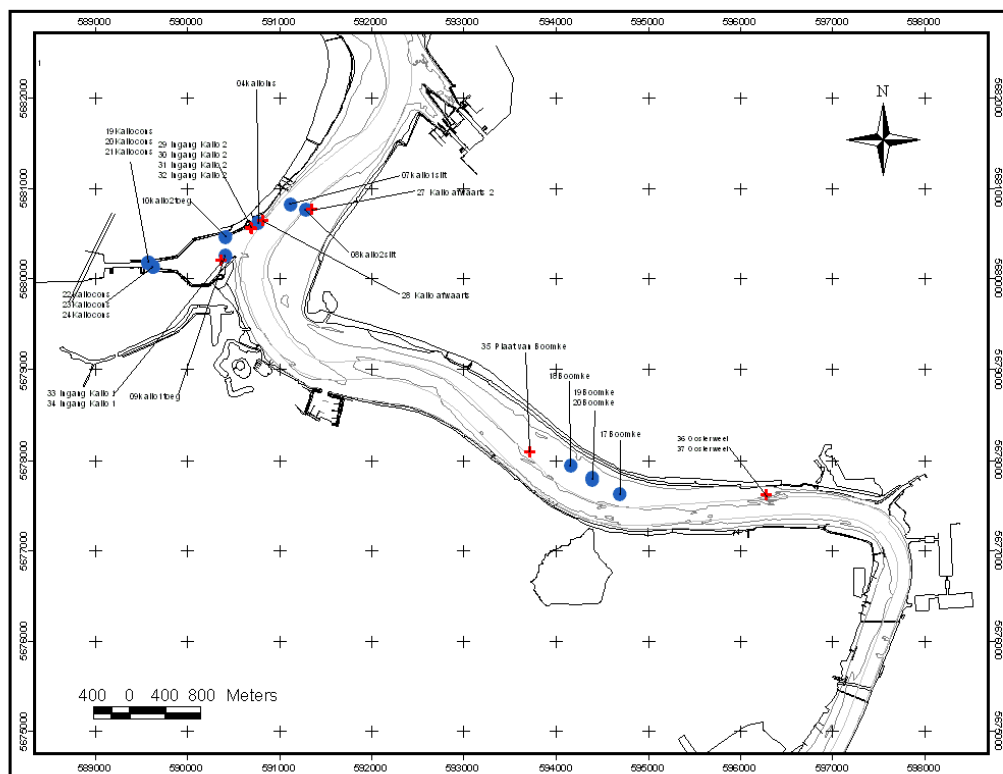


Figure 2.1: Maps of HCBS1 (blue o) and HCBS2 (red +) sample locations

Table 2-1: Sample analysis of HCBS1

Sample ID HCBS1	Cohesive sediment properties analysed by
01zandvltoeg	Geodelft and WL Delft Hydraulics
02berendtoeg	Geodelft
03dgdins	Geodelft
04kalloins	Geodelft and WL Delft Hydraulics
05dgd1silt	Geodelft
06dgd2silt	Geodelft
07kallo1silt	Geodelft
08kallo2silt	Geodelft and WL Delft Hydraulics
09kallo1toeg	Geodelft
10kallo2toeg	Geodelft
11zand1adcp	Geodelft
12zand2adcp	Geodelft
13liefk1adcp	Geodelft
14liefk2adcp	Geodelft and WL Delft Hydraulics
15B84don	Geodelft
16dgd1don	Geodelft and WL Delft Hydraulics
17Boomke	Geodelft
18Boomke	Geodelft
31GB10	Geodelft and WL Delft Hydraulics
32GB6	Geodelft
33PS1	Geodelft and WL Delft Hydraulics
34PS2	Geodelft
35GS2	Geodelft
36GS3	Geodelft and WL Delft Hydraulics
25Berendcons	WL Delft Hydraulics
26Berendcons	WL Delft Hydraulics

Table 2-2: Sample analysis of HCBS2

Sample ID HCBS2	Cohesive sediment properties analysed by
2 zandvlietsluis	Geodelft and WL Delft Hydraulics
5 Berendrechtsluis	Geodelft
7 Zandvliet 2	Geodelft
9 boei 84	Geodelft and WL Delft Hydraulics
10 DGD afwaarts 2	Geodelft
12 DGD 4	Geodelft and WL Delft Hydraulics
18 DGD 10	Geodelft and WL Delft Hydraulics
20 DGD 9	Geodelft
21 DGD 7	Geodelft and WL Delft Hydraulics
22 DGD 2	Geodelft
23 DGD 3	Geodelft
24 Sill (DGD opwaarts)	Geodelft and WL Delft Hydraulics
27 Kallo afwaarts 2	Geodelft
31 ingang Kallo 2	Geodelft and WL Delft Hydraulics
33 ingang Kallo 1	Geodelft and WL Delft Hydraulics
35 Plaat van Boomke	Geodelft
36 Oosterweel	Geodelft
GS2 galgenschor 2	Geodelft and WL Delft Hydraulics
GB10 groot buitenschor 10	Geodelft
PS2 Paardenschor	Geodelft and WL Delft Hydraulics

Table 2-3: Overview of samples taken and sample locations.

project	11291-zomer	pagina	1 van 1
datum	13/okt/06		
coord	UTM ED50		
schip	Scheldewacht 2		
operator	BQU		



Locatie						
	tijd UTC	naam locatie	Easting	Northing	staal	opm
1	8:10	zandvlietsluis	588802	5689436	1	
2	8:10	zandvlietsluis	588802	5689436	2	"+ 3 Waterstalen (Z)" extra
3	8:11	zandvlietsluis	588798	5689432	3	
4	8:21	Berendrechtsluis	588736	5689109	4	
5	8:21	Berendrechtsluis	588736	5689109	5	"+ 3 Waterstalen (B)" basis
6	8:21	Berendrechtsluis	588736	5689109	6	
7	8:38	Zandvliet 2	587402	5689616	7	basis
8	8:42	Zandvliet 1	587606	5689907	8	
9	8:58	boei 84	588948	5686185	9	extra
10	9:04	DGD afwaarts 2	588917	5685250	10	basis
11	9:09	DGD afwaarts 1	588724	5685017		geen staal (stenen, 4* nijs)
12	9:18	DGD afwaarts	588627	5684955	11	veel stenen, sluit slecht, (=slecht staal)
13	9:26	DGD 4	588558	5684506	12	extra
14	9:31	DGD 5	588533	5684487	13	
15	9:34	DGD 6	588446	5684331	14	
16	9:44	DGD 11	588013	5683221	15	
17	9:54	DGD 15	588054	5683260	16	
18	9:58	DGD 13	587945	5683303	17	
19	10:00	DGD 10	588102	5683460	18	extra
20	10:04	DGD 17	588354	5683521	19	
21	10:07	DGD 9	588425	5683856	20	basis
22	10:11	DGD 7	588617	5684173	21	extra
23	10:15	DGD 2	588692	5684361	22	basis
24	10:17	DGD 3	588780	5684317	23	basis
25	10:20	Sill (DGD opwaarts)	588827	5684154	24	extra
26	11:36	liefkenshoek 1	590512	5683935	25	(zeer zwart slib), vlakbij nieuwe steiger
27	11:39	Liefkenshoek 2	590320	5683608	26	
28	11:56	Kallo afwaarts 2	591316	5680772	27	zanderig basis
29	12:01	Kallo afwaarts 1	591100	5680909		schelpen, stenen, geen slib dus geen staal
30	12:12	Kallo afwaarts	590773	5680647	28	
31	12:14	ingang Kallo 2	590645	5680563	29	"+ 5 Waterstalen (K)"
32	12:14	ingang Kallo 2	590645	5680563	30	
33	12:15	ingang Kallo 2	590643	5680574	31	extra
34	12:15	ingang Kallo 2	590643	5680574	32	
35	12:20	ingang Kallo 1	590315	5680202	33	extra
36	12:20	ingang Kallo 1	590315	5680202	34	
37	12:40	Plaat van Boomke	593719	5678090	35	basis
38	12:45	Plaat van Boomke	593853	5677968		geen staal, teveel stenen
39	13:12	Oosterweel basis	596343	5677617	36	pas gedumpt door Marieke (uit DGD drempel)
40	13:12	Oosterweel	596343	5677617	37	pas gedumpt door Marieke (uit DGD drempel)

project	11291-zomer	pagina	2 van 2
datum	20/okt/06		
coord	UTM ED50		
schip	via oever		
operator	BQU		



Locatie						
	TIJD	naam locatie	Easting	Northing	staal	opm
46						
47	9:39	galgenschor 2	589474	5685475	GS2	extra
48	9:45	galgenschor 3	589408	5685480	GS3	
49	10:30	groot buitenschor 10	586930	5691083	GB10	basis
50	10:38	groot buitenschor 6	587097	5690778	GB6	
51	11:28	Paardenschor	587593	5688088	PS1	
52	11:32	Paardenschor	587512	5688038	PS2	extra

3. LABORATORY TEST RESULTS

3.1. Grain size distribution, organic and carbonate content

Appendix A shows the grain size distribution of all samples tested. Note that GeoDelft used a different sample identification. The conversion from IMDC/WL sampe ID to GeoDelft sample ID is as follows (Table 3-1):

Table 3-1: Renumbering of samples by GeoDelft

GeoDelft	IMDC/WL	GeoDelft	IMDC/WL
sample ID	sample ID	sample ID	sample ID
62	GB10 G. Buitenschor	72	no. 20 DGD 9
63	GS02 Galgenschor	73	no. 21 DGD 7
64	PS02 Paardenschor	74	no. 22 DGD 2
65	no. 2 Zandvlietsluis	75	no. 23 DGD 3
66	no. 5 Berendrechtsluis	76	no. 24 DGD opwaarts
67	no. 7 Zandvliet 2	77	no. 27 Kallo afwaarts 2
68	no. 9 Boei 84	78	no. 31 ingang Kallo 2
69	no. 10 DGD afwaarts 2	79	no. 33 ingang Kallo 1
70	no. 12 DGD 4	80	no. 35 Boomke
71	no. 18 DGD 10	81	no. 36 Oosterweel

From the grain size distributions it is concluded that samples 7 Zandvliet 2, 10 DGD afwaarts 2 and 27 Kallo afwaarts 2 are sandy, i.e. the sand skeleton dominates and the fines are only filling material reducing the permeability somewhat. The other samples are cohesive, in which sand is just a filling material (e.g. influencing the bulk density). From the grain size distributions 5 characteristic values are obtained: sand content ($> 63 \mu\text{m}$), silt content ($>2 \mu\text{m}$; $<63 \mu\text{m}$), clay content ($<2 \mu\text{m}$), D_{50} and D_{60}/D_{10} . These values are listed in Table 3-2. The uniformity coefficient D_{60}/D_{10} (Youd, 1973 and Winterwerp & Van Kesteren, 2004) is calculated from D_{60} and D_{10} from which the clay fraction was excluded. The uniformity coefficient is most relevant for sandy material with little clay (sand skeleton dominant). The higher the uniformity coefficient, the lower the porosity.

For classification the grain size distributions are plotted in the sand-silt-clay triangle as depicted in Figure 3.2. The sandy samples 7 Zandvliet 2, 10 DGD afwaarts 2 and 27 Kallo afwaarts 2 are found in the left lower corner: the sand dominated region. All other samples are gathered around a line with a constant silt/clay ratio of 1.74 (see also Figure 3.3). This constant ratio indicates that the different sample locations differ mainly in sand content. Sample 35 Boomke is also located near this line, which was not the case during the HCBS1 campaign. Also, its sand content has increased markedly. Probably the Boom clay layer has been covered locally with fresh deposits.

In the Deurganckdok, a clear trend in grain size distribution is observed. Going from the navigation channel in the river towards the back side of the harbour basin, the sand content gradually decreases from 88% (sample no. 10) to 28, 21, 13 and 7 for samples no. 22, 21, 20 and 18, respectively. This trend is shown in Figure 3.1.

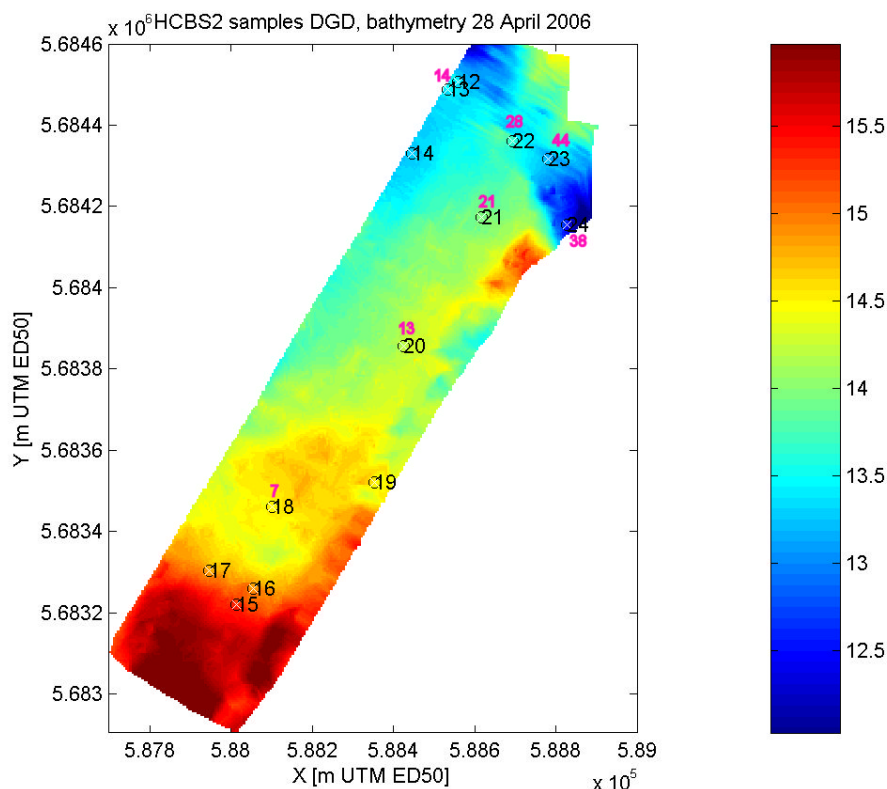


Figure 3.1: Bed composition in Deurganckdok. In black: sample no. In pink: percentage sand.

Table 3-2: Carbonate content, organic content (based on LOI), and grain size characteristics. ^aexcluding the clay fraction; ^baccording to Youd (1973)

GD	WL	Carbo nate %	Humus %	sand %	silt %	clay %	D ₅₀ μm	D ₆₀ /D ₁₀ ^a	n _{max} ^b
62	GB10 Buitenschor			48.9	38.7	12.4	62	5.3	42.3
63	GS02 Galgenschor	16.47	2.63	27.9	55.6	16.5	44	8.3	39.4
64	PS02 Paardensch.	17.00	2.81	28.0	53.7	18.3	42	8.1	39.6
65	2 Zandvlietsluis	20.56	5.84	9.5	54.0	36.5	4	6.7	40.8
66	5 Berendrechtsluis			15.2	50.4	34.4	6	14.0	36.1
67	7 Zandvliet 2			88.5	7.7	3.8	158	3.3	45.3
68	9 Boei 84	17.64	4.32	37.3	41.8	20.9	44	14.6	35.8
69	10 DGD afwaarts 2			88.1	7.9	4.0	114	2.0	48.4
70	12 DGD 4	16.43	5.41	14.4	54.4	31.2	7	10.0	38.2
71	18 DGD 10	21.67	5.63	7.4	61.1	31.5	5	4.3	43.6
72	20 DGD 9			13.3	74.1	12.6	6	4.0	44.0
73	21 DGD 7	15.74	5.21	20.7	47.2	32.1	9	13.3	36.4
74	22 DGD 2			27.6	46.0	26.4	23	15.5	35.5
75	23 DGD 3			44.4	35.1	20.5	55	12.8	36.7
76	24 DGD opwaarts	16.97	3.15	38.0	41.4	20.6	50	11.5	37.3
77	27 Kallo afwaarts 2			94.6	3.4	2.0	123	1.7	49.5
78	31 ingang Kallo 2	18.42	6.8	22.7	43.3	34.0	6	13.7	36.2
79	33 ingang Kallo 1	16.43	4.18	27.0	48.8	24.2	27	15.0	35.7
80	35 Boomke			34.2	35.0	30.8	8	27.5	31.8
81	36 Oosterweel			33.3	43.2	23.5	14	21.4	33.4

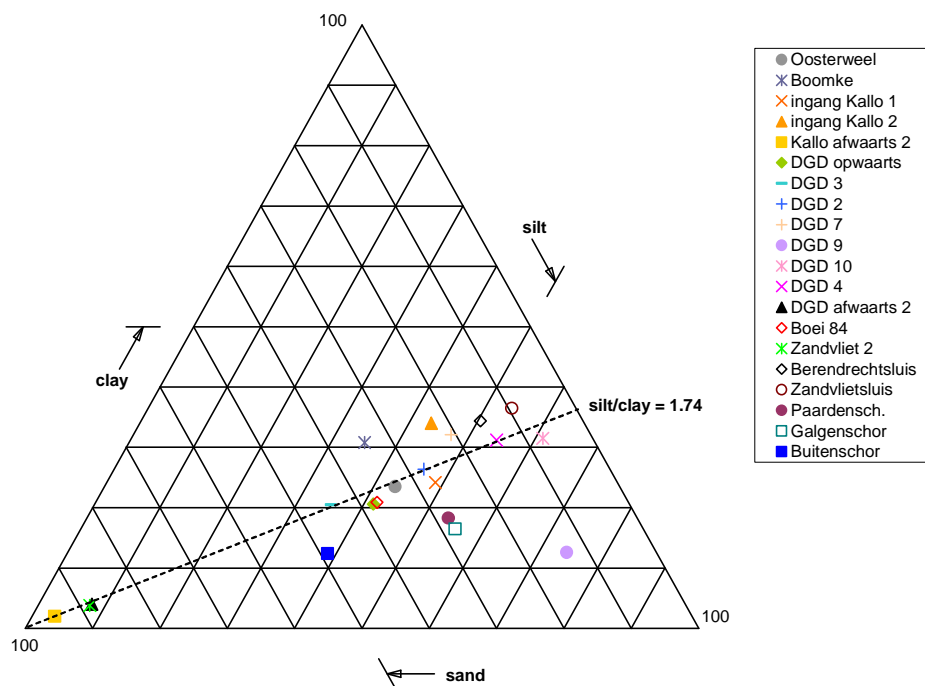


Figure 3.2: Sand-silt-clay triangle of soil samples

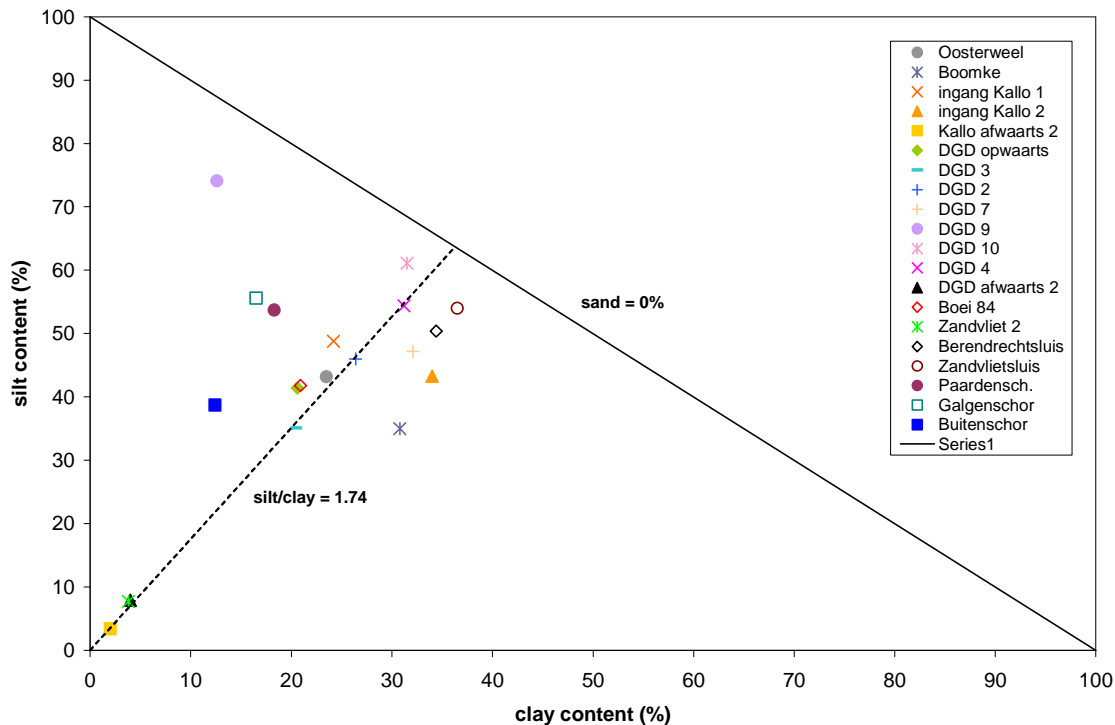


Figure 3.3: Silt content as a function of clay content ξ

3.2. Water content, undrained shear strength and Atterberg limits

The results on water content, undrained shear strength and Atterberg limits (plastic limit PL and liquid limit LL), organic content (humus) and carbonate content are shown in Table 3-3. The Atterbergs limits are water contents that are related to the plastic or cohesive behaviour of soils and are used for classification of soil plasticity. In the Plasticity Chart (Figure 3.4) the Plasticity Index (PI), defined by the difference between liquid and plastic limit ($PI = LL - PL$), is plotted as function of the liquid limit (LL). Figure 3.4 shows that most samples can be classified as inorganic clays with a plasticity ranging from high to extremely high. The plasticity of inorganic clays is also related to the amount and type of clay. This can be shown by plotting the Plasticity Index as function of the clay content in the so-called activity plot (see Figure 3.5). This plot shows that all samples are grouped along a single line with a constant gradient of 3.5 and an intercept at 11.4% clay content. The gradient is defined as the activity of the clay minerals present in the clay fraction ($< 2\mu\text{m}$). The intercept value indicates the minimal amount of clay that is required to obtain cohesive soil behaviour. From Figure 3.5 it is concluded that all cohesive samples contain mainly a single mixture of clay minerals with an activity of 3.5. This relative high activity indicates that montmorillonite must be present (activity 7 to 9) besides less active minerals like kaolinite (0.4) and illite (0.9). The activity of 3.5 corresponds to the activity of cohesive sediments that are transported along the Dutch coast, in which the montmorillonite originates from the French coast and the Ypresian clay that is exposed in the Dover Strait. It is remarkable that the activity is higher than the activity of the samples analysed in the framework of the HCBS1 campaign, which equalled 2.5. This may be explained by the surface area of exposed Boom clay, which has an activity of 1.13 (see HCBS1 data report 4). The higher activity of the HCBS2 samples may indicate a smaller exposed area of Boom clay.

Table 3-3: Water content, undrained shear strength and Atterberg limits

GD	WL	W %	C _u Pa	LL %	PL %	PI %	LI
63	GS02 Galgenschor	57.30	1283	51.30	33.00	18.40	1.33
64	PS02 Paardenschoor	58.80	2418	57.70	28.30	29.50	1.04
65	2 Zandvlietsluis	188.20	171	131.20	37.80	93.40	1.61
68	9 Boei 84	109.2	199	75.9	29.7	46.10	1.72
70	12 DGD 4	119.5	737	108.4	33.4	75.00	1.15
71	18 DGD 10	214.6	104	131.60	39.50	92.10	1.90
73	21 DGD 7	109.7	1135	98.1	33.1	65.10	1.18
76	24 DGD opwaarts	91.2	169	61.4	28.4	32.90	1.90
78	31 ingang Kallo 2	154.2	513	124.7	39.6	85.20	1.35
79	33 ingang Kallo 1	116.4	177	80.50	32.40	48.10	1.75

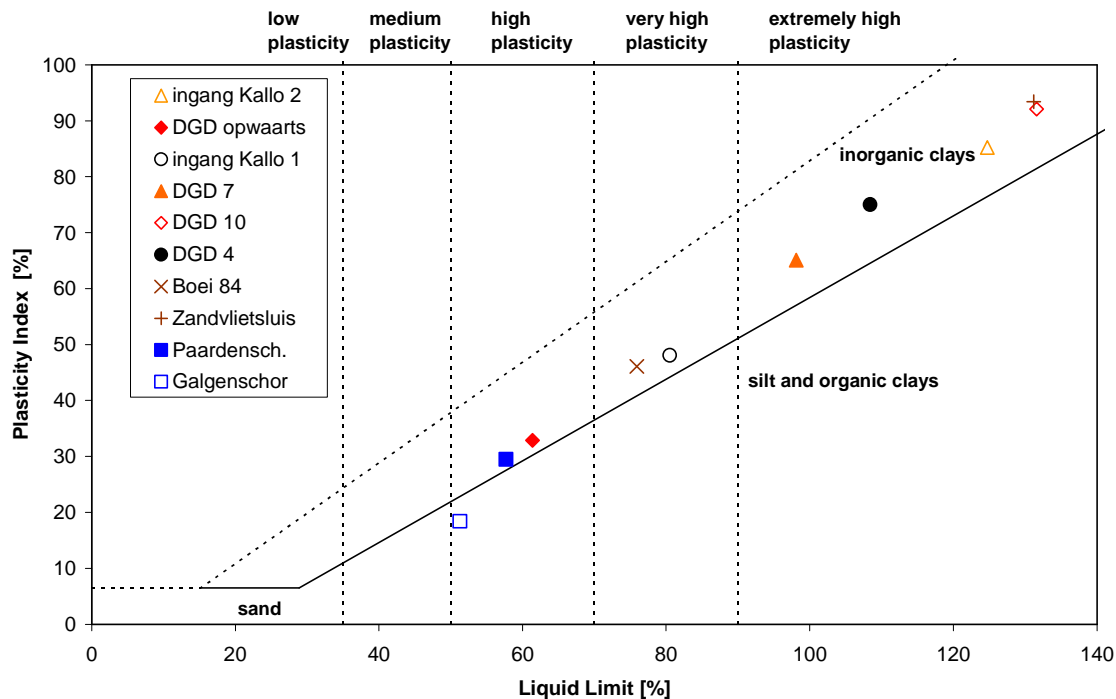


Figure 3.4: Plasticity Index (PI) as a function of liquid Limit (LL) (Plasticity Chart)

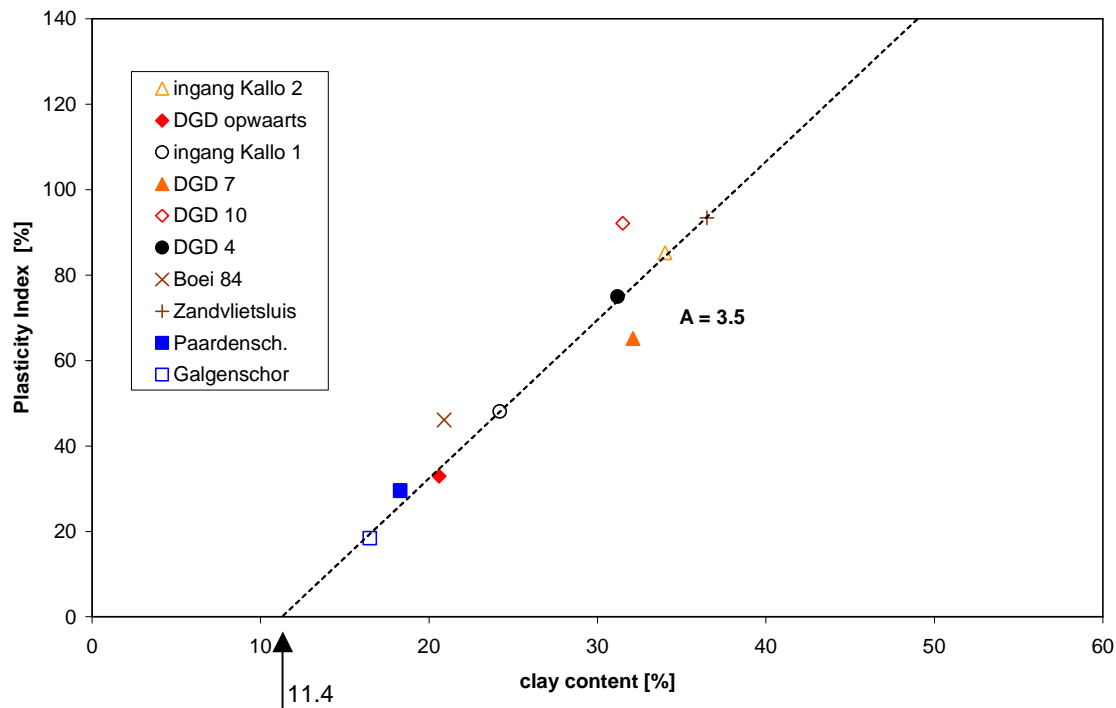


Figure 3.5: Plasticity Index (PI) as a function of clay content ξ (Activity Plot)

Therefore it can be concluded that most of the fines in the cohesive sediments of the lower Sea Scheldt are of marine origin. Verlaan (1998) concluded that about 50% of the sediment is of marine origin. It is recommended to compare the present results with those of Verlaan (1998) in more detail.

In Figure 3.6 and Figure 3.7 the measured organic or humus content and carbonate content is given as function of the clay content. It shows that both are well related to the clay content and therefore cohesive behaviour of the sediments is mainly determined by the clay content and not by the carbonate or organic matter. It is remarkable that the carbonate content is about 5% lower than for the samples analysed in the framework of the HCBS1 campaign. Although a seasonal variation of the carbonate content may be expected, a lower value in summer than in winter seems illogical.

In Figure 3.8 the undrained shear strength is plotted as function of the Liquidity Index (LI), which is a relative water content, defined by:

$$LI = \frac{W - PL}{PI} \quad (35)$$

Most of the cohesive samples are gathered around one line. Fig. 3.5 indicates that the same clay mineral mixture is active in all sediments. Therefore, the undrained shear strength can also be plotted as function of the water content with respect to the clay fraction ξ_{cl} (see Figure 3.9). The data can be fitted by:

$$C_u = a \left[\frac{W}{\xi_{cl}} \right]^b = 1.4 \times 10^8 \left[\frac{W}{\xi_{cl}} \right]^{-2.27} \quad (36)$$

The coefficients in (36) are equal to those determined for the HCBS1 campaign, which demonstrate that the physical properties of the clay fraction remain unchanged.

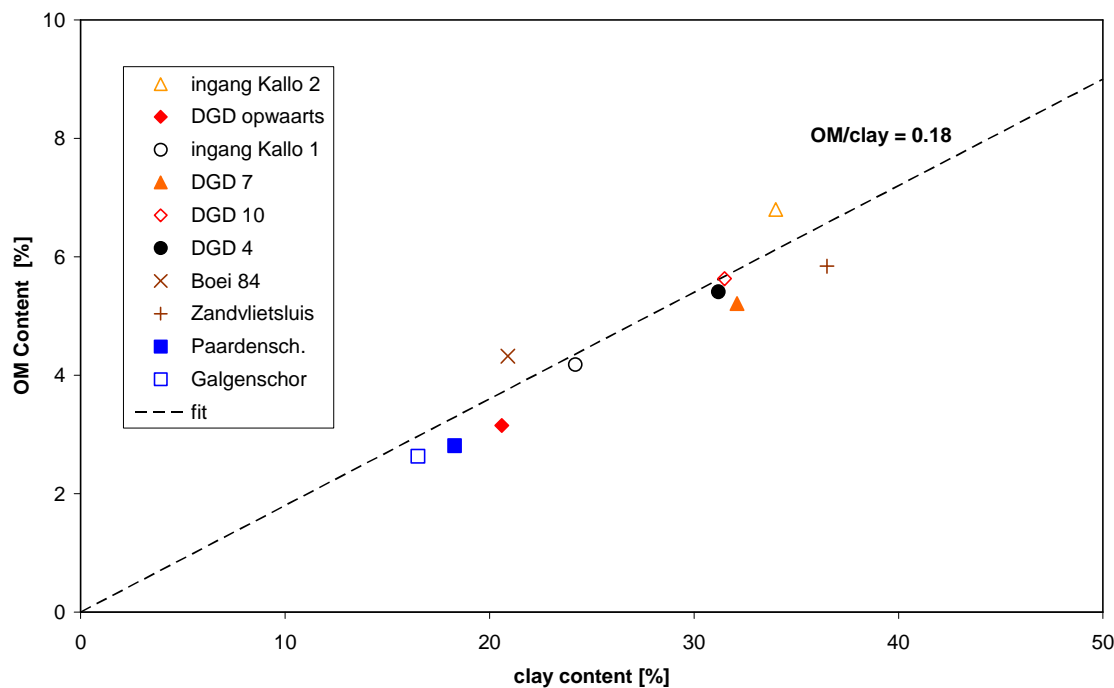


Figure 3.6: Percentage Organic Matter (OM) as a function of clay content ξ .

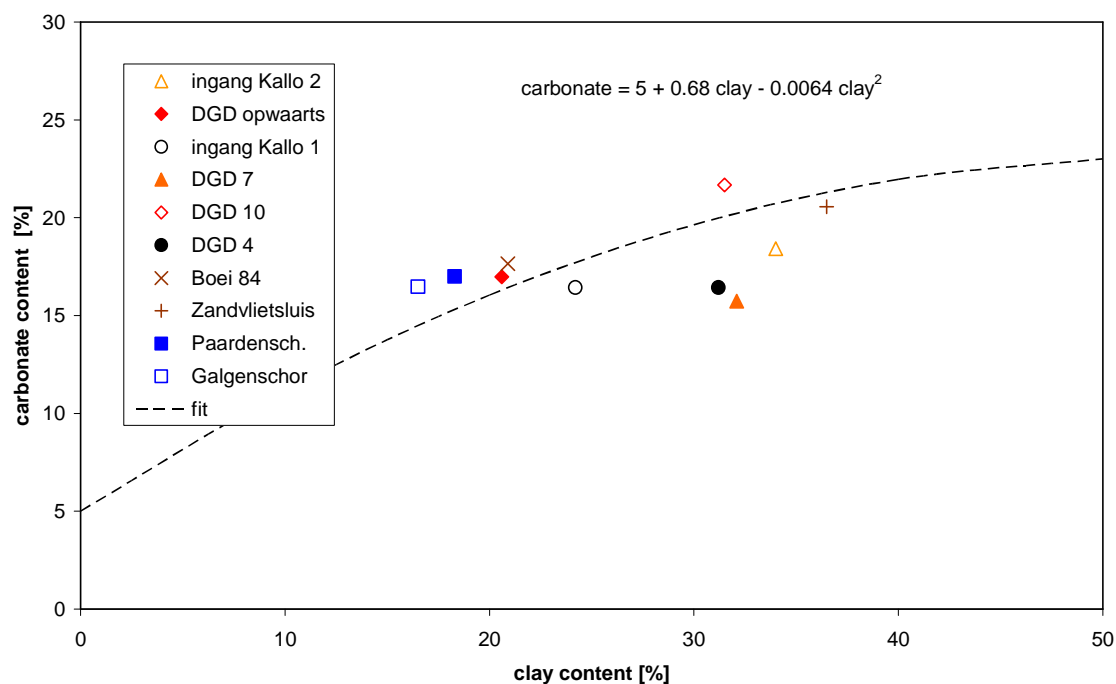


Figure 3.7: Carbonate Content as a function of clay content ξ .

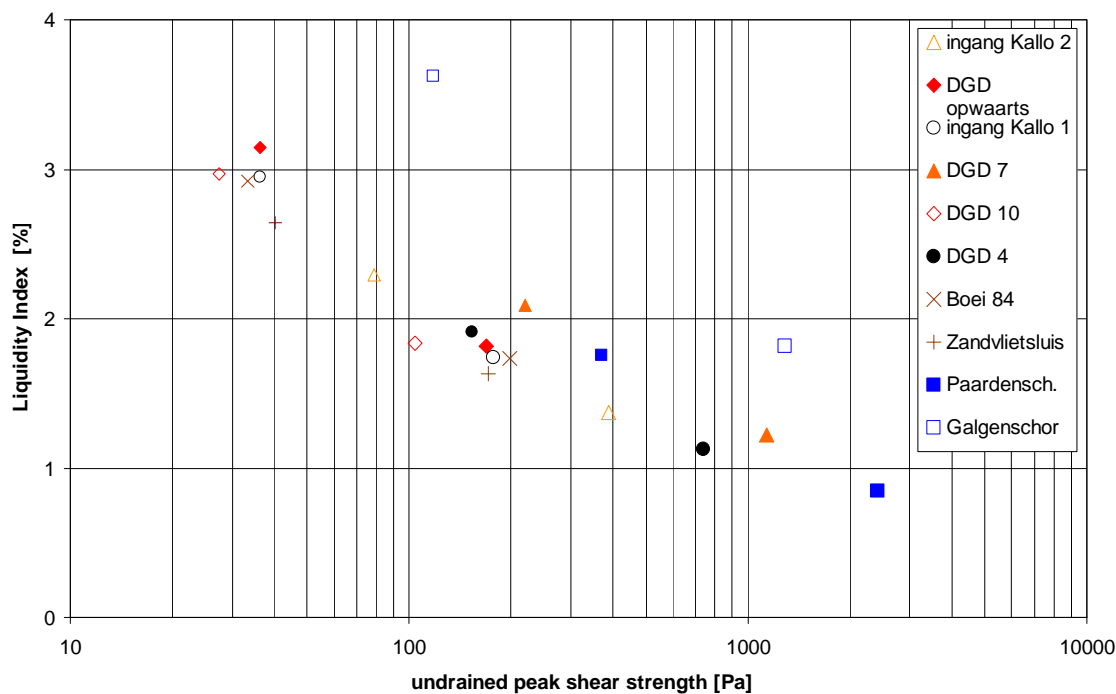


Figure 3.8: Undrained shear strength C_u as a function of Liquidity Index (LI)

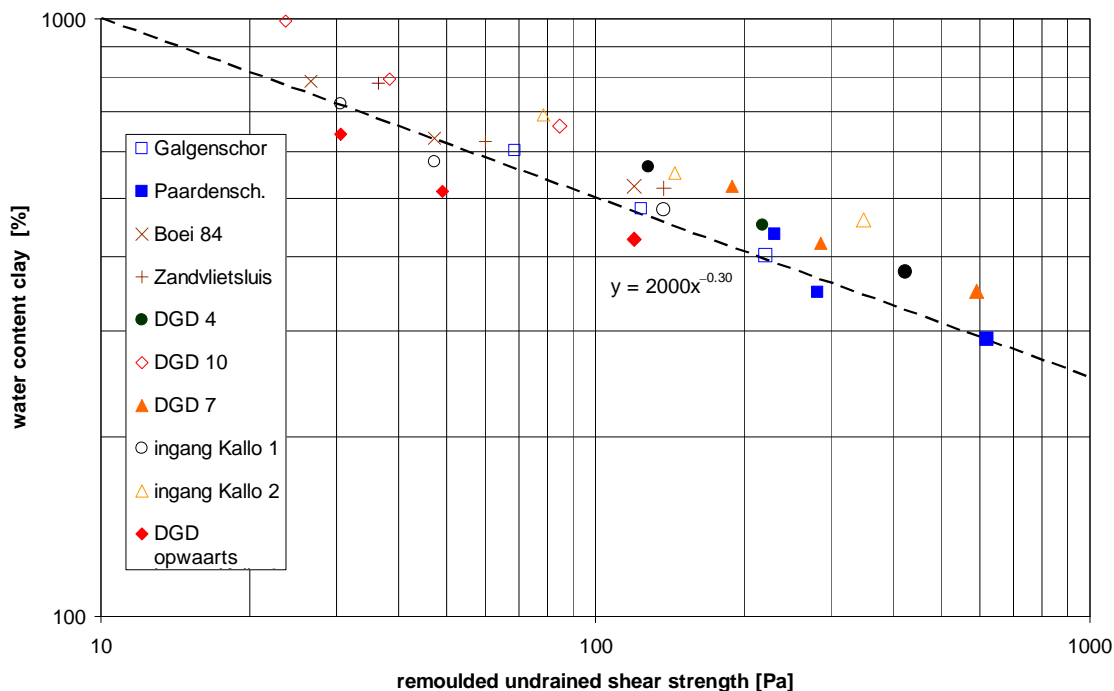


Figure 3.9: Undrained shear strength C_u as a function of clay water content w/n_{cl} .

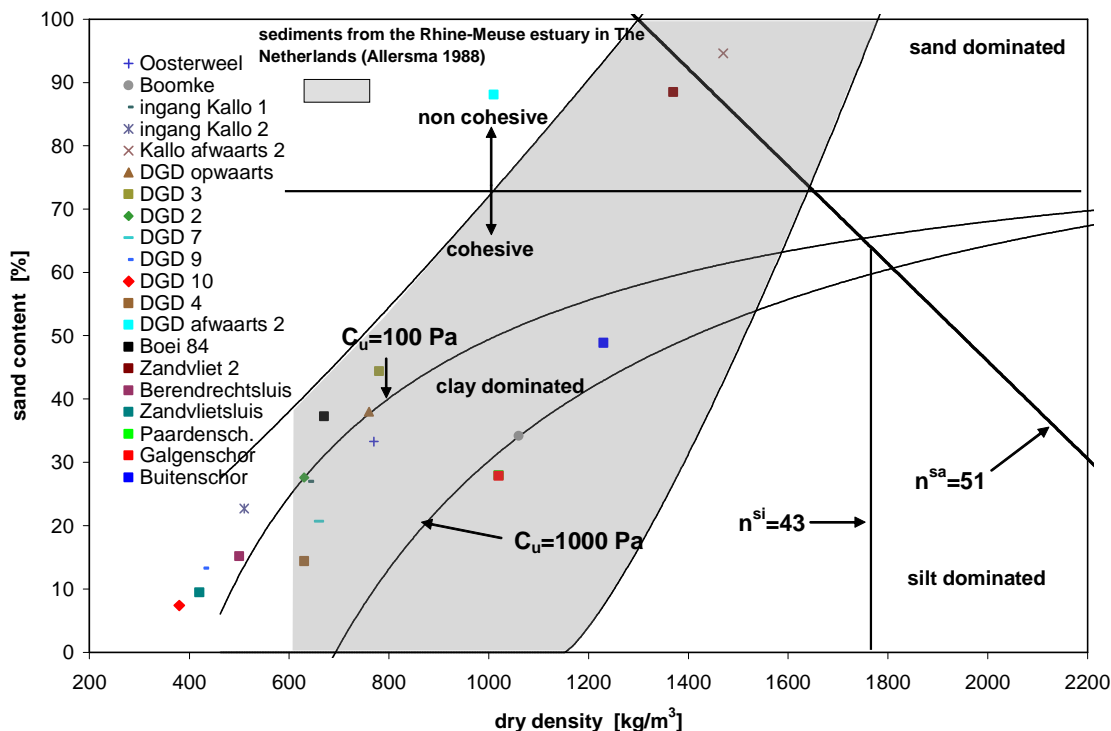


Figure 3.10: Sediment phase diagram for the lower Sea Scheldt

With Equation (36) and the constant ratio between silt and clay of 1.74 (see Figure 3.2 and Figure 3.3) the properties of the cohesive sediment can be given as function of sand content only. This is depicted in Figure 3.10 in the so-called sediment phase diagram for the lower Sea Scheldt, in which the sand content is plotted against the dry density. Most Scheldt samples are cohesive and dominated by a clay skeleton, but some samples are non-cohesive and dominated by a sand skeleton. When the distribution of sand content in the lower Sea Scheldt is known as a function of time, the sediment behaviour (erosion, consolidation, settling) can be determined from the dry density or water content as function of time.

3.3. Zeta potential

The zeta potential of a mud or silt particle determines its sensitivity to flocculation. A high zeta-potential (either negative or positive) results in strong repulsive forces and a stable suspension. A low zeta-potential (close to zero) results in weak repulsive forces and an instable suspension, i.e. the particle may easily flocculate and settle.

In Table 3-4 the measured data are listed for samples suspended in both demineralised water and salt water. Variations in salinity were realised by dilution with 0.1M solutions of NaCl. In Figure 3.11 the measured data are plotted against the activity. The zeta-potential is similar of all samples at equal salinity, which demonstrates that the physical properties of the fine sediment fraction are quite uniform in the sampling area.

Table 3-4: Zeta-potential of mud samples in freshwater (conductivity 0.5 mS/cm) and saltwater (conductivity 7.9 mS/cm at 25 °C).

sample ID	zeta-potential in fresh water (mV)	zeta-potential in salt water (mV)
GS02 Galgenschor	-15.2	-25.3
PS02 Paardenschoor	-16.2	-26.7
2 Zandvlietsluis	-16.2	-25.7
9 Boei 84	-15.5	n.a.
12 DGD 4	-16.1	-26.8
18 DGD 10	-16.1	-32.0
21 DGD 7	-16.3	-26.5
24 DGD opwaarts	-16.1	-26.3
31 ingang Kallo 2	-16.1	-25.2
33 ingang Kallo 1	-16.0	-25.3

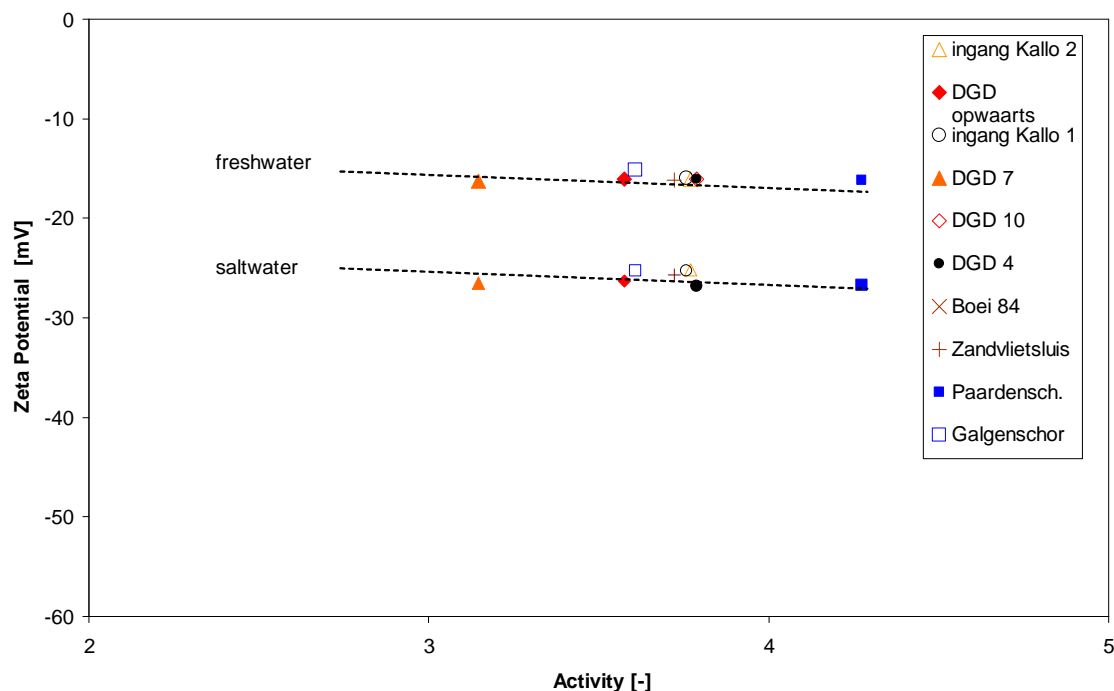


Figure 3.11: Zeta-potential of samples as a function of their activity

3.4. CST tests

The CST test is a test to determine the **Capillary Suction Time** (CST) of a sample. It is a simple test to determine the permeability of a sample at the water content applied. The capillary suction pressure generated by a standard filter paper is used to ‘suck’ water from the sample. The rate at which water permeates through the filter paper varies as a function of the permeability of the sample. The CST is obtained from two electrodes placed at a standard interval from the centre of the instrument (see Figure 3.13). The time necessary for the waterfront to pass between the two electrodes constitutes the CST. As the force generated by capillary suction is much greater than the hydrostatic head within the sample funnel, the CST is independent of the amount of cohesive sediment tested, as long as there is sufficient sediment to generate a CST (Winterwerp and Van Kesteren, 2004).

As the test is simple and little time-consuming, it has been applied to all samples. The theory behind the CST-test is explained in Huisman and Van Kesteren (1998). Results from the CST-test are shown in Table 3-5 and in Figure 3.12.

Table 3-5: Capillary suction time and initial water content of samples

sample ID	water content (%)	CST (s)
GS02 Galgenschor	66.21	545.0
PS02 Paardenschoor	53.26	741.4
2 Zandvlietsluis	189.87	448.2
9 Boei 84	109.81	344.7
12 DGD 4	117.76	995.7
18 DGD 10	208.53	349.3
21 DGD 7	112.54	560.9
24 DGD opwaarts	88.23	417.4
31 ingang Kallo 2	156.54	611.5
33 ingang Kallo 1	116.24	404.7

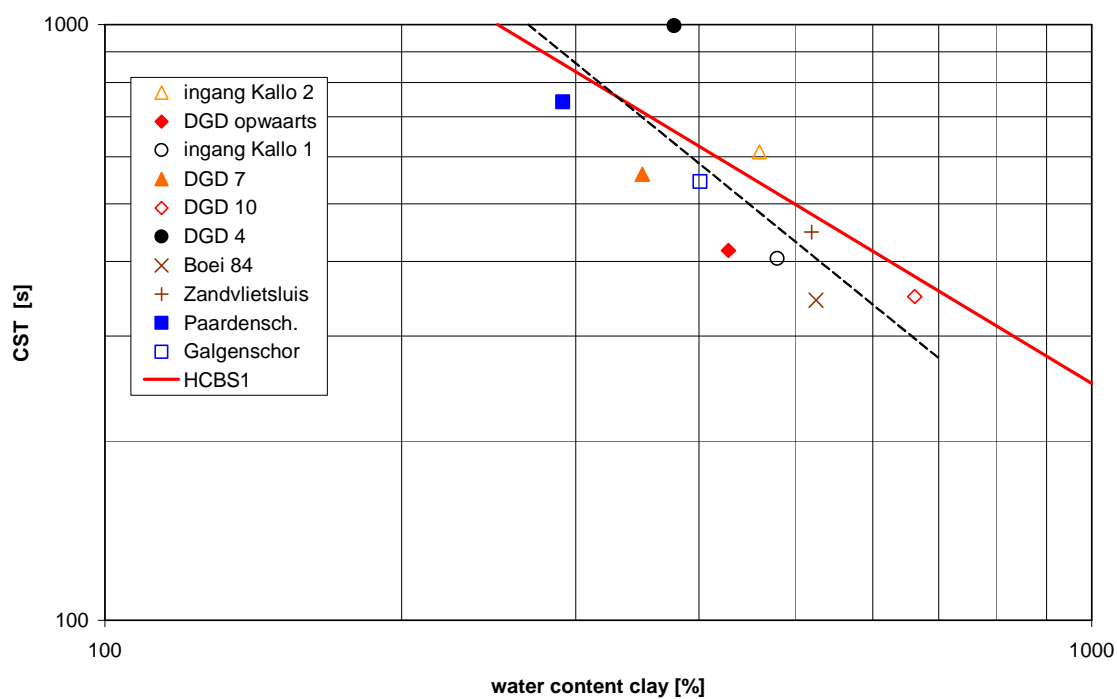


Figure 3.12: Results from CST-tests

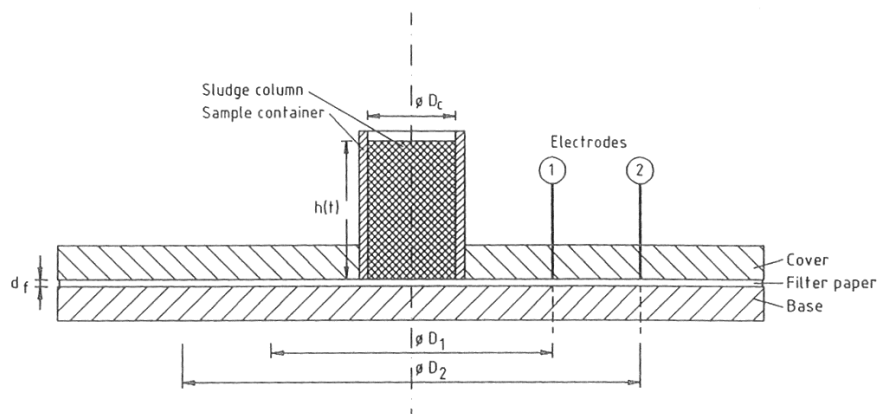


Figure 3.13: Overview of CST-apparatus. $d_f = 1.10 \times 10^{-3} \text{ m}$, $D_c = 0.018 \text{ m}$; $D_1 = 0.032 \text{ m}$; $D_2 = 0.045 \text{ m}$.

3.5. Consolidation tests

The consolidation tests were carried out according to the procedure proposed by Merckelbach (2000). The tests were carried out on 10 samples using 10 perspex columns with inner diameter 0.12 m and height 1 m.

The experimental procedure was as follows. All samples were diluted with Scheldt water to a concentration of about 30 g/L (water content of about 33). The samples were poured into the columns, after which sedimentation and subsequently consolidation started. The interface between the mud suspension and the clear water was continuously monitored with a digital multiple-camera imaging system derived from the ARGUS system (www.wldelft.nl/argus). At the start of the experiments the image capture frequency was set at 0.2 Hz. The capture frequency was decreased exponentially during the column tests, as also the velocity at which the interface lowers decreased exponentially. The exponential decrease in sampling frequency was chosen such that the total consolidation experiment was captured with 2000 images. The height of the interface as a function of time was detected automatically from these images using customised image processing software.

According to Merckelbach (2000), the settlement of the interface $h(t)$ may be expressed as:

$$h(t) = \left(\zeta \frac{2-n}{1-n} \right)^{\frac{1-n}{2-n}} \left(K_K \frac{\rho_s - \rho_w}{\rho_w} (n-2) \right)^{\frac{1}{2-n}} t^{\frac{1}{2-n}}, \quad (39)$$

where ζ is the material height (m), K_K the permeability parameter and $n = 2/(3-D)$, where D is the fractal dimension. The fractal dimension D can therefore easily be determined from the slope R of the settlement curve versus time on a double logarithmic scale: $R = 1/(2-n) = (3-D)/(4-2D)$. Subsequently, K_K is found by substitution of the interface height and corresponding time. The parameter K_K is used in the following expression for the permeability k :

$$k = K_K \phi^{\frac{2}{3-D}}, \quad (40)$$

where ϕ is the sediment volume fraction.

Note that expression (39) is only valid for $t_1 < t < t_2$, where t_1 is the time that the interface between clear water and mud suspension meets the interface between mud suspension and mud bed. At t

= t_1 , the entire suspension has reached the gelling point and a single discontinuity remains. At $t = t_2$, effective stress starts to become important and (39) is not valid anymore.

The effective stress parameter K_σ can be determined from the final density profile after consolidation according to:

$$h - z = 2 \frac{K_\sigma}{(D-1)(\rho_s - \rho_w)g} \phi^{\frac{D-1}{3-D}}, \quad (41)$$

By plotting the particle volume fraction ϕ , obtained from a measured density profile in the final stage of consolidation, versus the distance below the interface on double logarithmic scales, the fractal dimension can be derived directly from the slope R of the plot: $R = (D-1)/(3-D)$. Subsequently, the parameter K_σ is obtained by substitution of ϕ and corresponding z .

The parameter K_σ is used in the following expression for the effective stress $\sigma_v' = \sigma_{\text{eff}}$:

$$\sigma_v' = K_\sigma \phi^{\frac{2}{3-D}} \quad (42)$$

The final density profile was measured with a conductivity probe, assuming an inverse linear relationship between sediment concentration C and conductivity K :

$$C = A / K$$

The calibration factor A was derived from the known material height in the columns. Concluding, all parameters of the material functions between effective stress and particle volume fraction and permeability and particle volume fraction can be determined from a single settling test.

The settlement curves and final density profiles are shown in Appendix B. The resulting values for D , K_κ and K_σ are shown in Table 3-6, including data such as initial height h , water content w and material height ζ .



Figure 3.14: Example of image captured with CANON digital SLR (3888 x 2592) to determine interface settlement. Column height = 1 m; ruler length = 0.20 m; distance between two ruler ticks = 0.01 m.

Table 3-6: Results from consolidation tests

Sample ID	h (m)	w (-)	ζ (m)	D (-)	K_K ($\times 10^{-10}$ m/s)	K_σ ($\times 10^3$ Pa)	c_v ($\times 10^{-9}$ m ² /s)
GS02 Galgenschor	0.94	38.38	0.00934	2.63	0.37	0.657	0.033
PS02 Paardenschoor	0.934	41.61	0.00857	2.63	0.19	1.29	0.0347
2 Zandvlietsluis	0.947	19.74	0.0181	2.65	0.019	224	0.68
9 Boei 84	0.947	42.57	0.00850	2.44	25.	13.7	3.23
12 DGD 4	.945	21.22	0.0169	2.63	0.070	53.3	0.665
18 DGD 10	0.952	24.08	0.0150	2.62	0.057	34.2	0.564
21 DGD 7	0.958	23.76	0.0153	2.63	0.062	279	1.79
24 DGD opwaarts	0.948	20.63	0.0174	2.45	100.	13.2	42.2
31 ingang Kallo 2	0.935	24.98	0.0142	2.64	0.026	73.3	0.504
33 ingang Kallo 1	0.943	27.48	0.0130	2.45	38	45.1	8.93

4. CONCLUSIONS AND APPLICATION METHOD

4.1. Conclusions

The sample analysis demonstrates that all samples contain a silt and clay fraction with comparable properties. This implies that although the sample properties are highly variable, these variations can be attributed to variations in water content and sand fraction only. This makes numerical modelling of sediment exchange between the water column and the bed relatively straightforward if the spatial distribution of the water content and the sand fraction of the river bed is known. Most sample properties of the HCBS2 campaign are similar to those of the HCBS1 campaign taken at the same location, which suggests that the temporal variability of the sediment composition and properties is limited in the Lower Sea Scheldt. Only the carbonate content showed a significant decrease, and the sample 35 Boomke showed a much higher sand content and much lower silt/clay ratio than the sample taken at the same position during the HCBS2 campaign. This may be caused by the (partial) coverage of the Boom clay layers, which also explains the observed minor increase in activity.

In the next section it is explained how properties such as the critical shear stress for erosion and the erosion constant can be calculated from the water content and the sand fraction of the soil.

4.2. Application of results to numerical modelling

In numerical models, the Partheniades-Krone formulation is often used to calculate the (surface) erosion of sediment:

$$E = M_E (\tau_b - \tau_{crit}) \quad (43)$$

where E is the erosion rate in kg/m²/s. If the critical shear stress for erosion τ_{crit} (Pa) and the erosion constant M_E (s/m) are known, the erosion rate at the actual bed shear stress τ_b can be evaluated.

The critical shear stress for erosion is calculated according to the following procedure:

1. From the sand fraction, calculate the clay fraction according to $n_{clay} = 1 - n_{sand} / (1 + 1.74)$. This expression follows from $n_{clay} + n_{silt} + n_{sand} = 1$ and $\xi_{silt} / \xi_{clay} = 1.74$, as the ratio between the silt and clay fraction is nearly constant for River Scheldt sediment (see Figure 3.2).
2. Calculate the Plasticity Index PI according to $PI = A (\xi_{clay} - \xi_0)$ with $A = 3.5$ and $\xi_0 = 11.4 \%$. This expression is based on the Activity Plot (Figure 3.5). $\xi_{clay} = 100 n_{clay}$.
3. The critical shear stress for erosion can be calculated from the Plasticity Index PI according to (Smearnon and Beasley, 1959): $\tau_{crit} = 0.163PI^{0.84}$ (44)

The erosion parameter M_E is calculated from the basic soil properties according to (Winterwerp and Van Kesteren, 2004):

$$M_E = \frac{c_v \phi_s \rho_{dry}}{10 D_{50} c_u} \quad (45)$$

where c_v is the consolidation coefficient (m²/s), ϕ_s the initial sediment volume concentration (-), ρ_{dry} is the dry density (kg/m³), D_{50} is the median grain size and c_u the undrained shear strength.

The parameters ϕ_s , ρ_{dry} and D_{50} follow directly from sample analysis. The undrained shear strength is directly related to the clay fraction and the water content, see Eq. (36): $c_u = a [W/n_{clay}]^b$. Note that mass erosion may occur if $\frac{1}{2}\rho U^2 > (2 \text{ to } 5)c_u$, which is a much faster process than surface erosion.

The consolidation coefficient c_v can be computed from the permeability and effective stress as function of the void ratio (Eqs. 37 and 38) with:

$$c_v = -\frac{k(1+e)}{\rho_w g} \frac{d\sigma'}{de} = -\frac{1}{\rho_w g} \frac{(1+e)}{e} \frac{C}{B} A^{-1/2} = \frac{2}{3-D} \frac{K_\sigma K_K (1+e)}{\rho_w g e} \quad (46)$$

in which e is the void ratio.

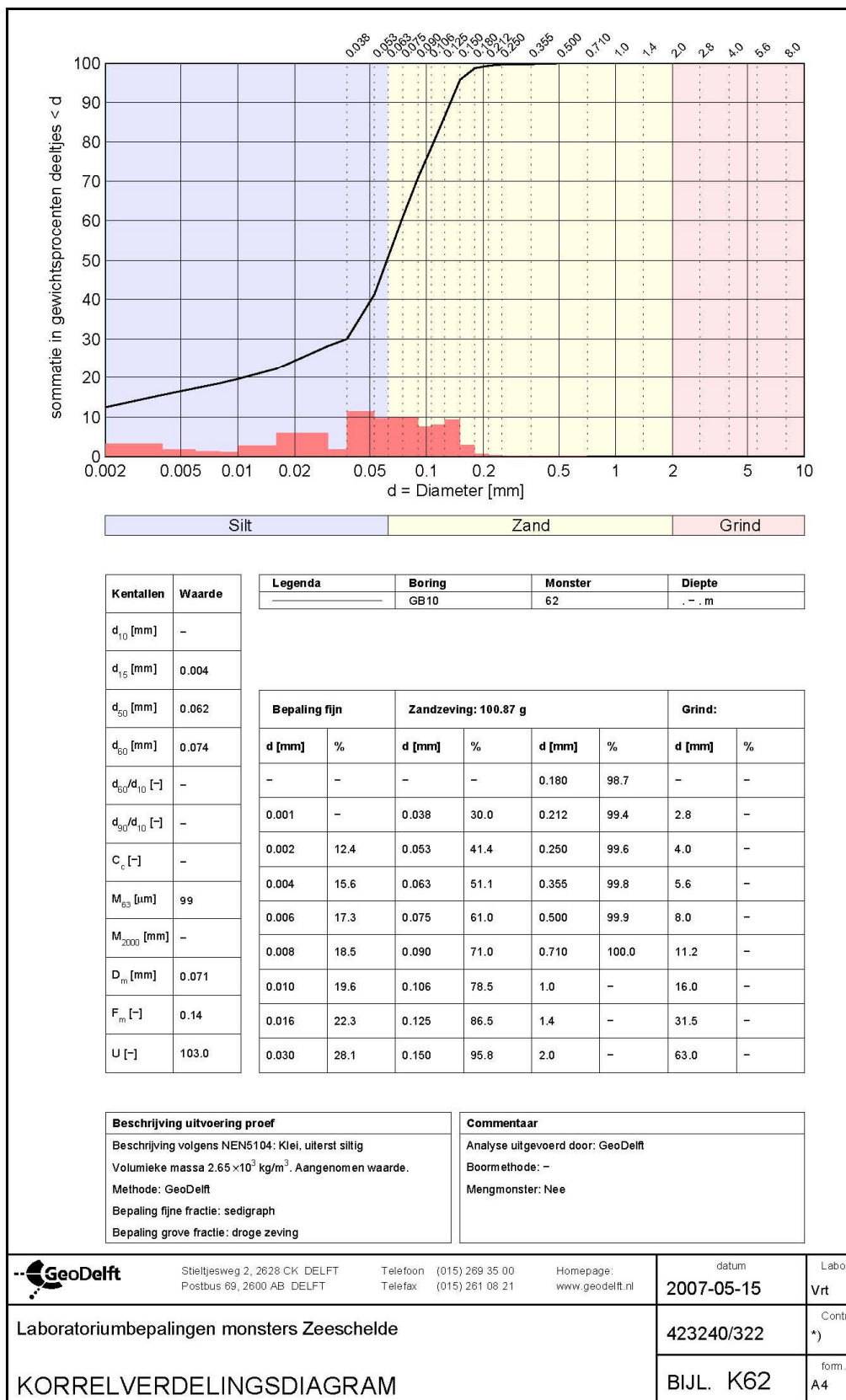
Table 4-1: Erosion parameters determined from sediment analysis.

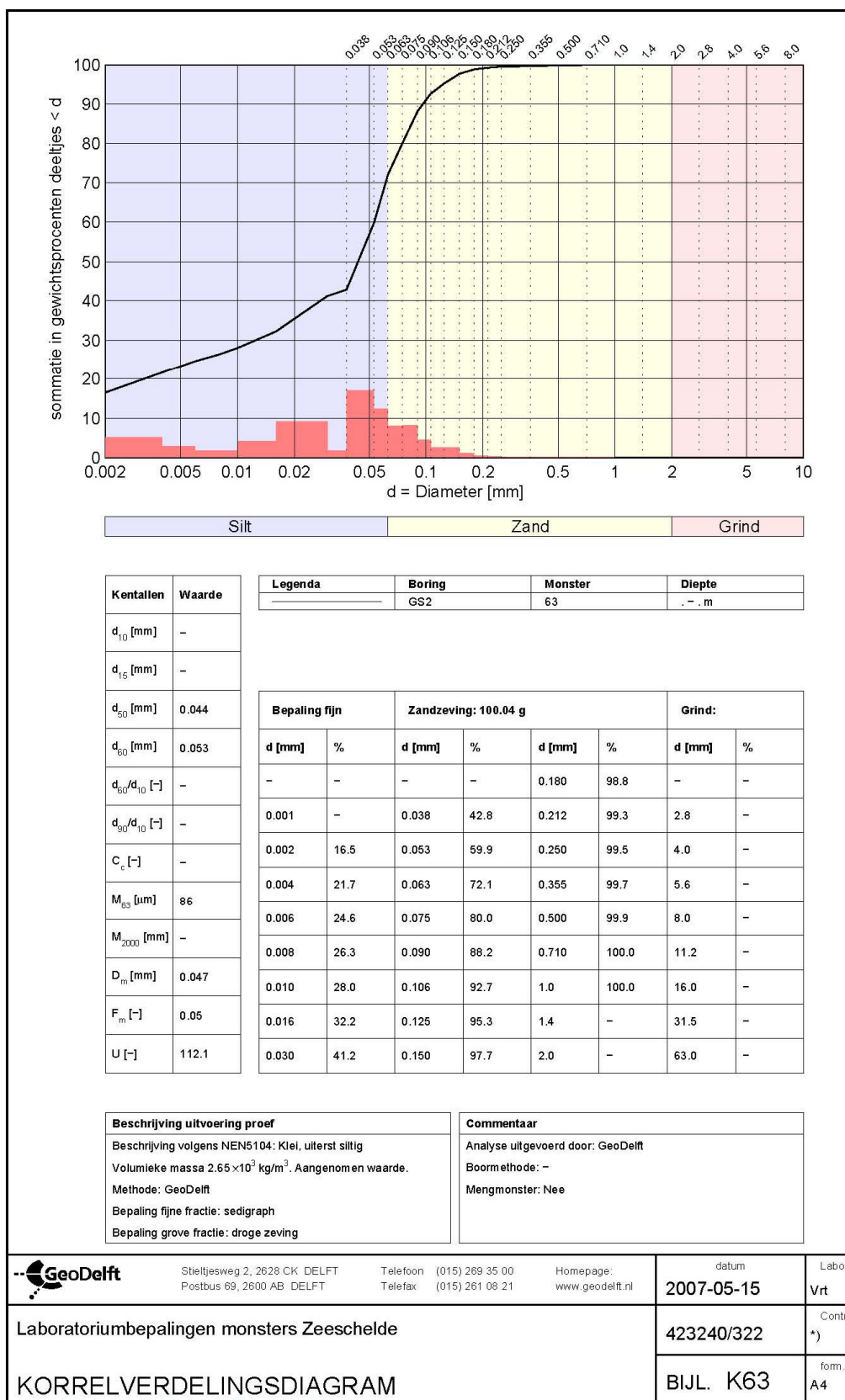
sample ID	τ_{crit} (Pa)	ϕ_s (-)	ρ_{dry} (kg/m ³)	D_{50} (μ m)	c_u (Pa)	e (-)	c_v $\times 10^{-9}$ (m ² /s)	M_E $\times 10^{-6}$ (s/m)
GS02 Galgenschor	3.1	0.402	1,020	44	1283	1.49	0.0330	0.0239
PS02 Paardenschoor	2.7	0.395	1,020	42	2418	1.53	0.0347	0.0138
2 Zandvlietsluis	3.4	0.170	420	4	171	4.89	0.680	7.08
9 Boei 84	2.8	0.260	670	44	199	2.84	3.23	6.45
12 DGD 4	3.1	0.243	630	7	737	3.11	0.666	1.98
18 DGD 10	3.6	0.152	380	5	104	5.58	0.564	6.26
21 DGD 7	3.1	0.260	660	9	1135	2.85	1.79	2.99
24 DGD opwaarts	2.7	0.297	760	50	169	2.37	42.2	112.5
31 ingang Kallo 2	3.6	0.200	510	6	513	4.01	0.504	1.67
33 ingang Kallo 1	3.0	0.248	640	27	177	3.03	8.93	29.7

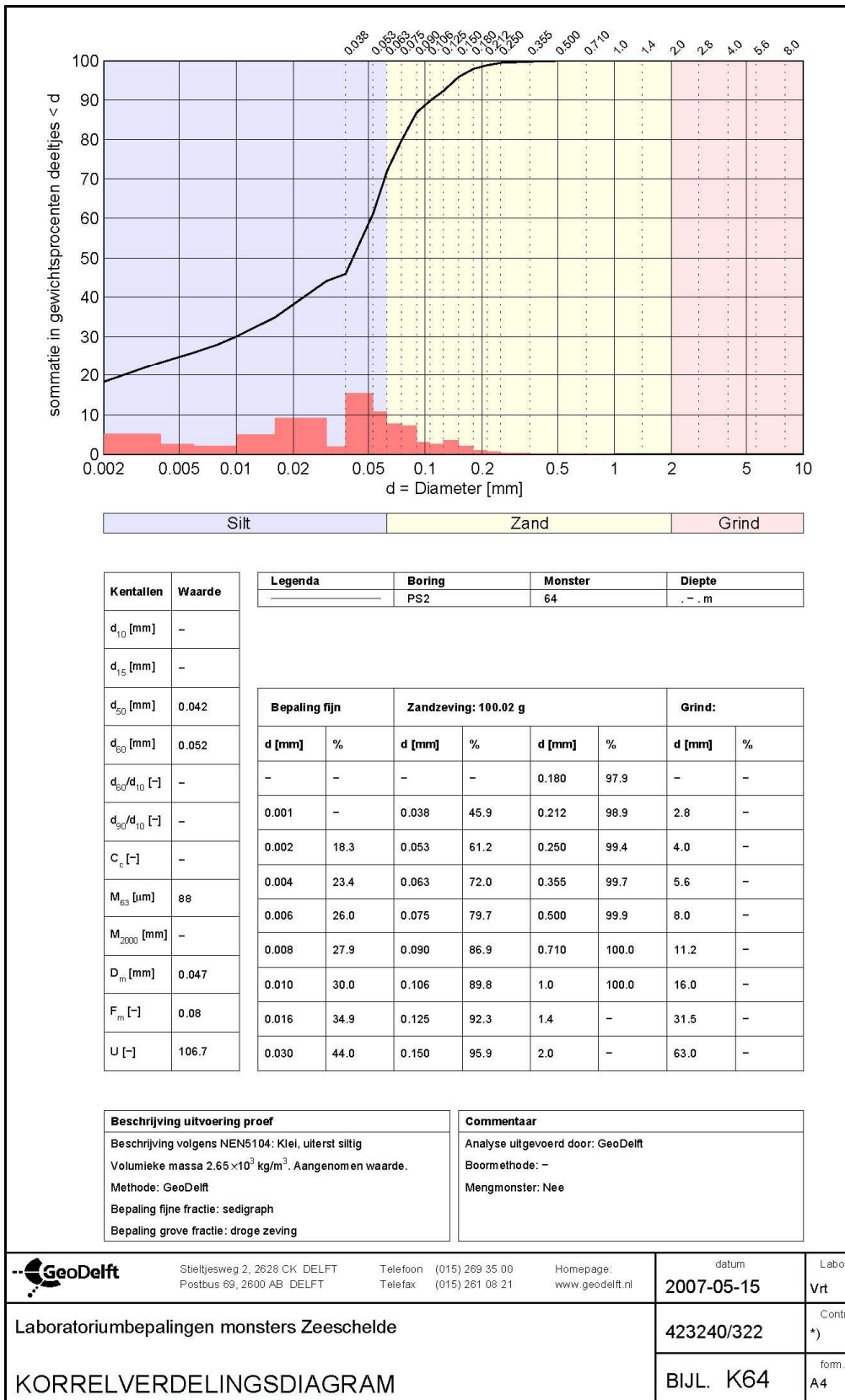
5. REFERENCES

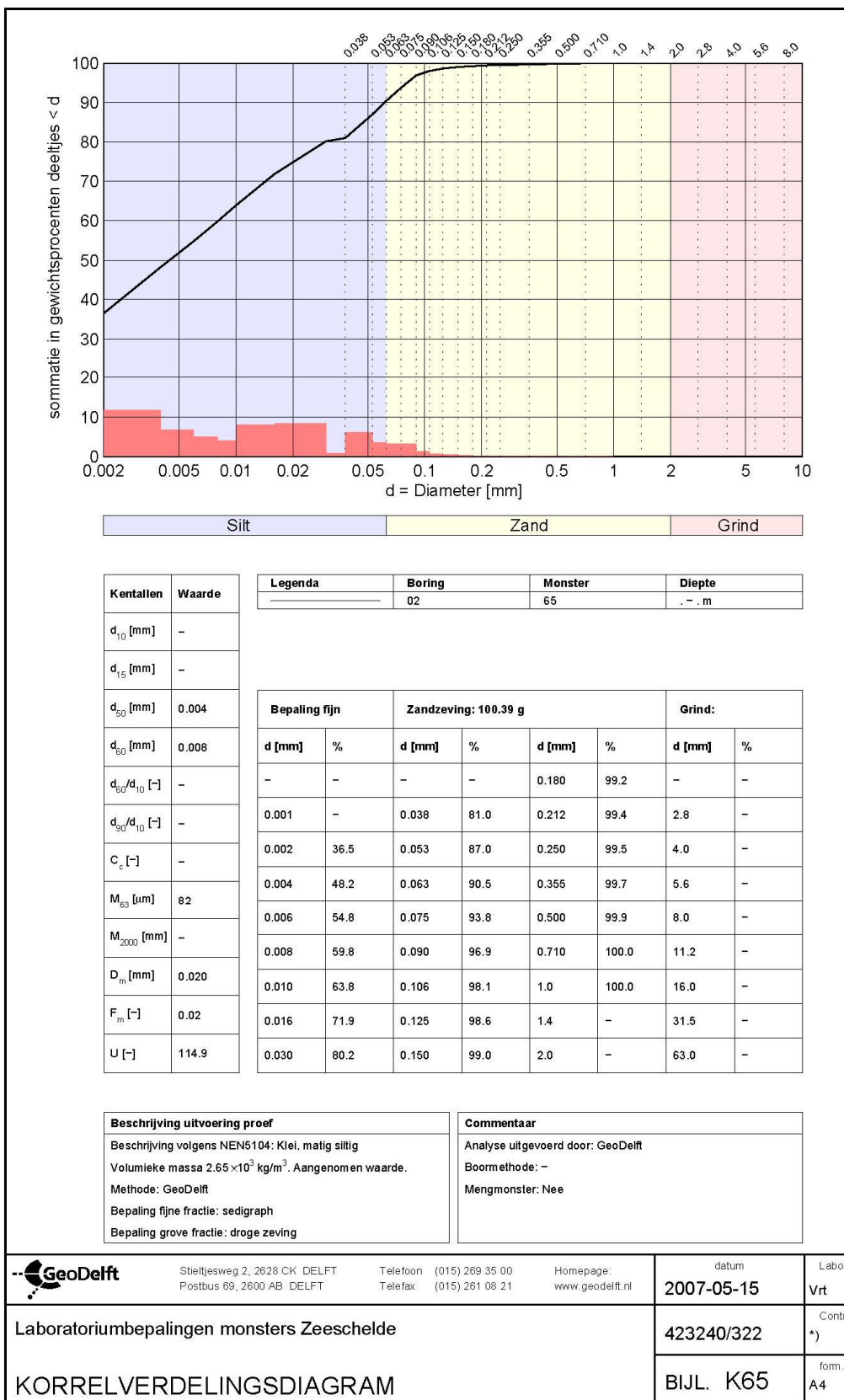
- Huisman, M. and W.G.M. van Kesteren (1998). Consolidation theory applied to the capillary suction time (CST) apparatus. *Wat. Sci. Tech.* Vol. 37, No. 6-7, pp. 117-124.
- Hunter, R.J. (1991). Measuring zeta-potential in concentrated industrial slurries. *Colloids and Surfaces A.* 195, pp. 205–214.
- IMDC-IN, (1998). Containerdok West, Hydraulic-sedimentological investigations. Report 4: In situ measurements of the erodibility of mud from the river Scheldt, I/RA/11128/98.005/WFE (in Dutch).
- IMDC (2005). Uitbreiding studie densiteitsstromingen in de Beneden Zeeschelde in het kader van LTV Meetcampagne naar hooggeconcentreerde slibsuspensies Deelrapport 4: Cohesive sediment properties february 2005, I/RA/11265/05.017/MSA, in opdracht van AWZ.
- Lubking, P.A. (1982). Begeleidende proeven op klei; snijproevenprogramma's X, XI en XII (1979-1981). *GeoDelft report no. CO256440 (Bagt 338).*
- Merckelbach, L.M., (2000), Consolidation and strength evolution of soft mud layers, PhD-thesis, Delft University of Technology; also: Delft University of technology, Faculty of Civil Engineering and Geosciences, Communications on Hydraulic and Geotechnical Engineering, Report 00-2, ISSN 0169-6548.
- Merckelbach, L.M. and Kranenburg, C., (2004), "Determining effective stress and permeability equations for soft mud from simple laboratory experiments", *Géotechnique*, Vol 54, No 9, pp 581-591.
- Smerdon, E.T., Beasley, R.P., (1959), The tractive force applied to stability of open channels in cohesive soils, University of Missouri, Research Bulletin 715.
- Van Kesteren, W.G.M. (2002). Analysis of the characteristics of mud from the outer harbour of IJmuiden. *WL | Delft Hydraulics report no. Z3252 (in Dutch).*
- Verlaan, P.A.J. (1998). Mixing of marine and fluvial particles in the Scheldt estuary. Ph.D. thesis Delft University of Technology.
- Winterwerp J.C, R.E Uittenbogaard and Z.B. Wang, (2006) New developments in the mud transport module of Delft3D; implementation of new functionalities, Delft Hydraulics Report Z3824, in preparation
- Winterwerp, J.C. and W.G.M. van Kesteren (2004). Introduction to the physics of cohesive sediment in the marine environment. *Developments in Sedimentology* 56. Elsevier, Amsterdam.
- Youd, T.L. (1973). Factors controlling maximum and minimum densities of sand. *ASTM Special Technical Publications*, no. 523, pp. 98-112.

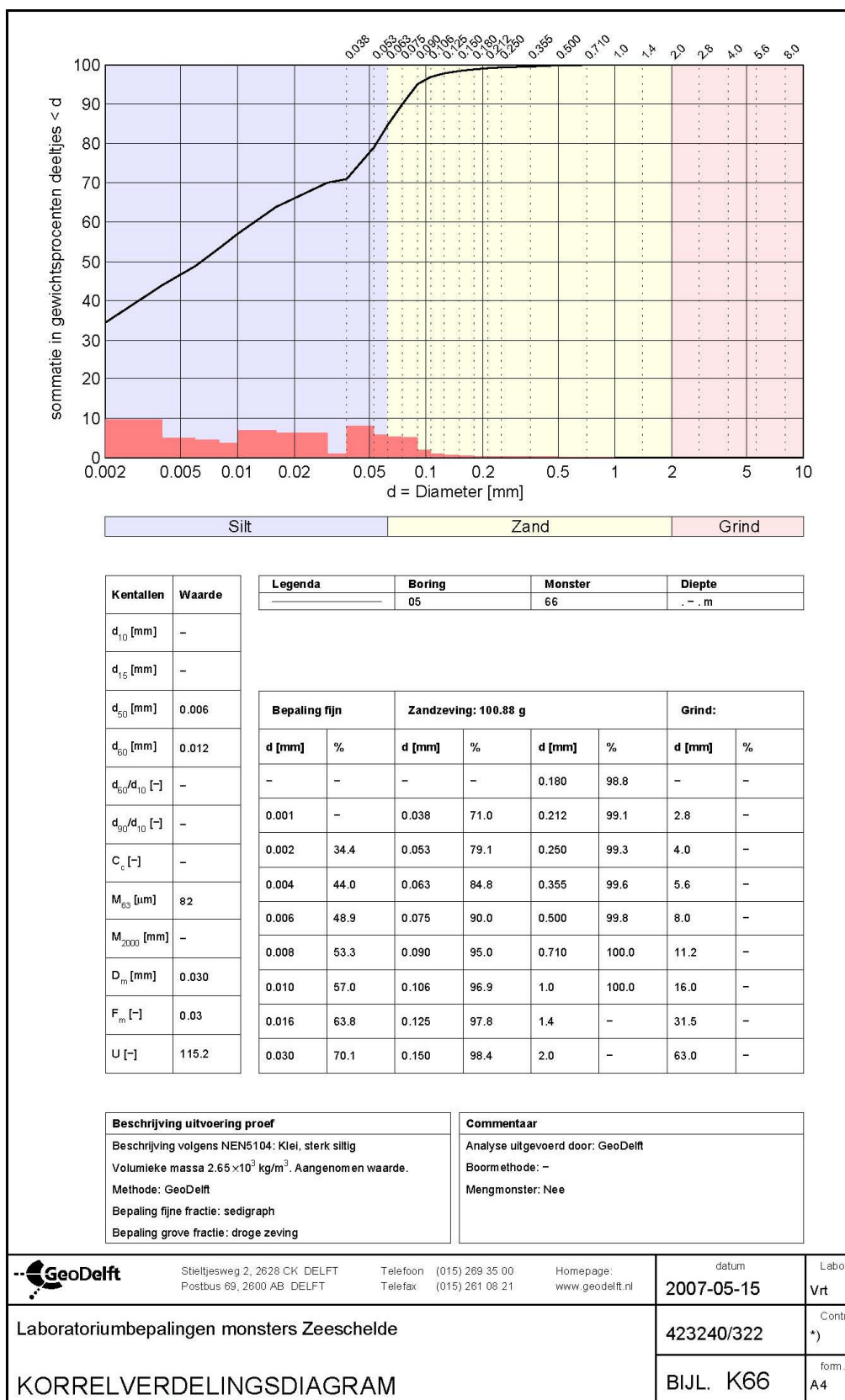
ANNEX A. GRAIN SIZE DISTRIBUTIONS

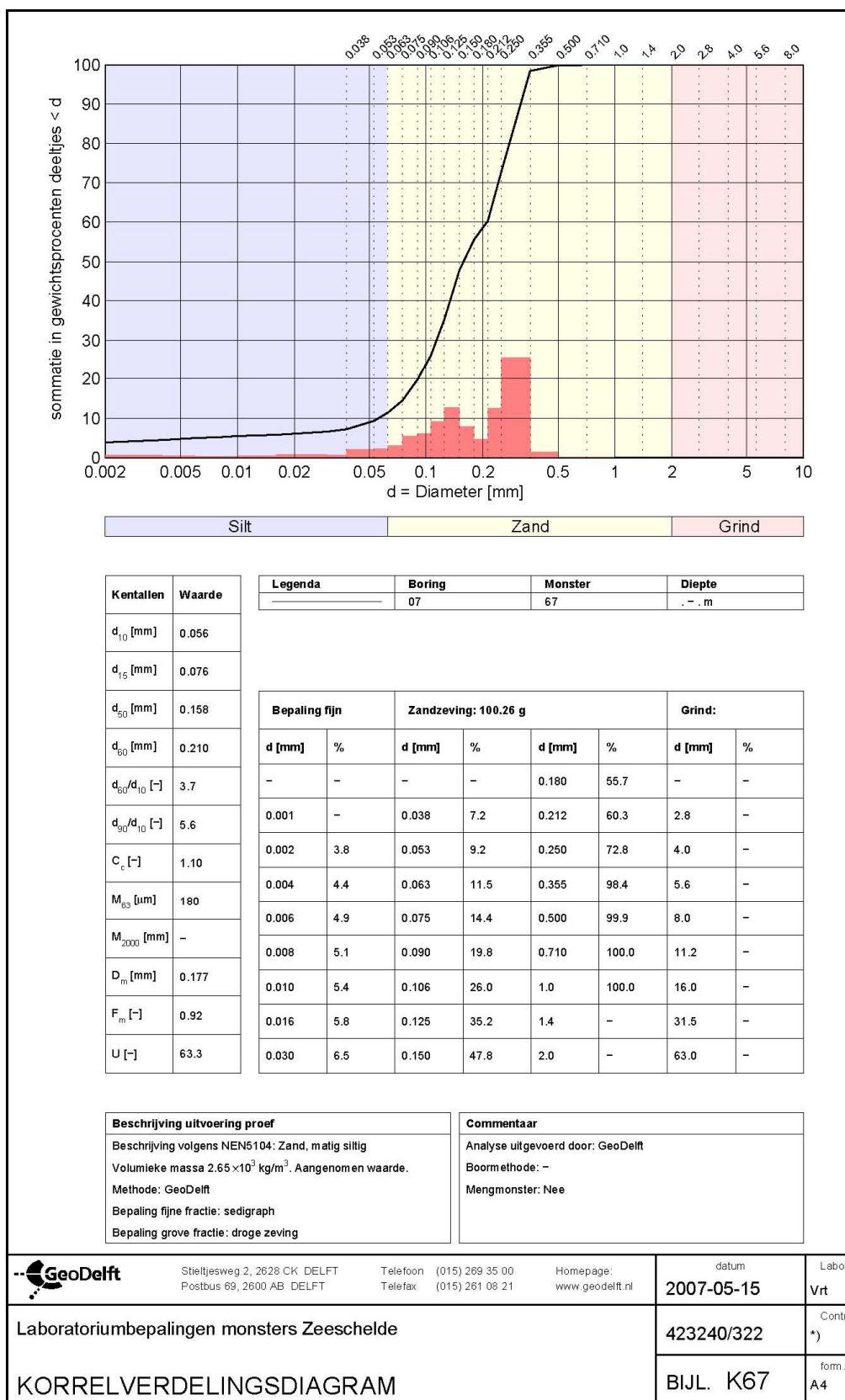


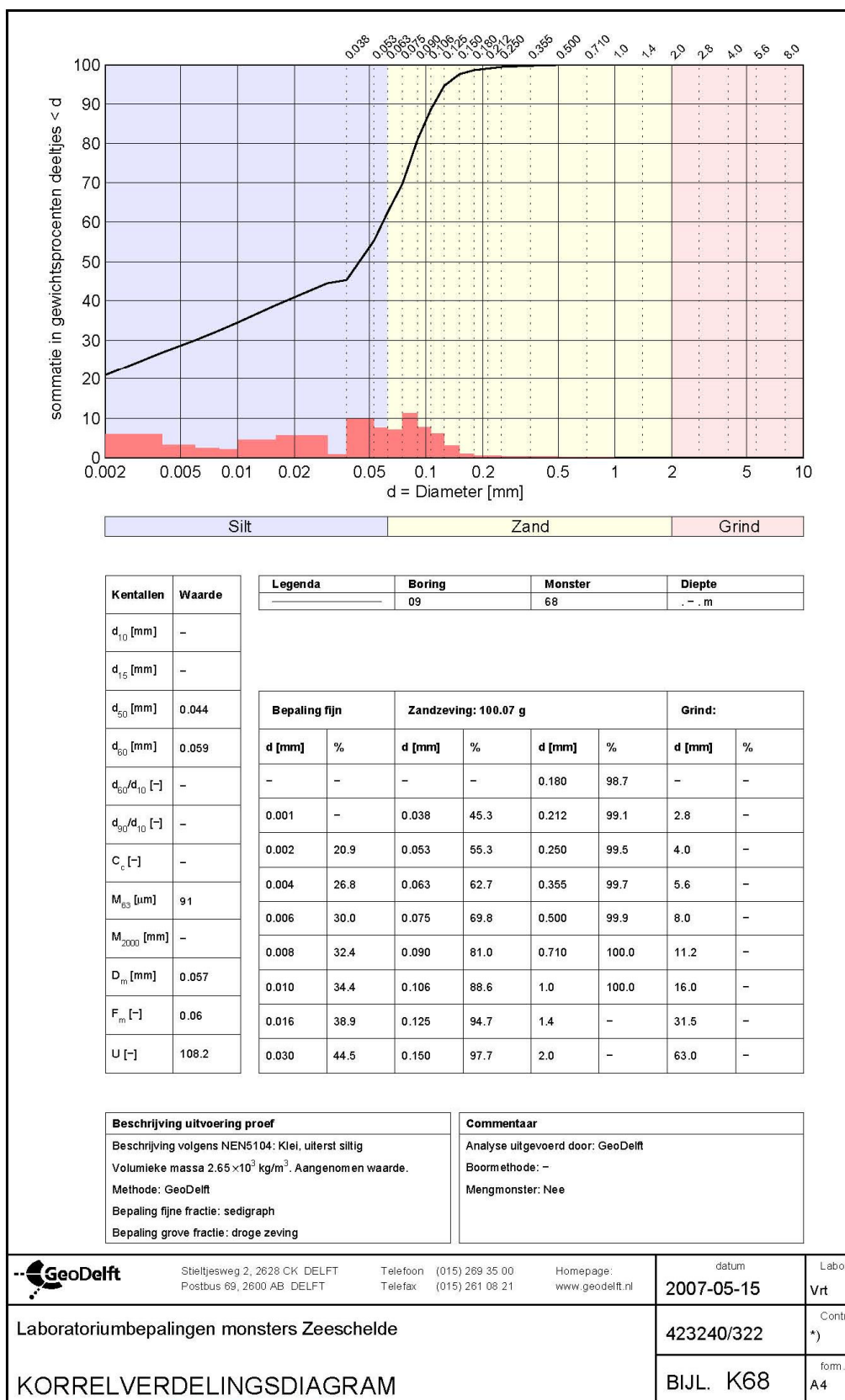


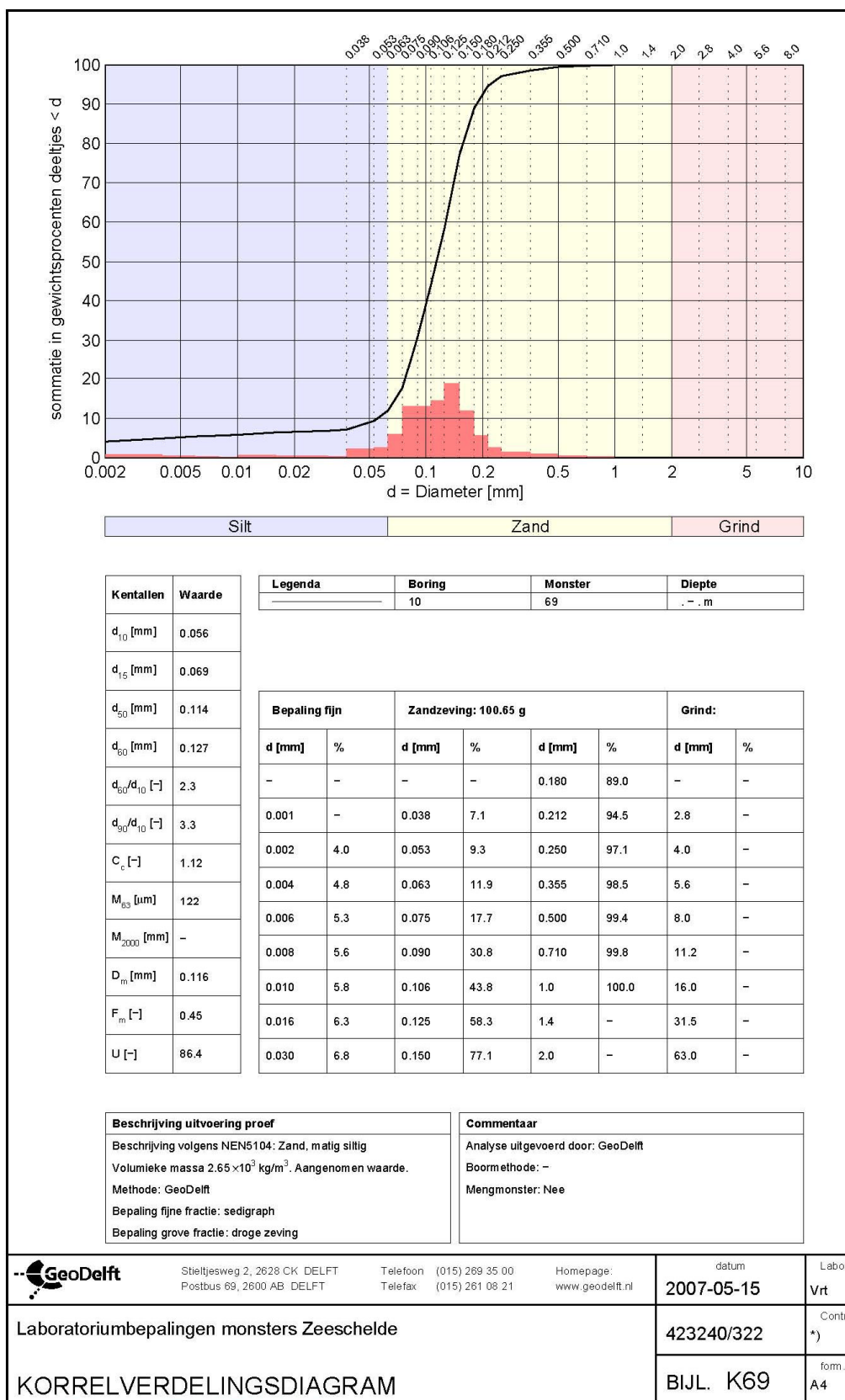


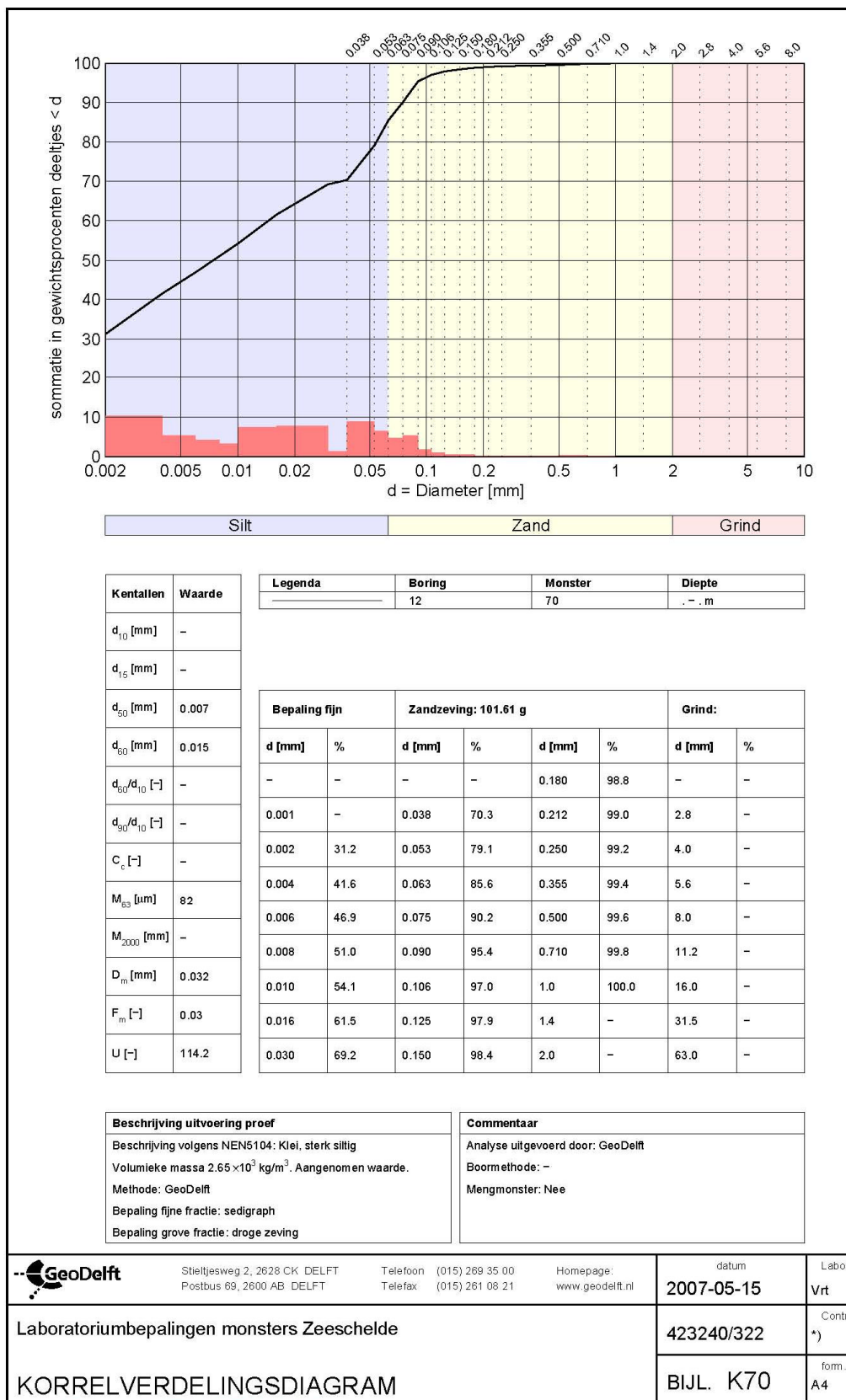


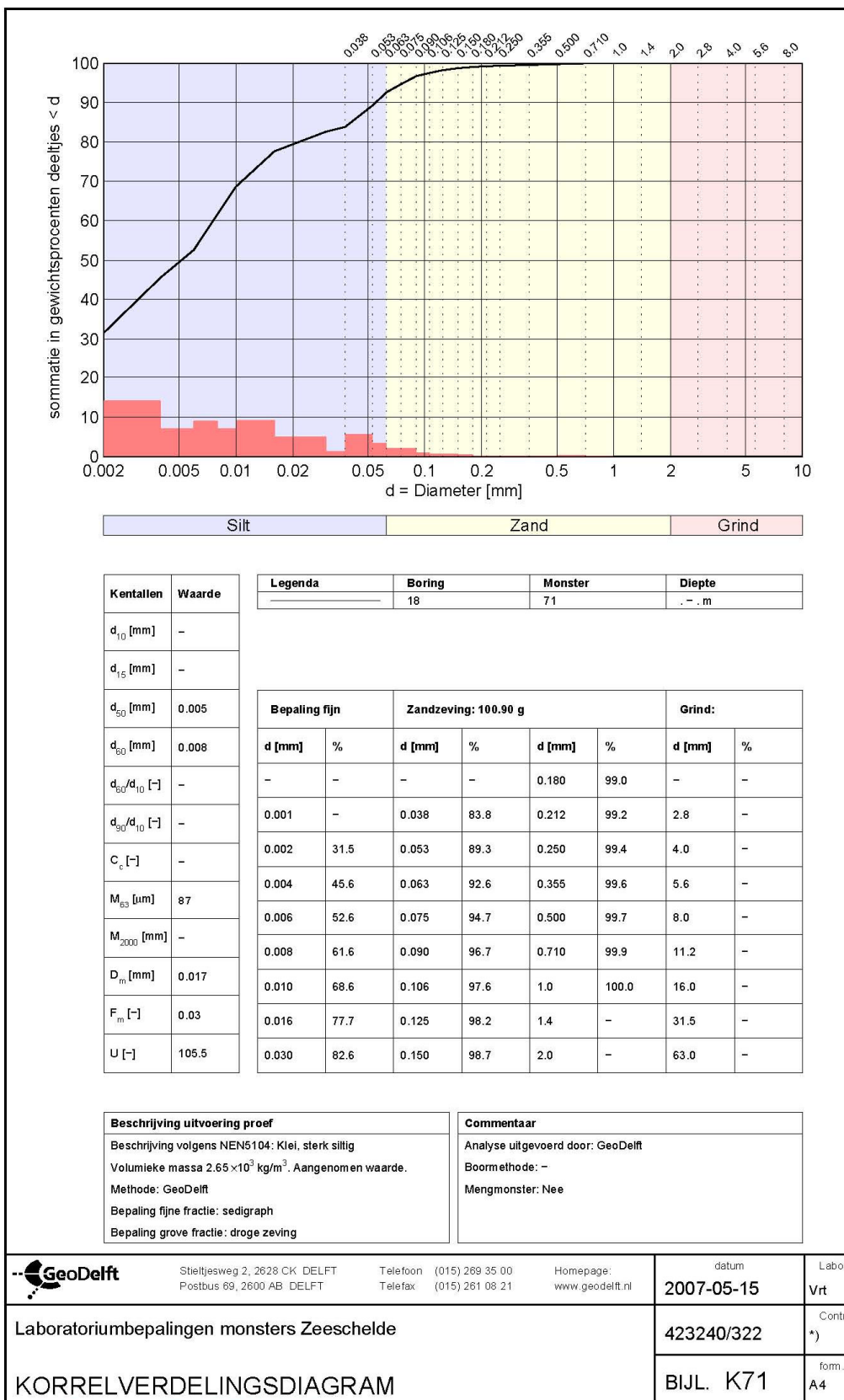


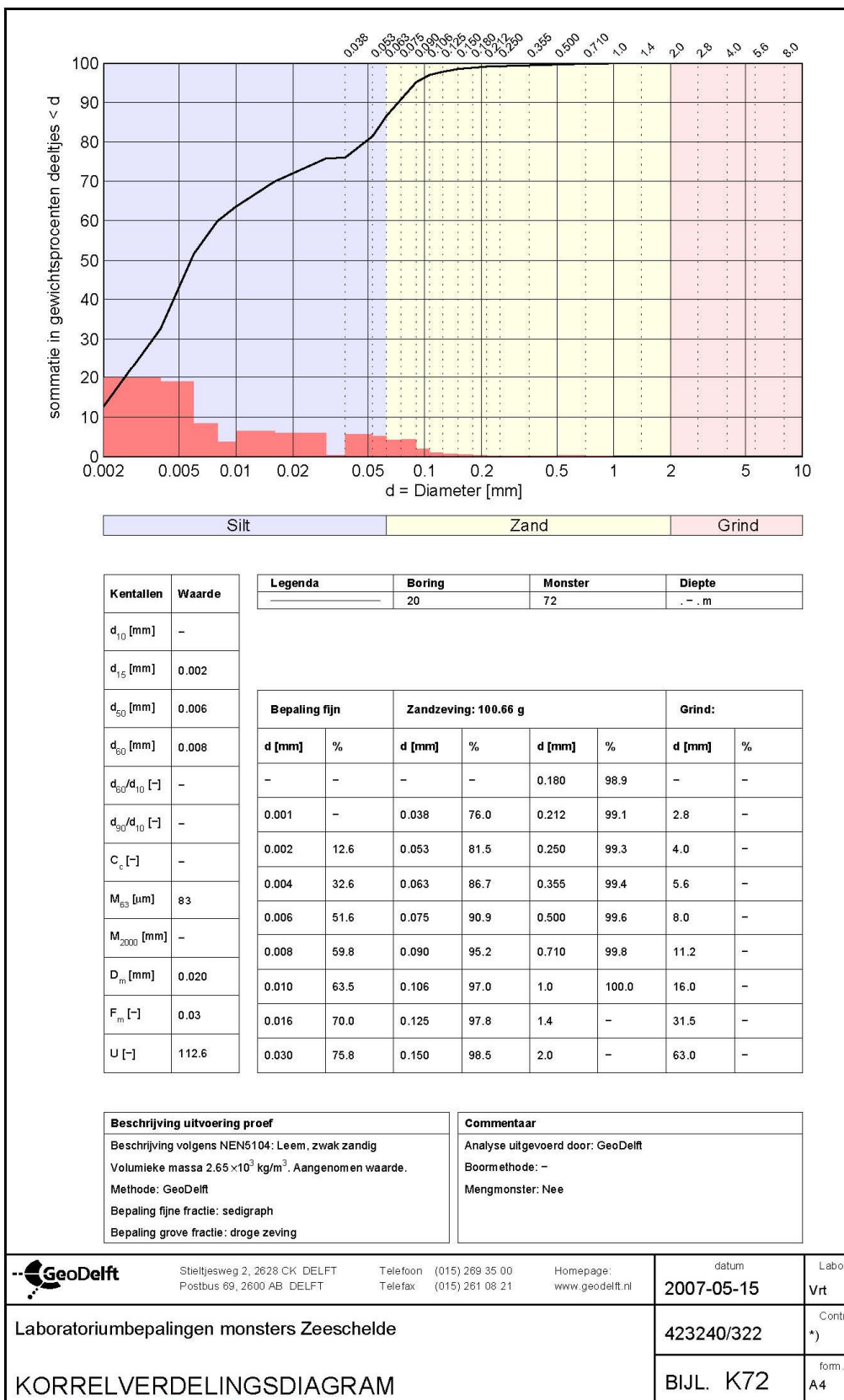


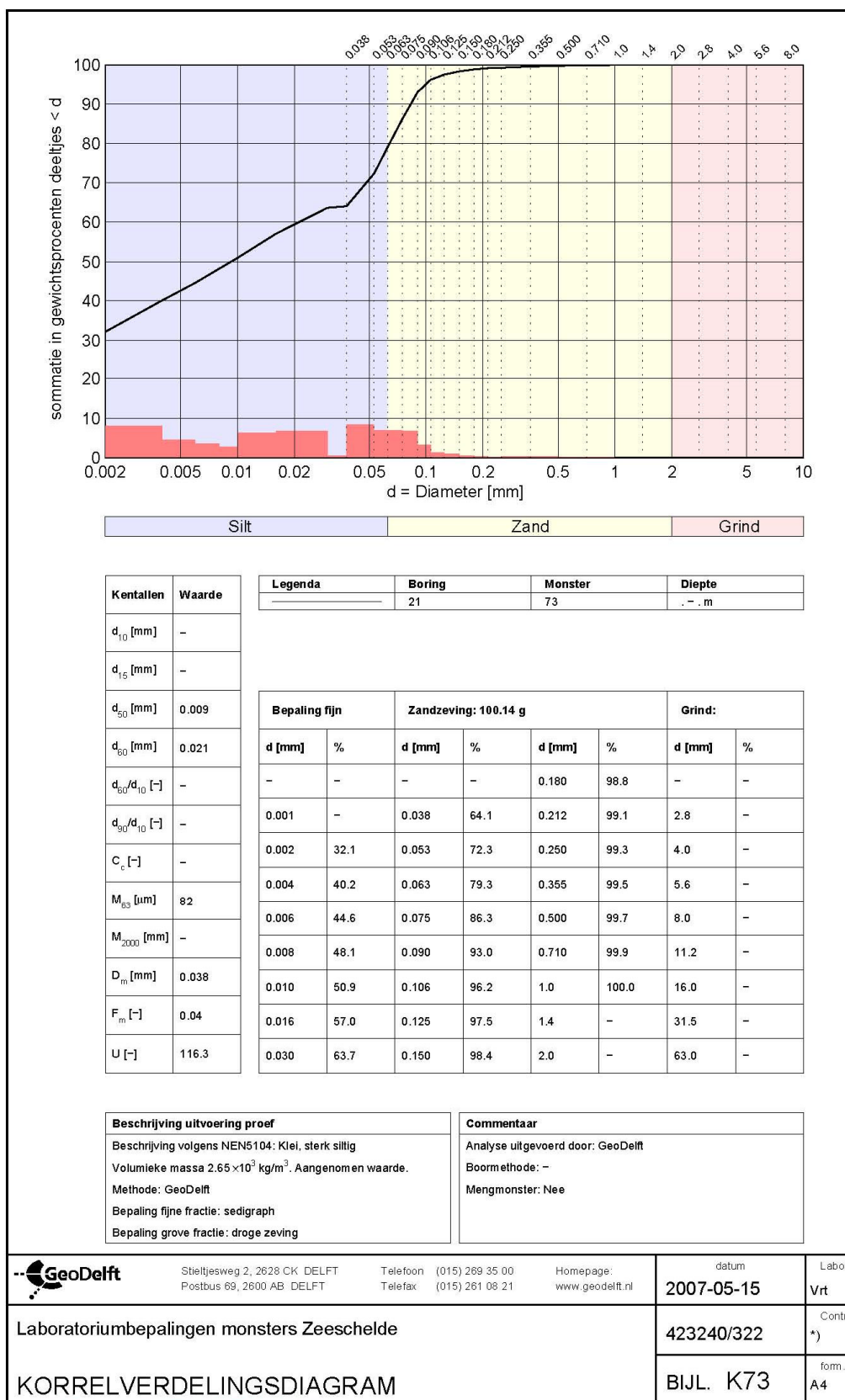


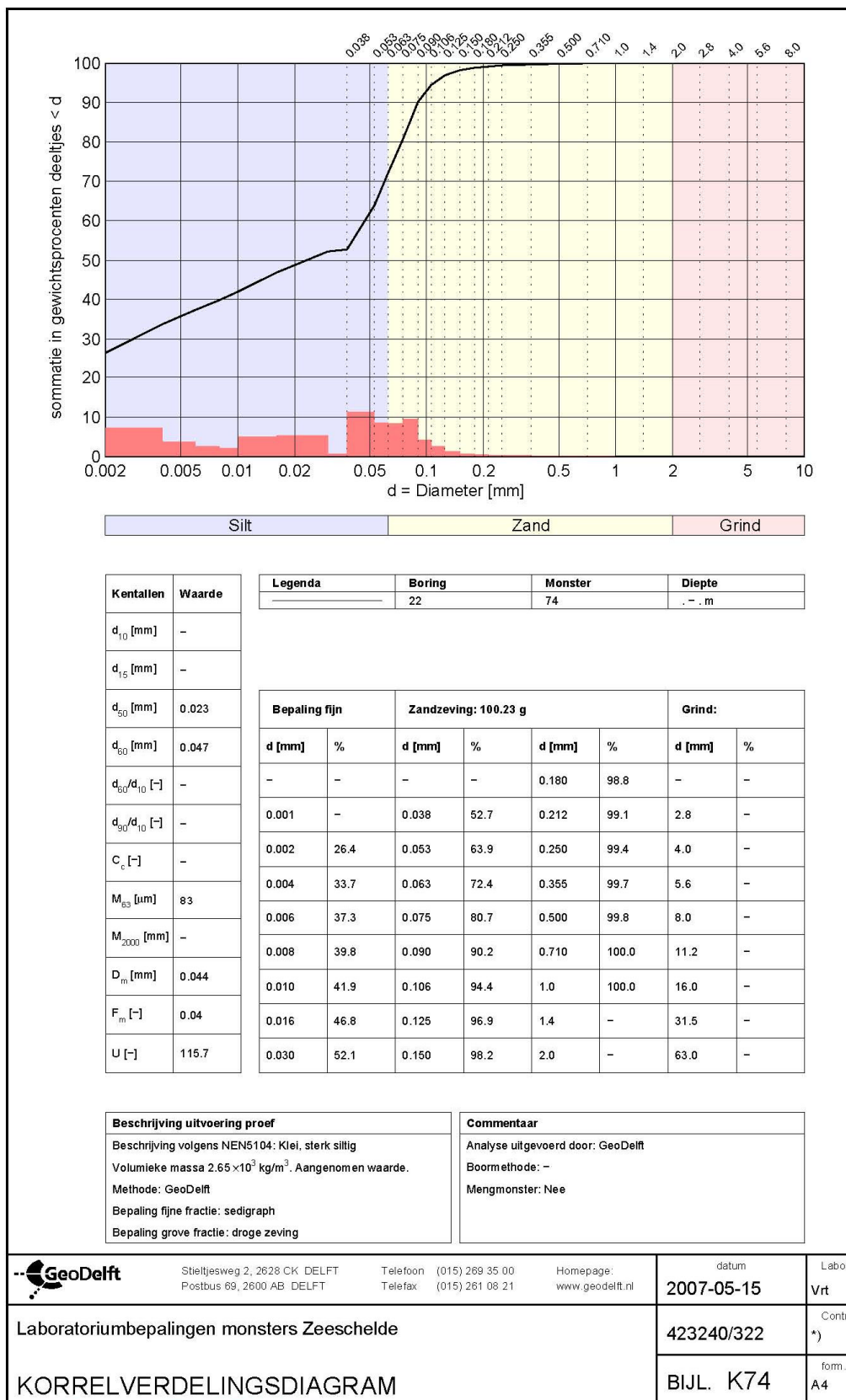


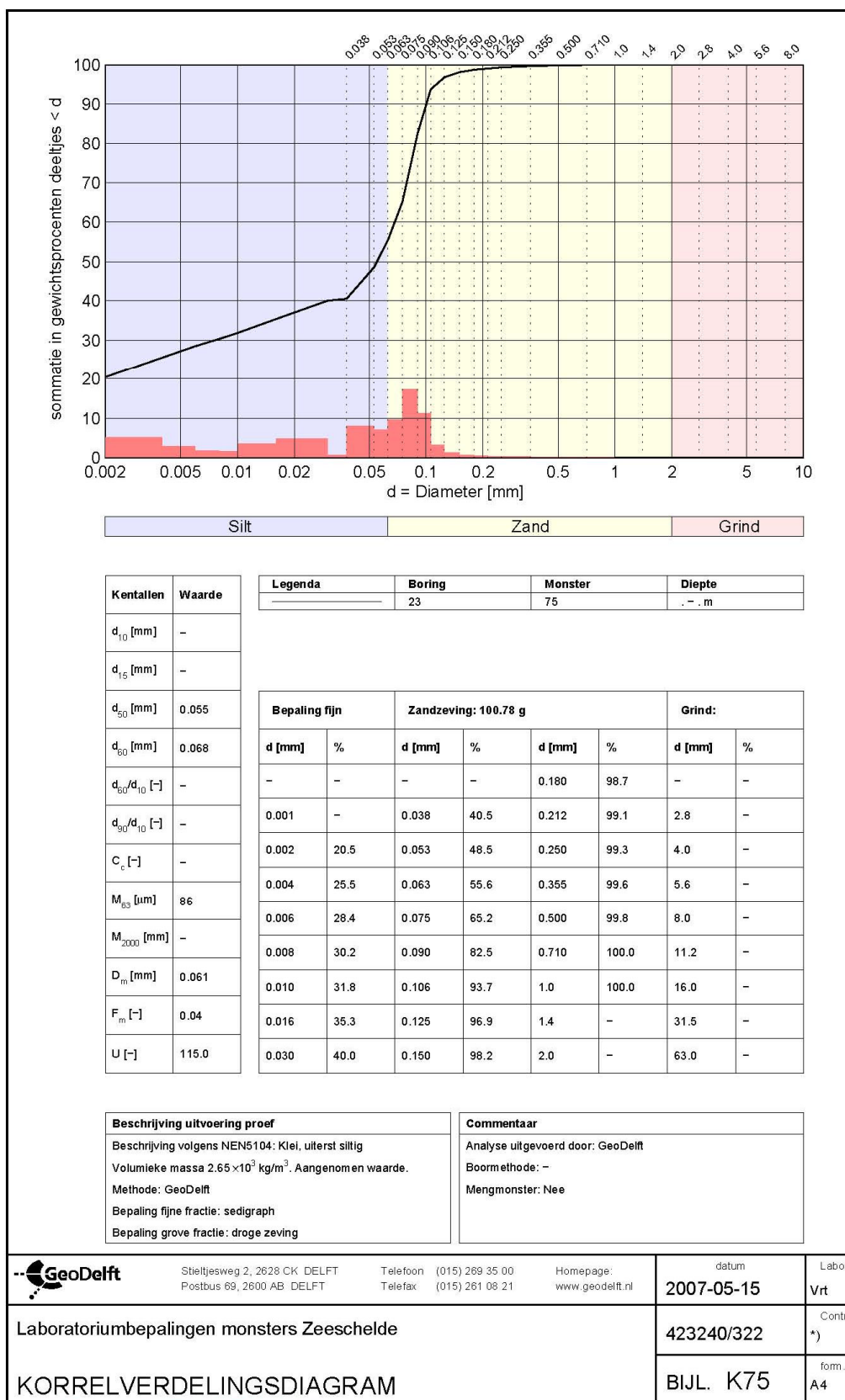


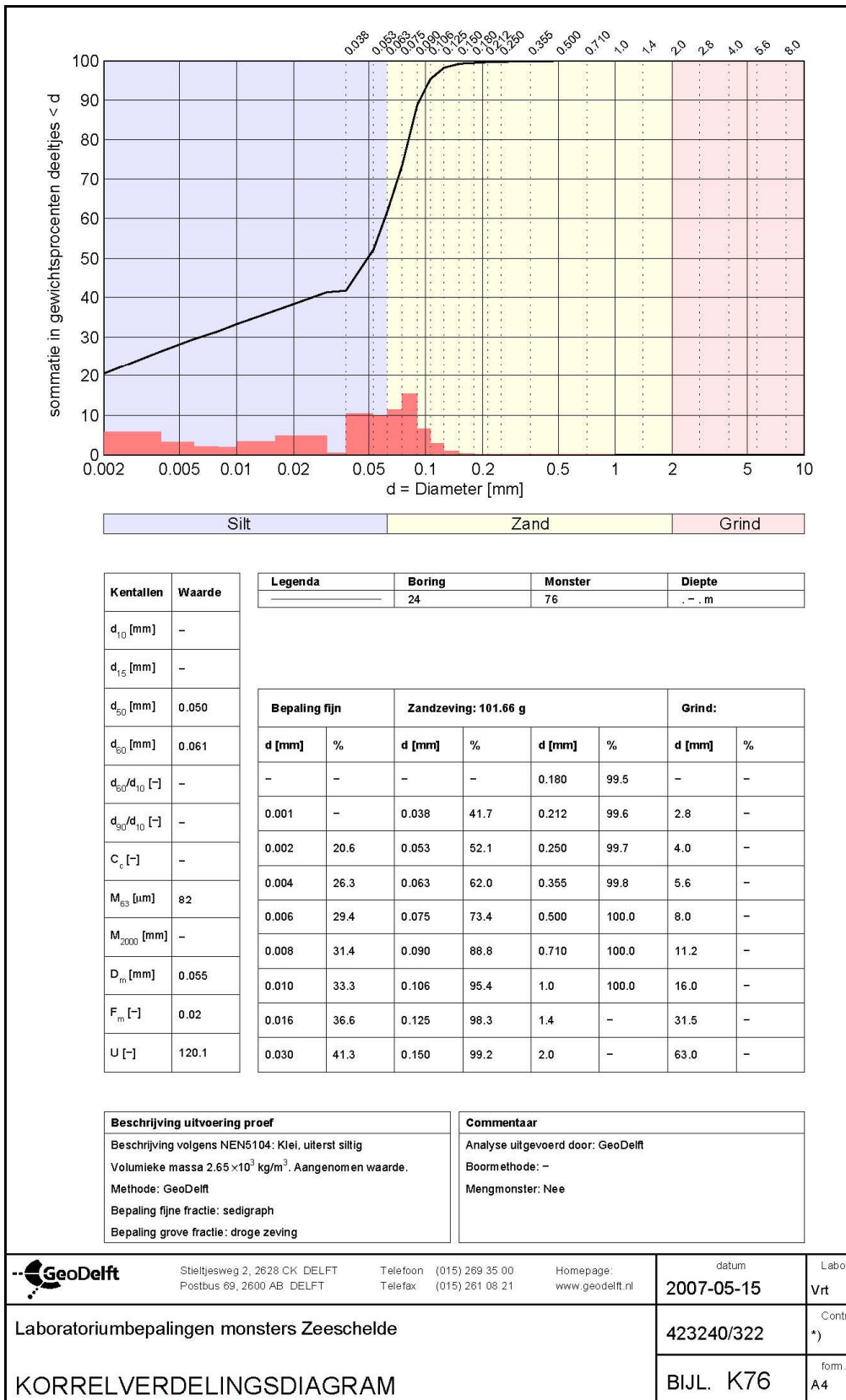


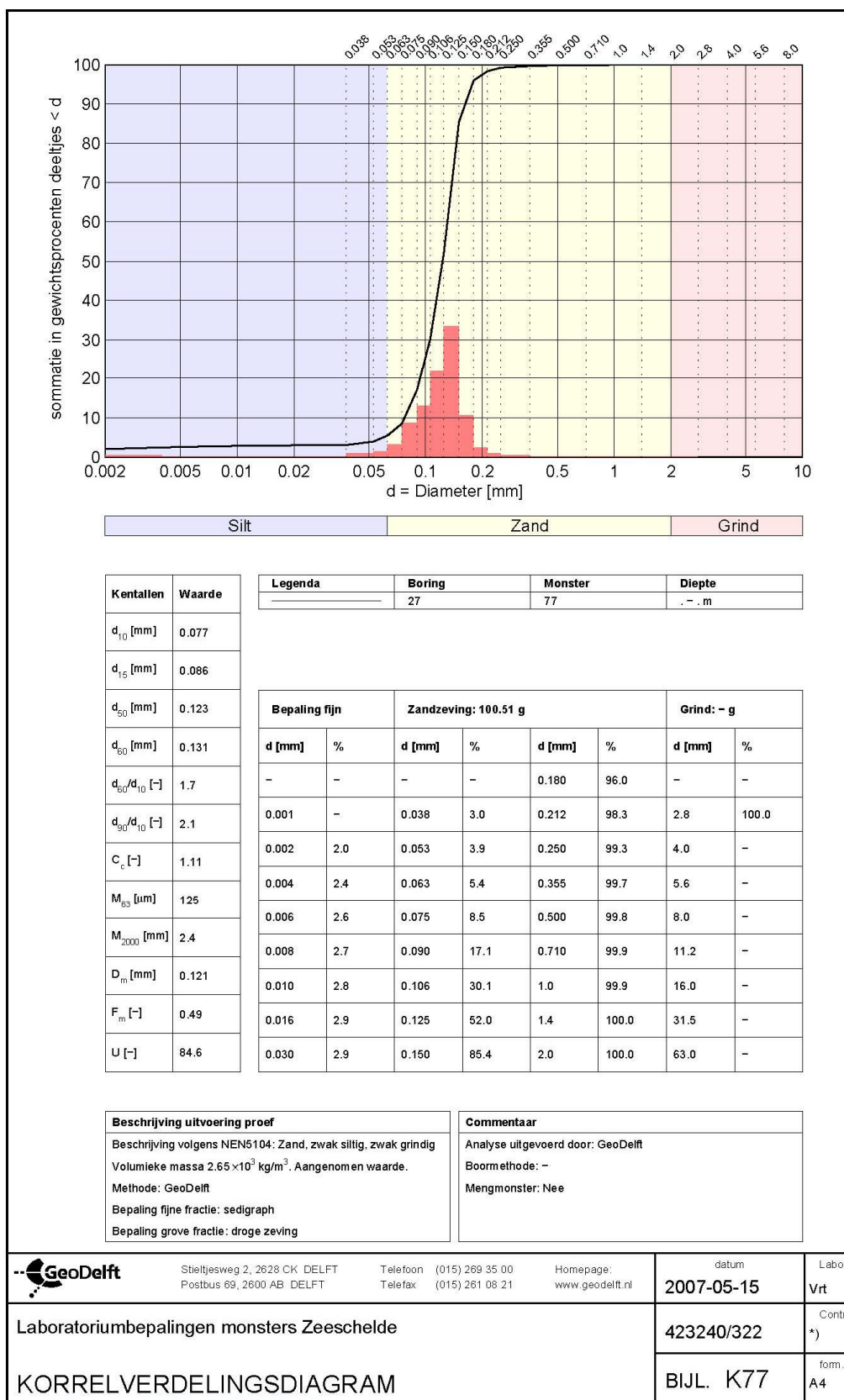


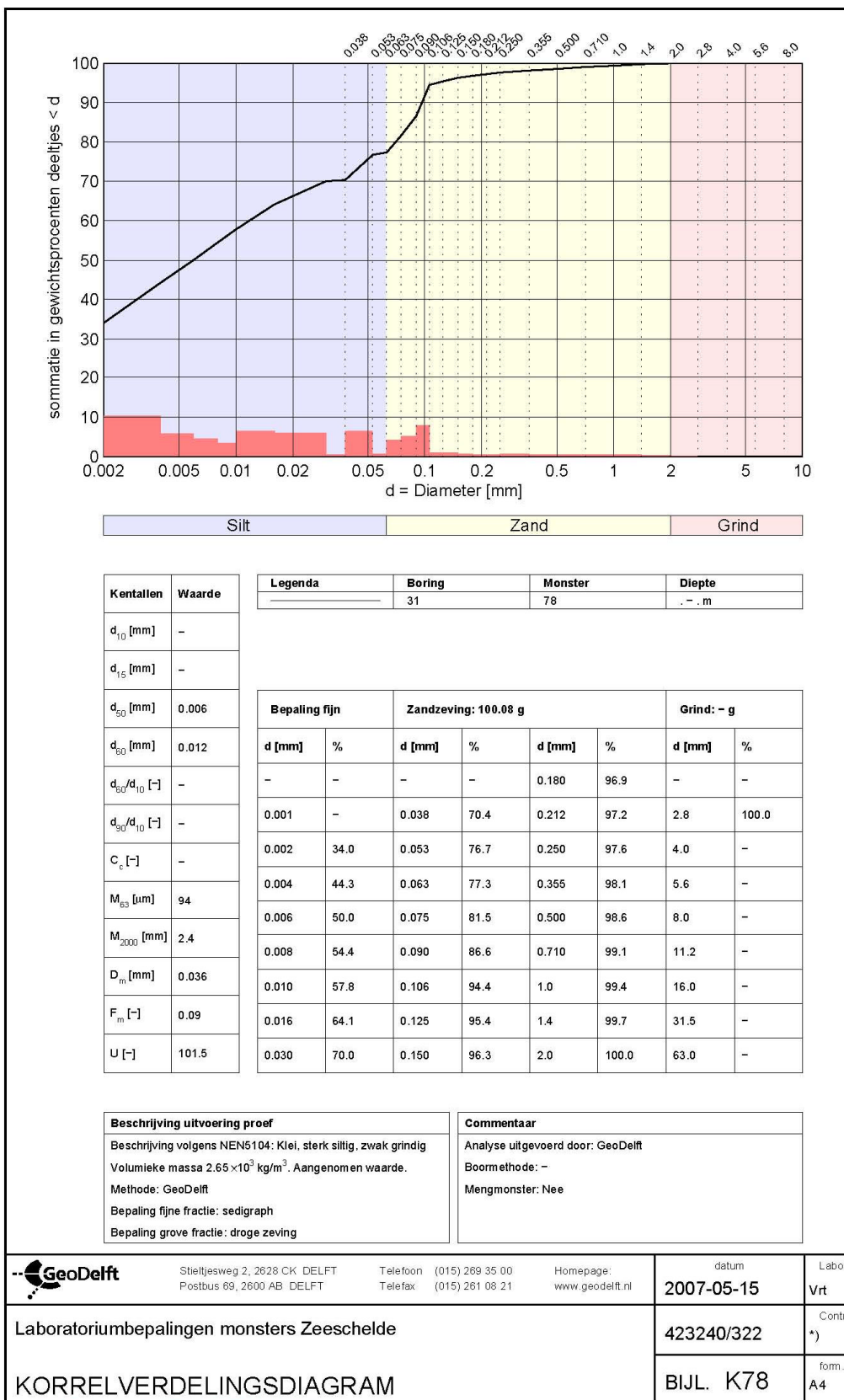


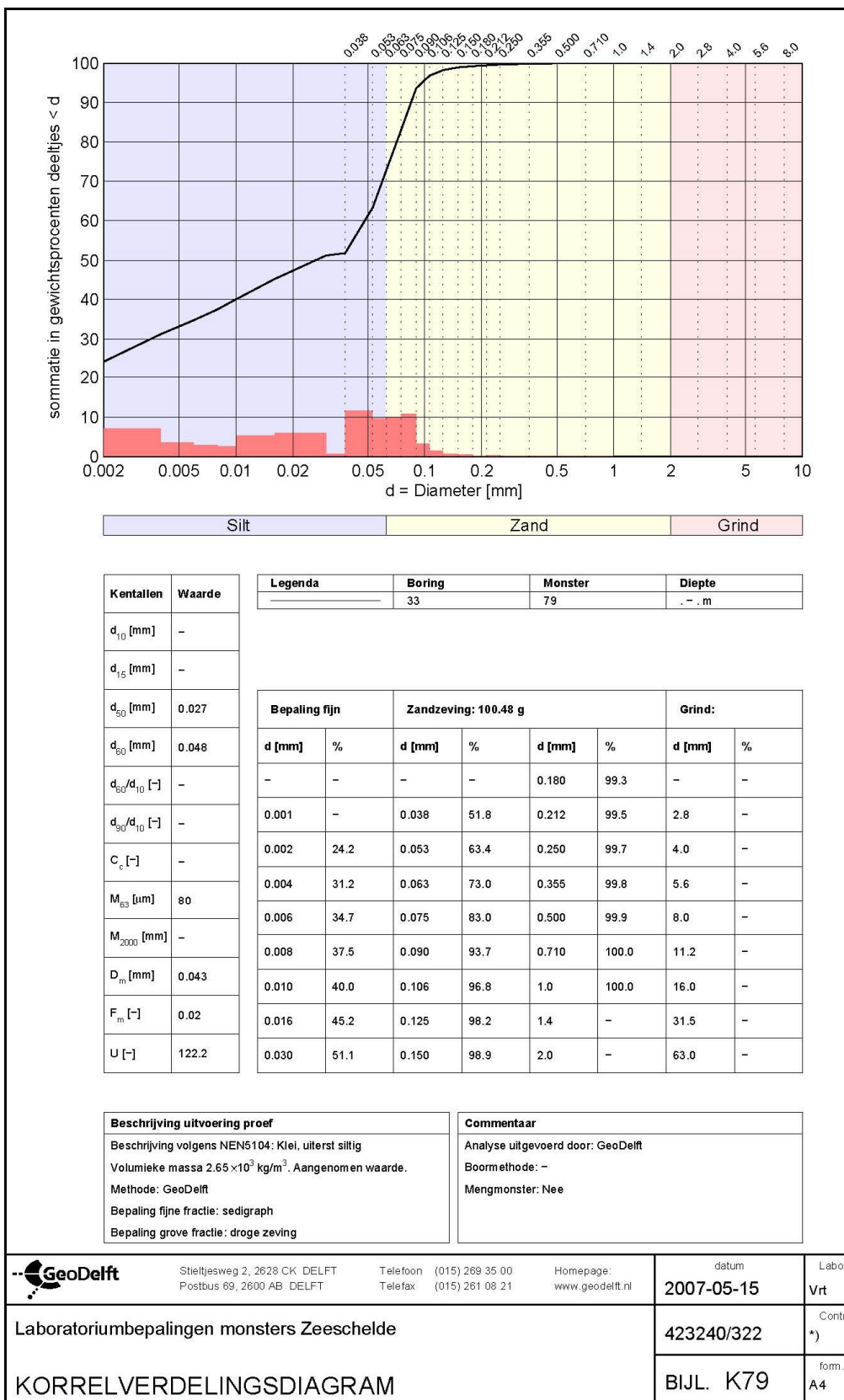


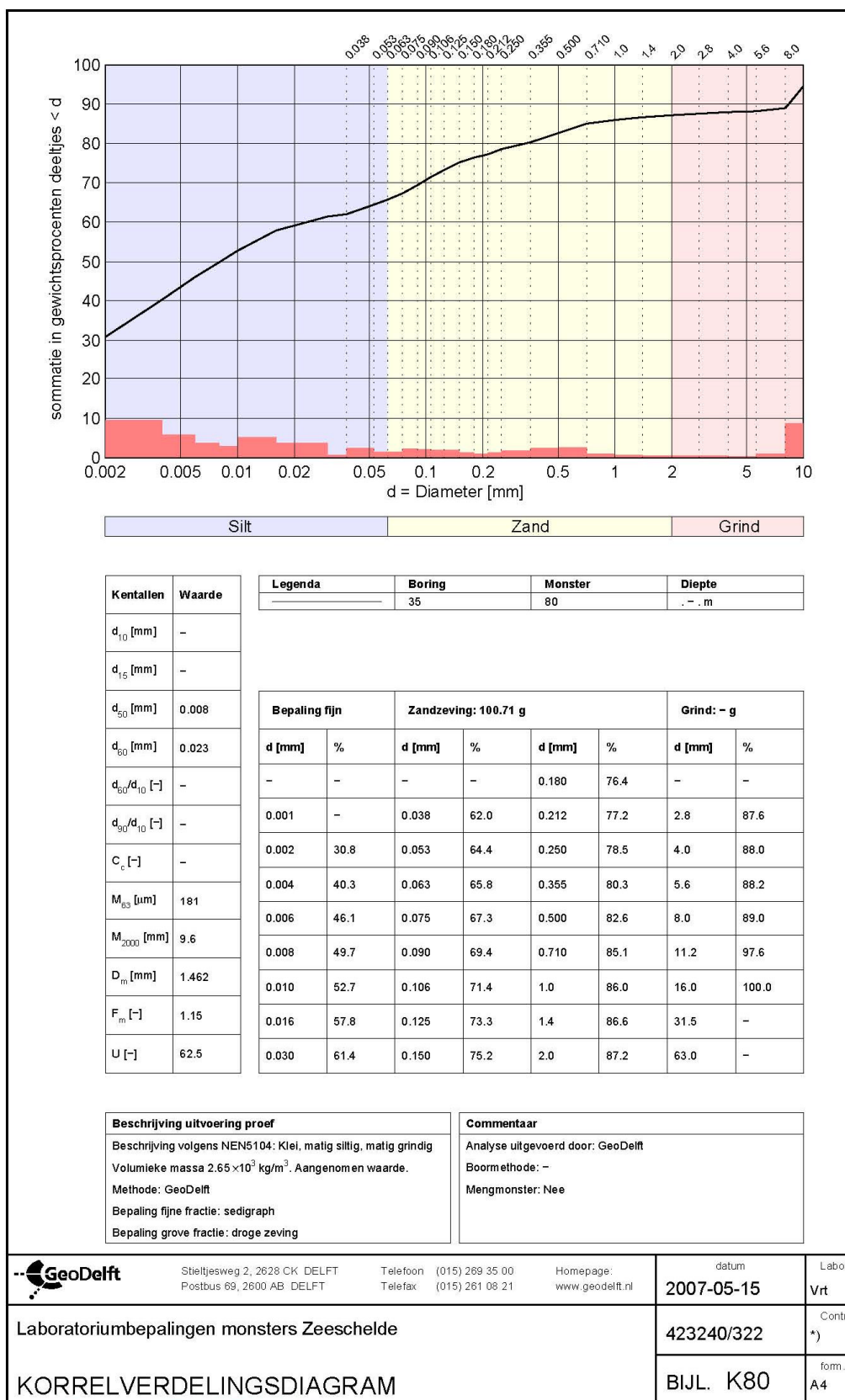


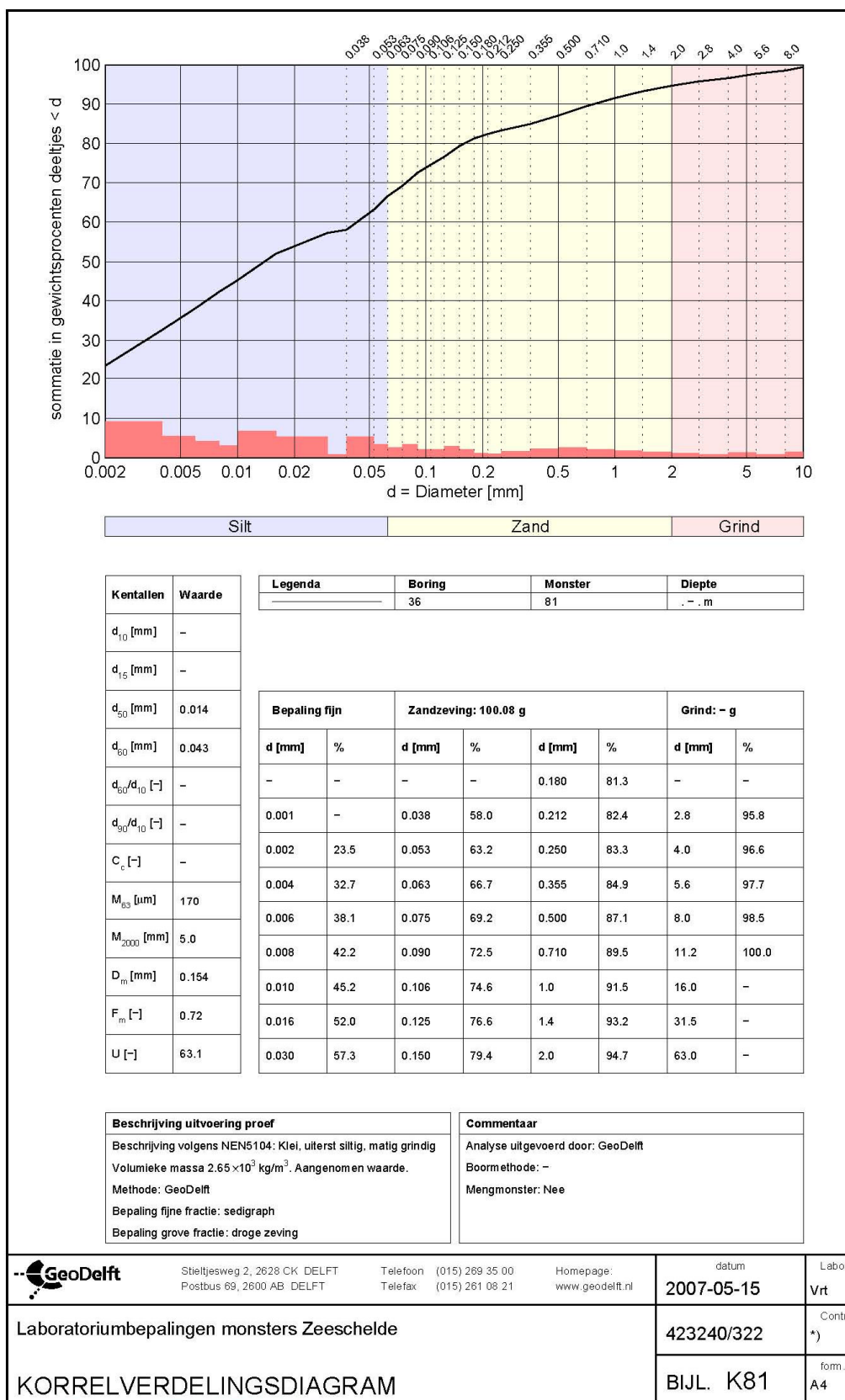












ANNEX B. CONSOLIDATION TEST RESULTS

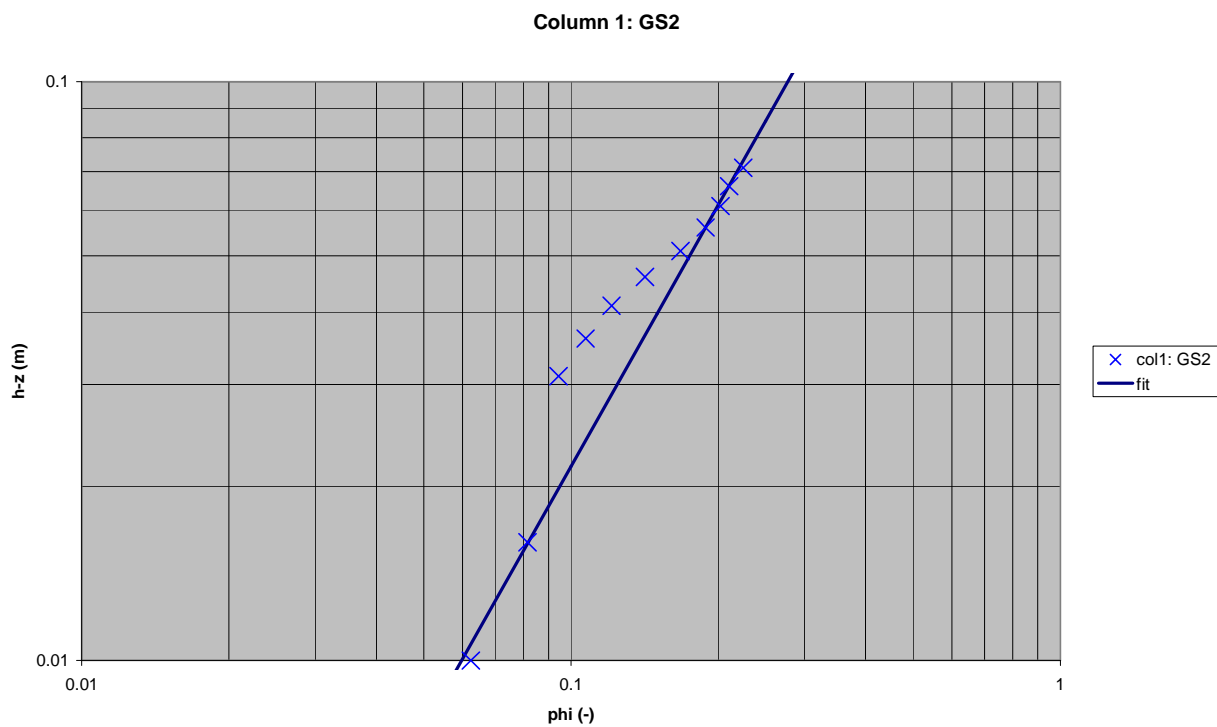
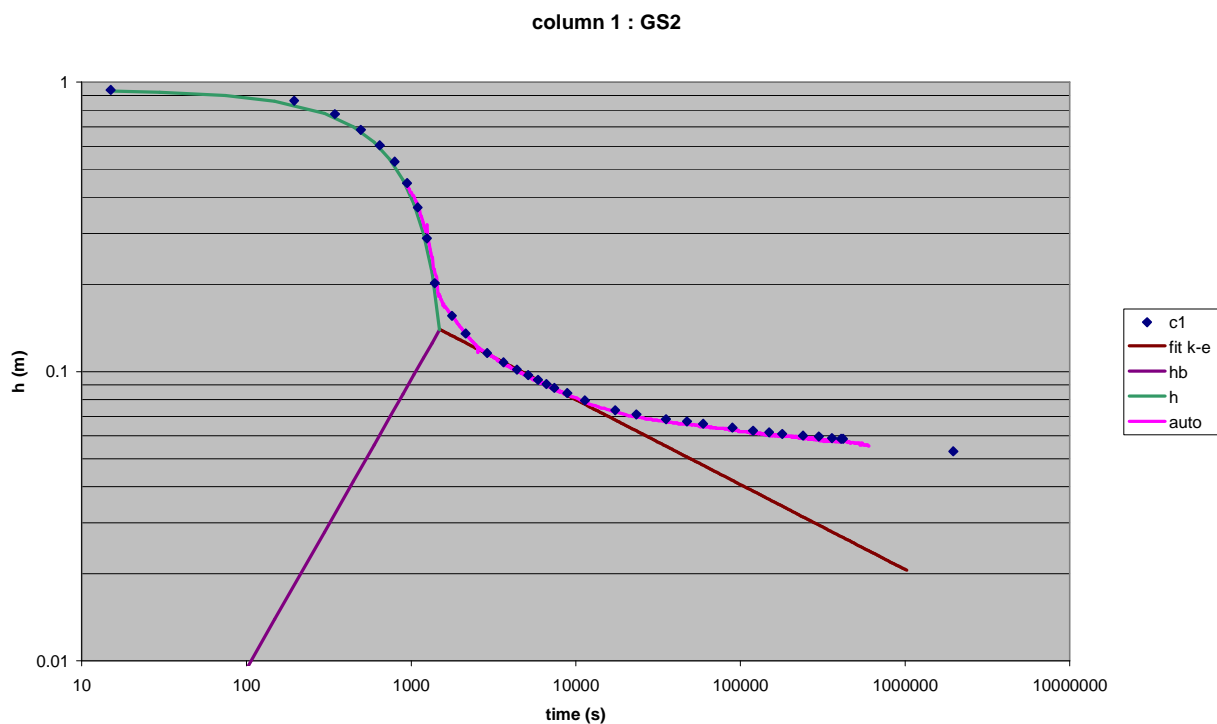


Figure annexe B-1: Settling curve (top) and final density profile (bottom) for sample GS02 Galgenschor

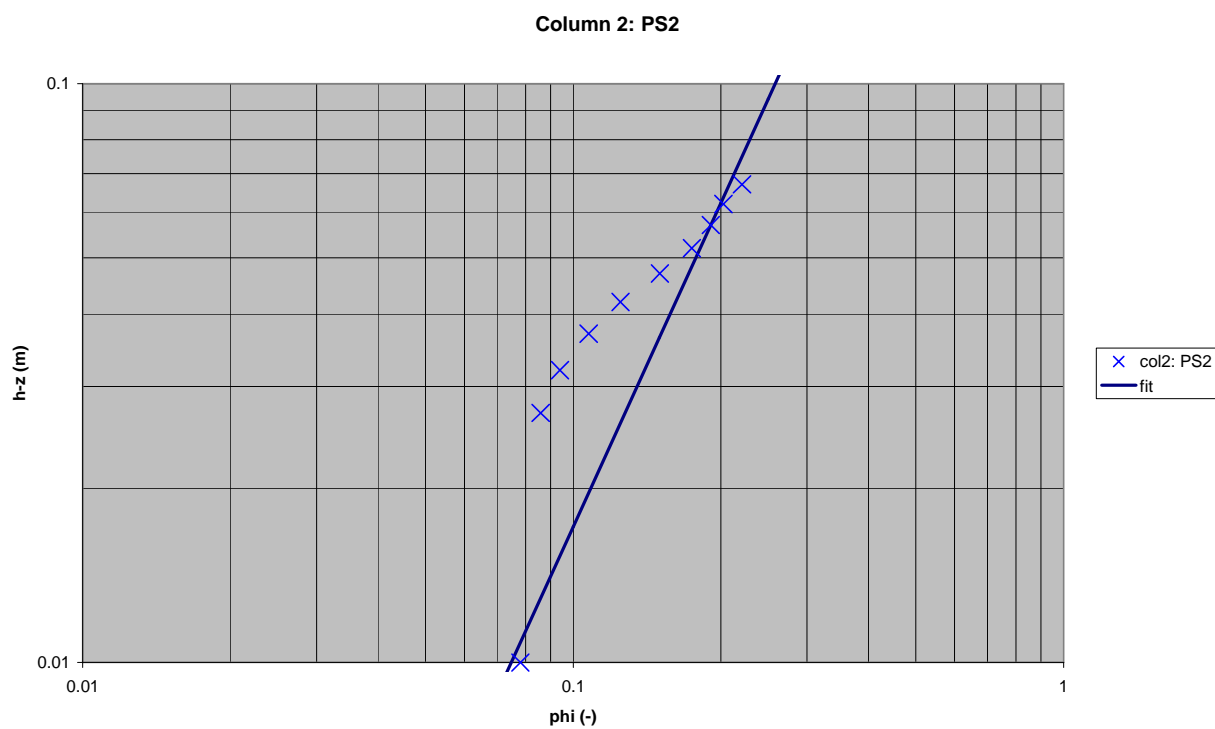
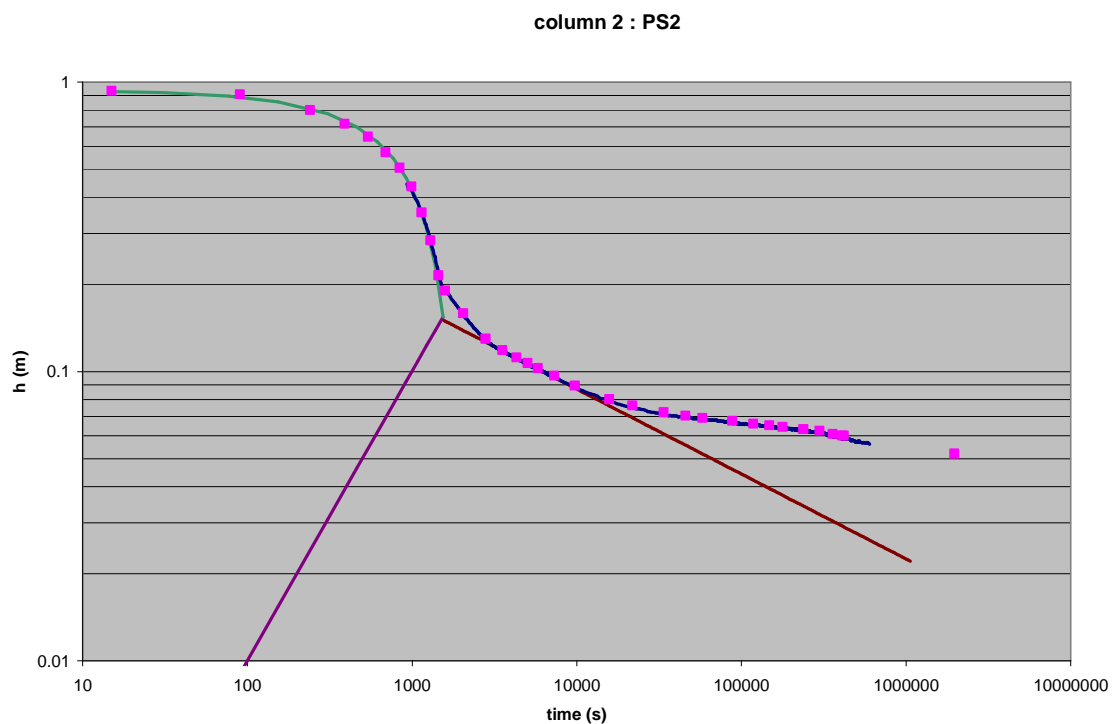


Figure annexe B-2: Settling curve (top) and final density profile (bottom) for sample PS02 Paardenschor

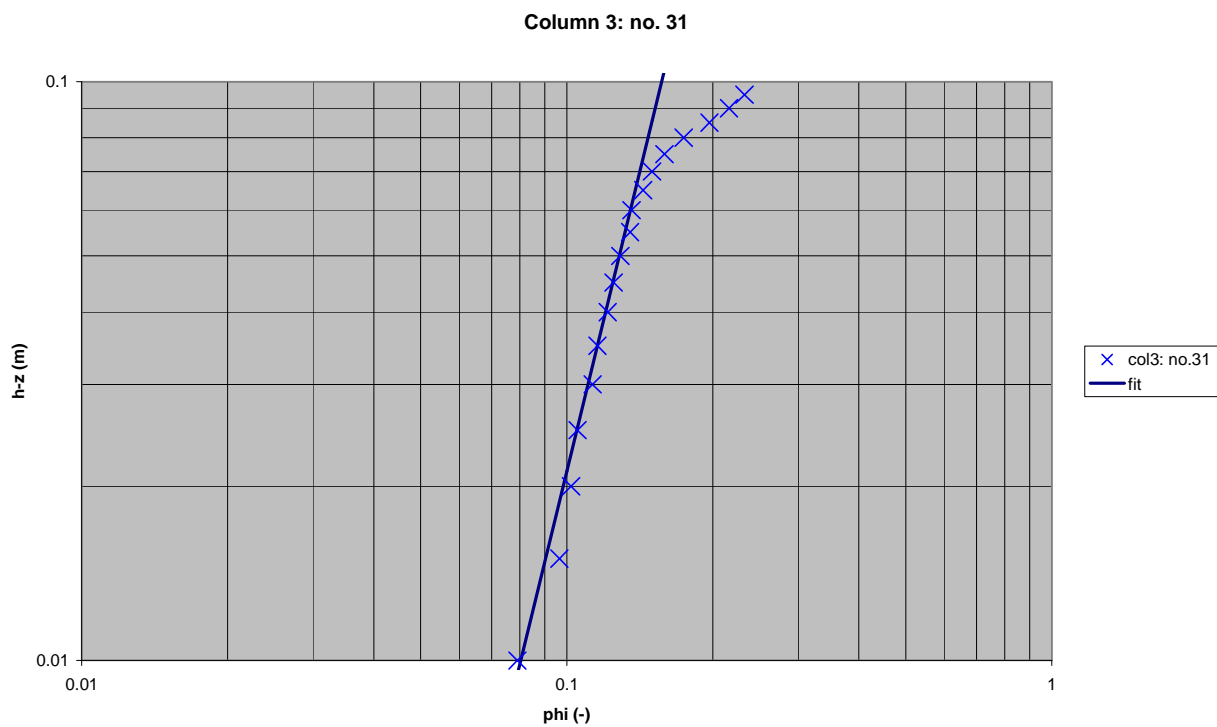
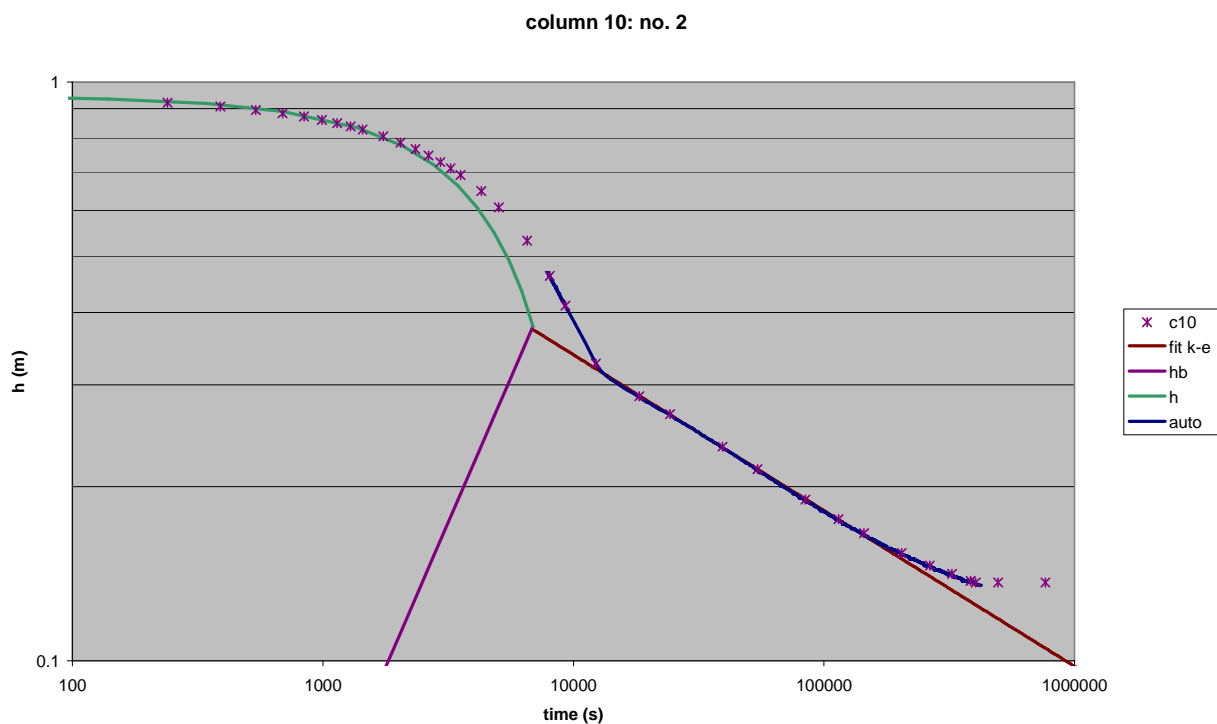


Figure annexe B-3: Settling curve (top) and final density profile (bottom) for sample 2 Zandvlietsluis

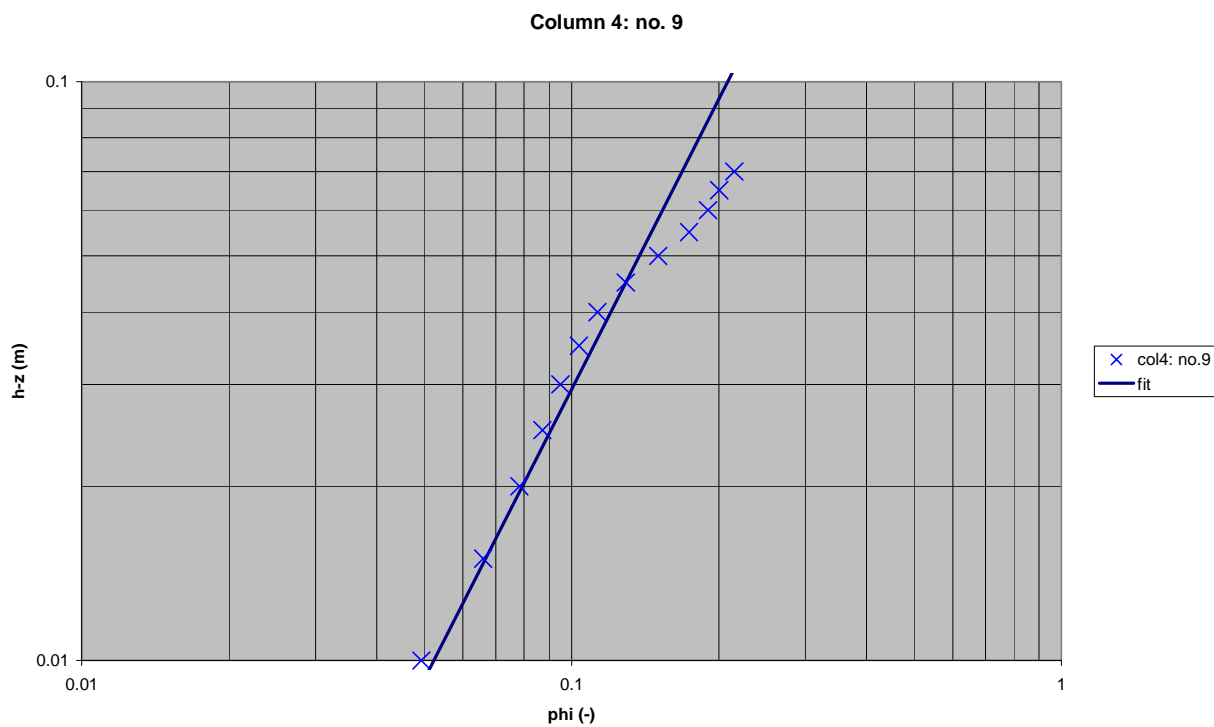
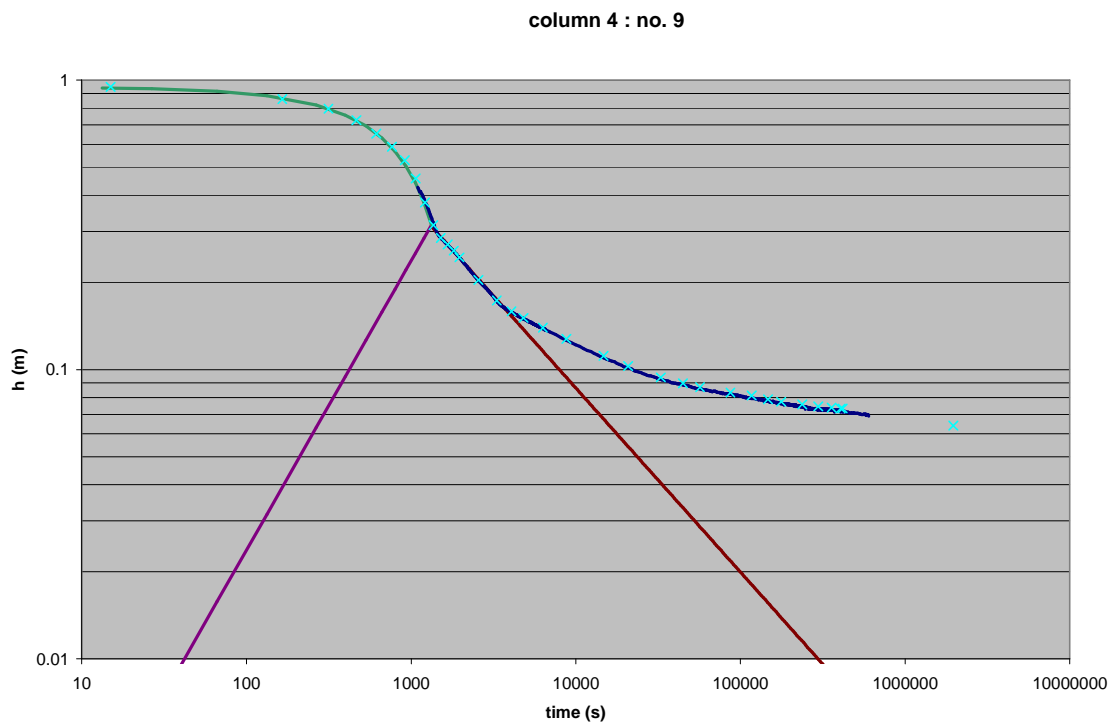
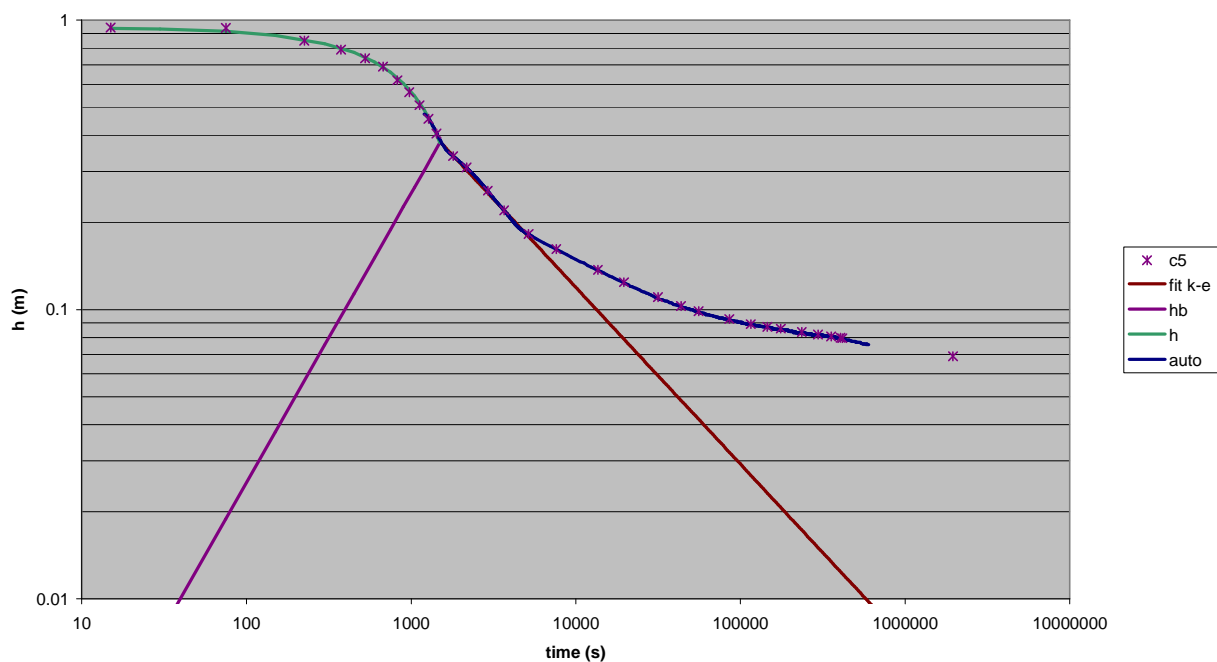


Figure annexe B-4: Settling curve (top) and final density profile (bottom) for sample 9 Boei 84

column 5 : no. 33



Column 5: no. 33

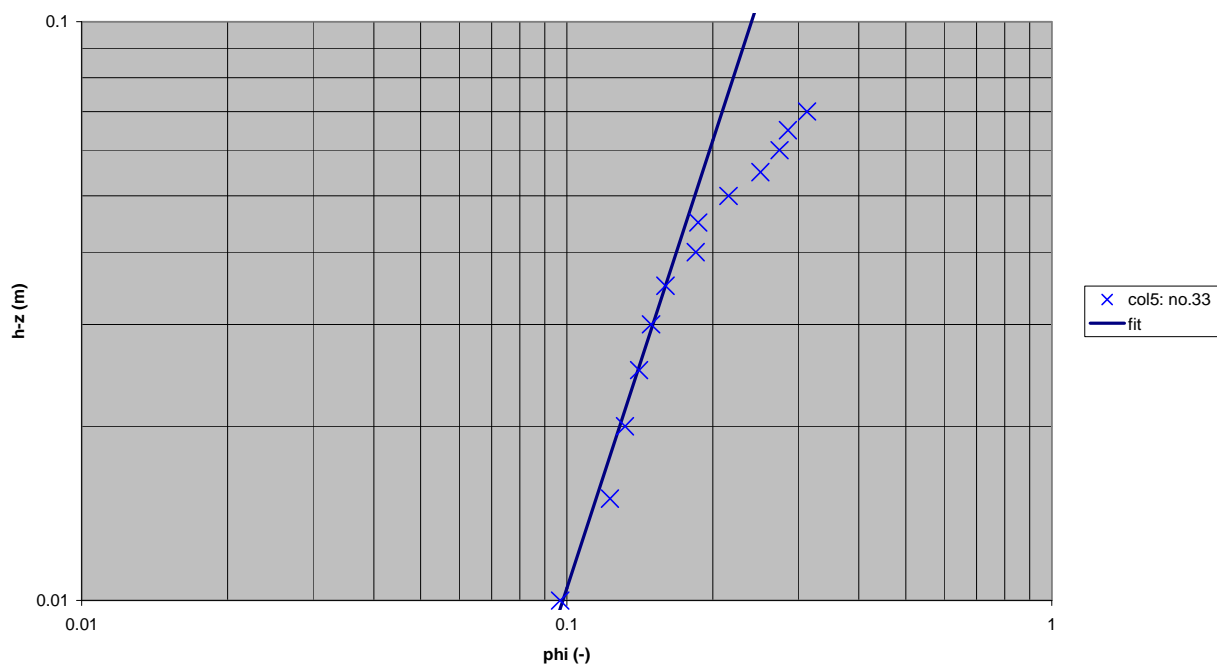


Figure annexe B-5: Settling curve (top) and final density profile (bottom) for sample 33 ingang Kallø 1

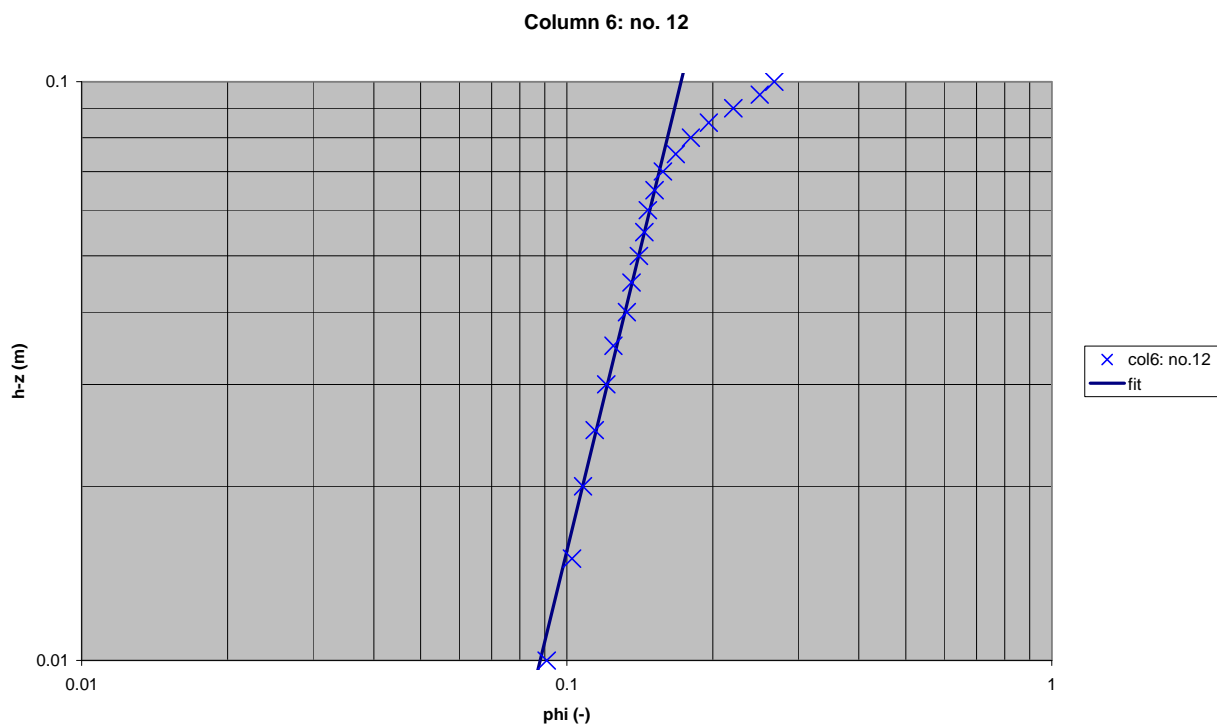
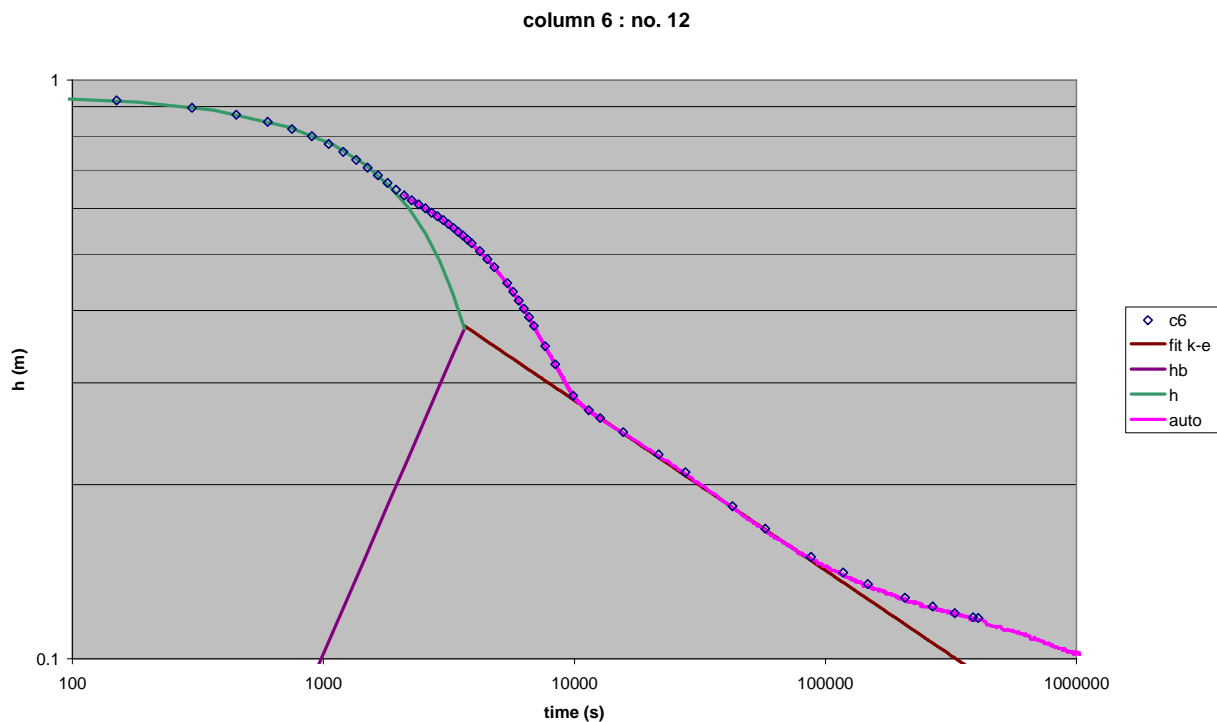
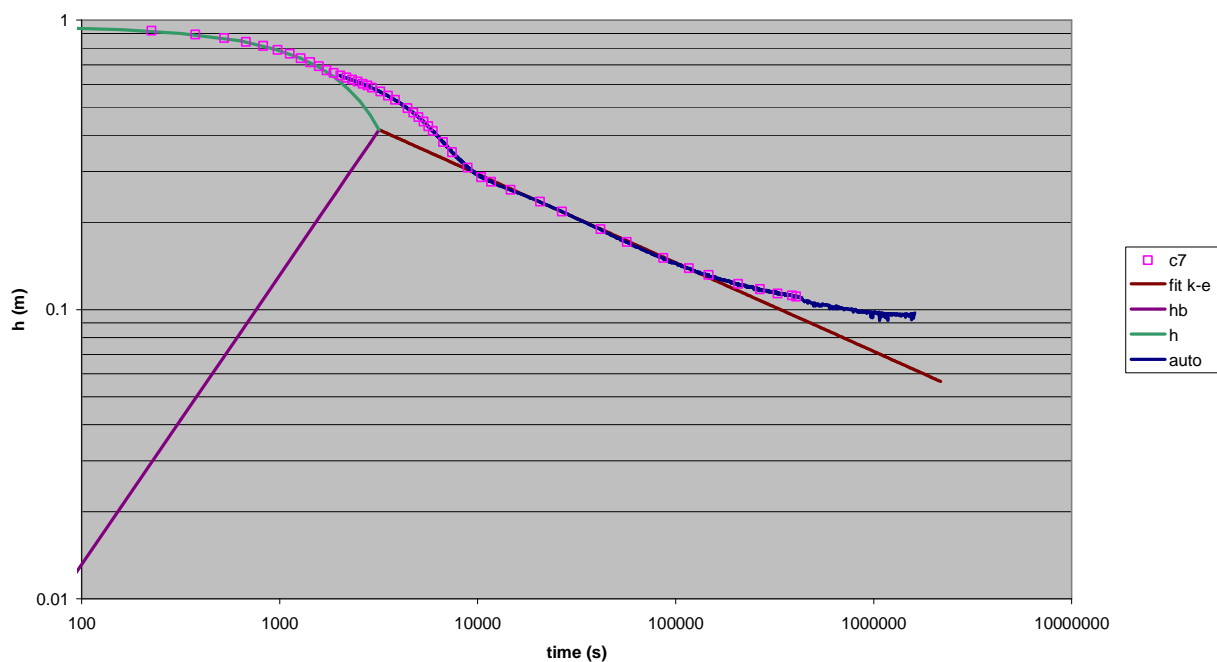


Figure annexe B-6: Settling curve (top) and final density profile (bottom) for sample 12 DGD 4

column 7 : no. 18



Column 7: no. 18

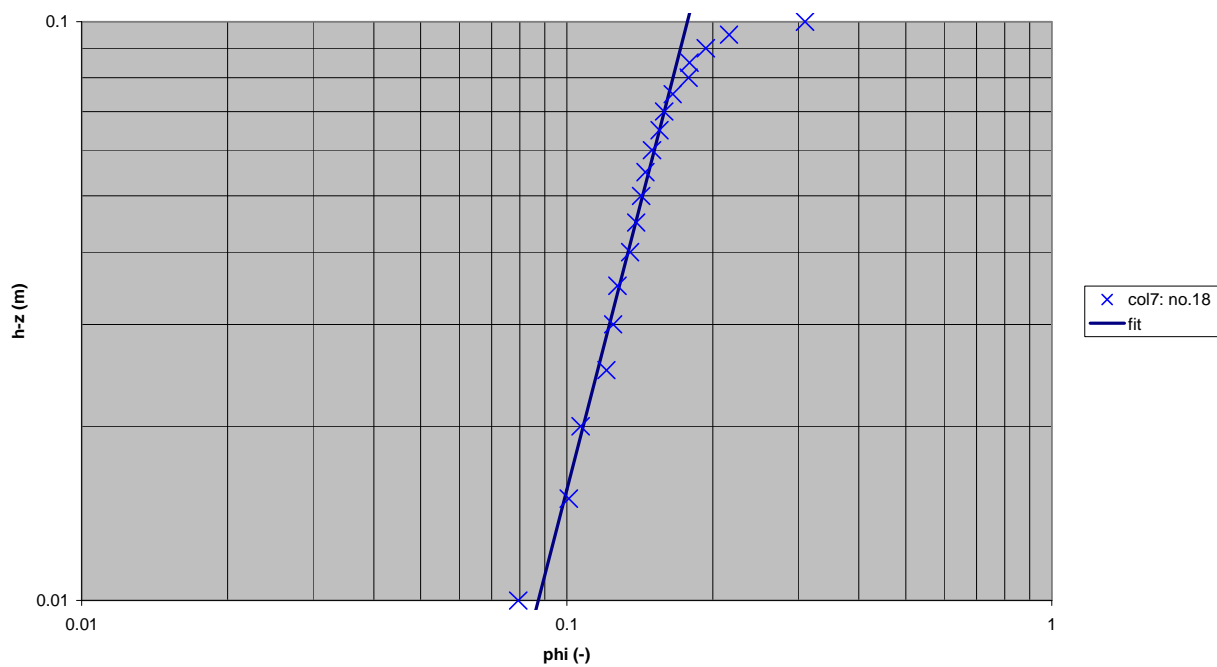
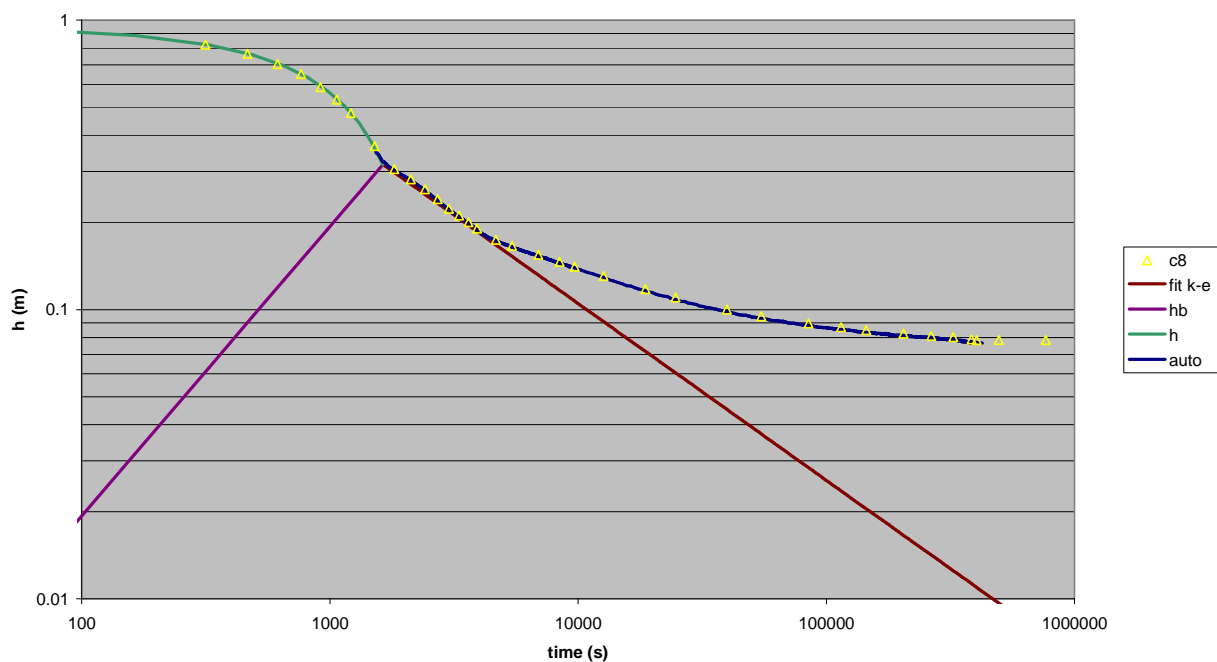


Figure annexe B-7: Settling curve (top) and final density profile (bottom) for sample 18 DGD 10

column 8 : no. 24



Column 8: no. 24

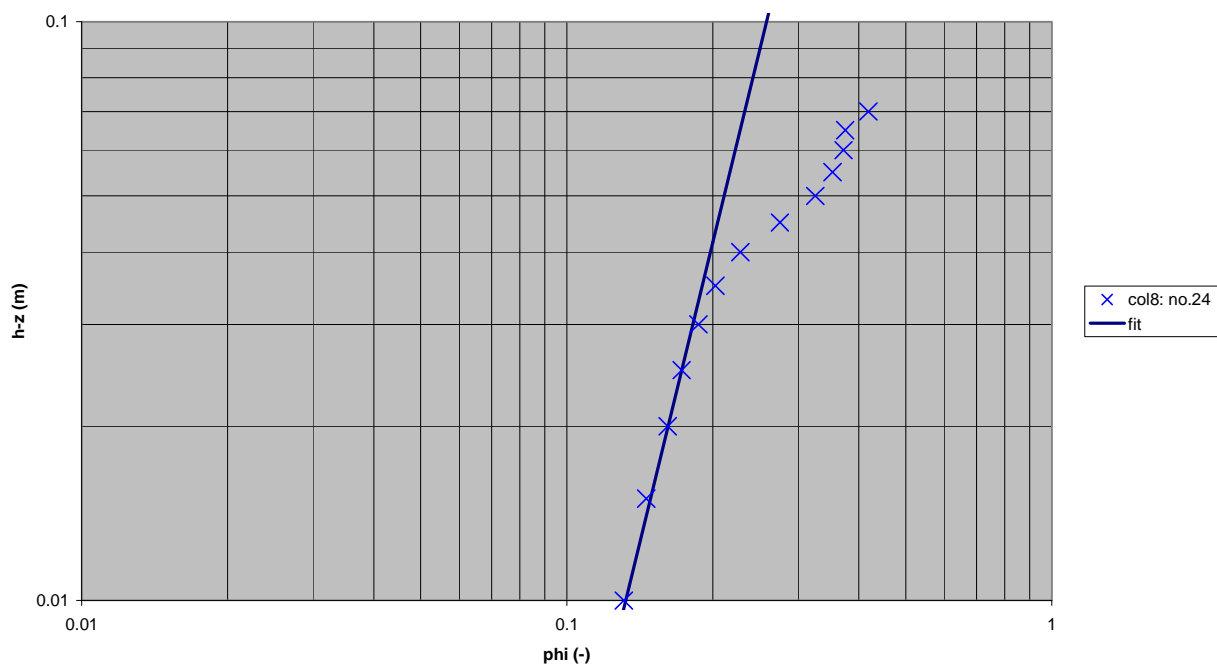
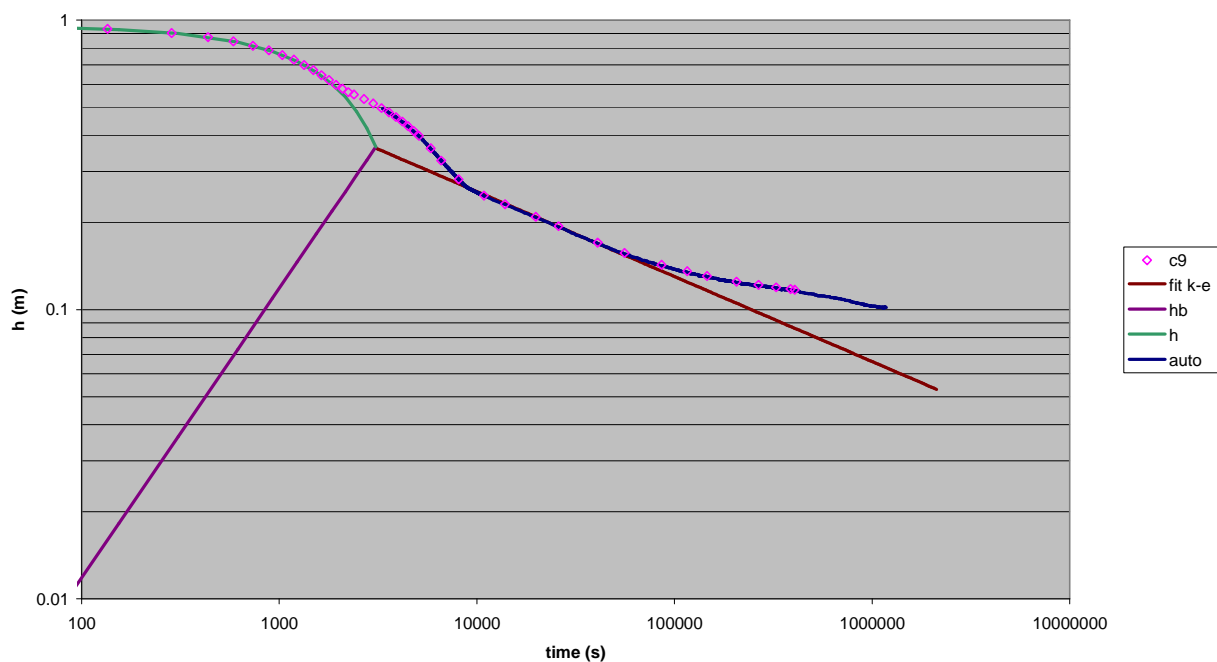


Figure annexe B-8: Settling curve (top) and final density profile (bottom) for sample 24 DGD opwaarts

column 9 : no. 21



Column 9: no. 21

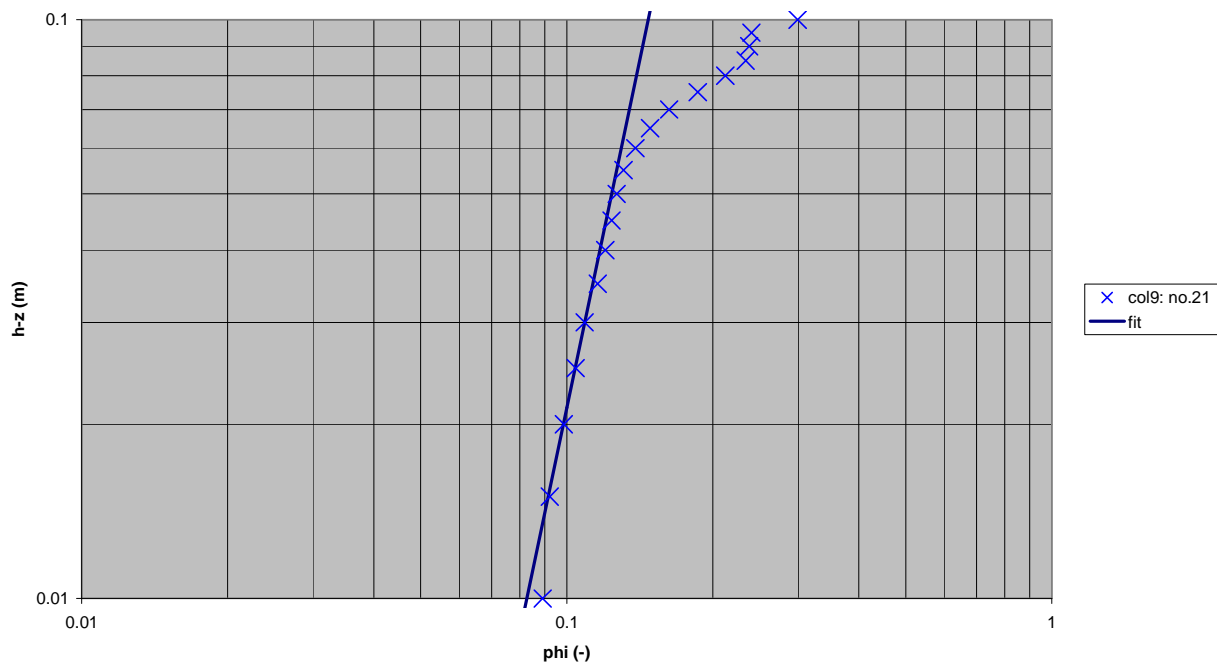


Figure annexe B-9: Settling curve (top) and final density profile (bottom) for sample 21 DGD7

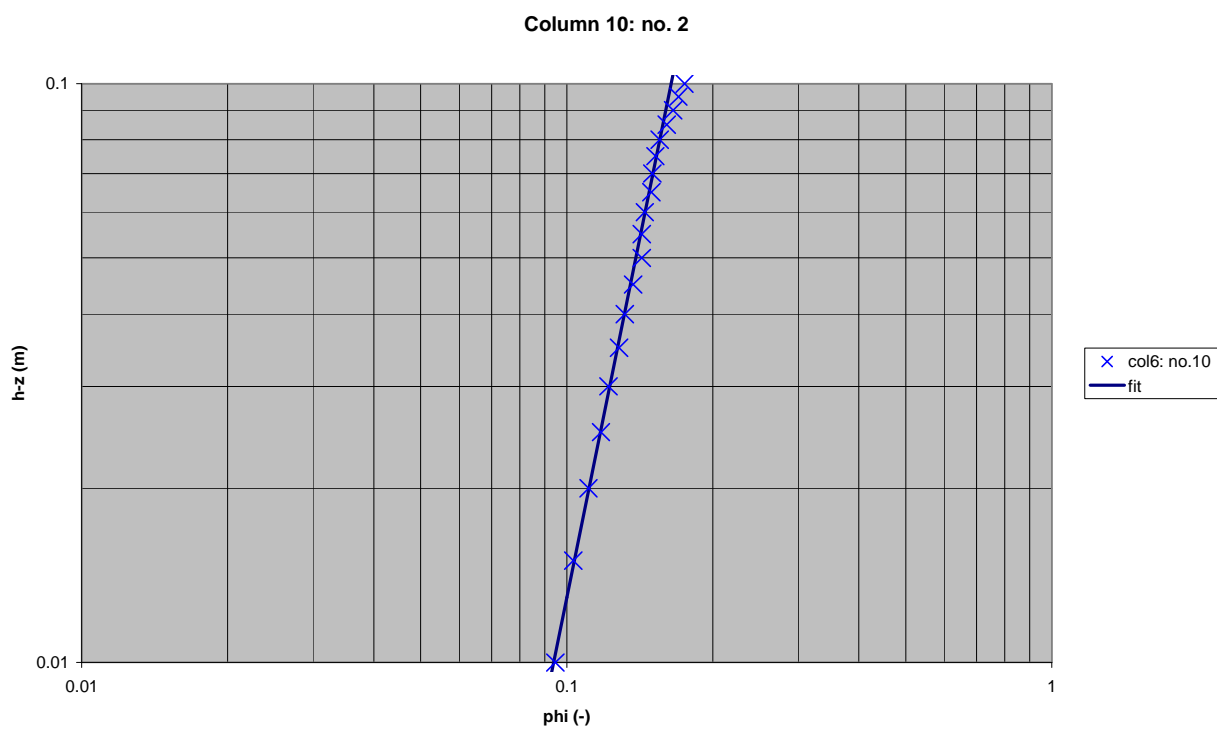
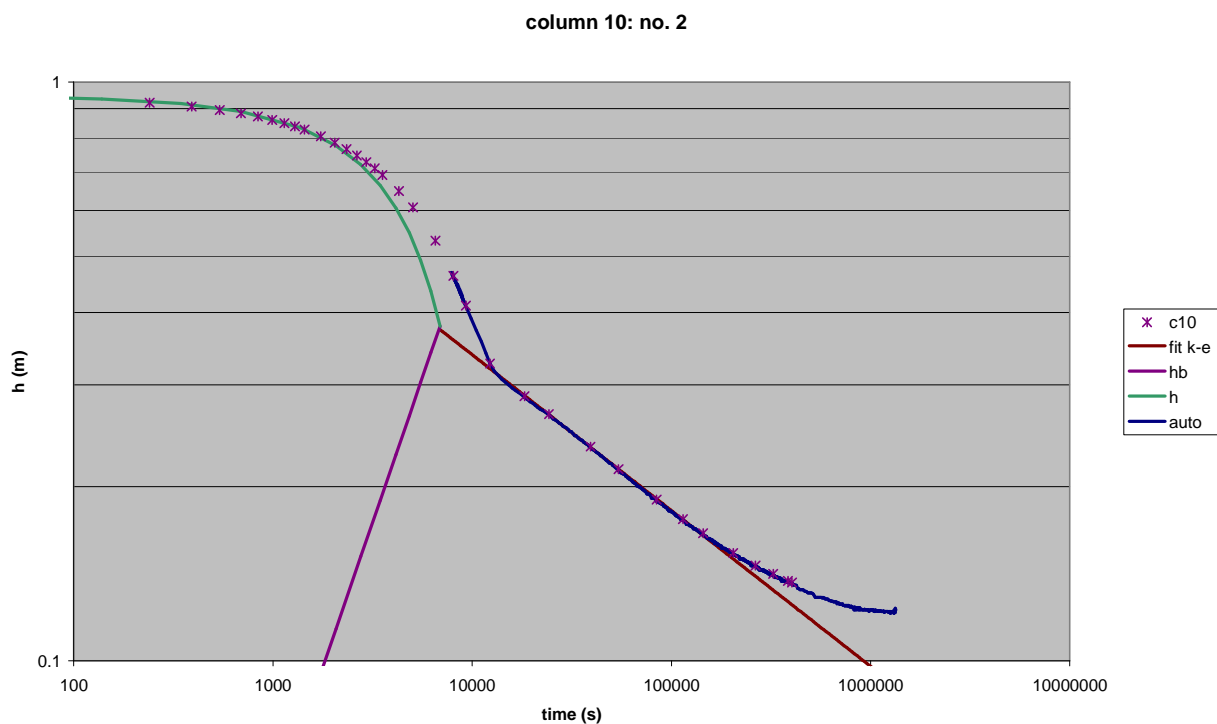


Figure annexe B-10: Settling curve (top) and final density profile (bottom) for sample 2 Zandvlietsluis